APPLICATION OF MICRONEEDLES AND ELECTROPORATION FOR ANTIGEN DELIVERY TO ENHANCE THE EFFICIENCY OF SKIN VACCINATION

By
MISS Boonnada PAMORNPATHOMKUL

A Thesis Submitted in Partial Fulfillment of the Requirements
for Doctor of Philosophy (PHARMACEUTICAL TECHNOLOGY)
Department of PHARMACEUTICAL TECHNOLOGY
Graduate School, Silpakorn University
Academic Year 2017

การประยุกต์ใช้ไมโครนีเดิลส์และอิเล็กโทรพอเรชันสำหรับนำส่งแอนติเจนเพื่อเพิ่มประสิทธิภาพการเสริมสร้างภูมิคุ้มกันทางผิวหนัง

โดย
นางสาวบุณฌดา ภมรปฐมกุล

วิทยานิพนธ์นี้เป็นส่วนหนึ่งของการศึกษาตามหลักสูตรปรัชญาดุษฎีบัณฑิต
สาขาวิชาเทคโนโลยีเภสัชกรรม แบบ 1.2 ปรัชญาดุษฎีบัณฑิต
ภาควิชาเทคโนโลยีเภสัชกรรม
บัณฑิตวิทยาลัย มหาวิทยาลัยศิลปากร
ปีการศึกษา 2560

APPLICATION OF MICRONEEDLES AND ELECTROPORATION FOR ANTIGEN DELIVERY TO ENHANCE THE EFFICIENCY OF SKIN VACCINATION

By
MISS Boonnada PAMORNPATHOMKUL

A Thesis Submitted in Partial Fulfillment of the Requirements
for Doctor of Philosophy (PHARMACEUTICAL TECHNOLOGY)
Department of PHARMACEUTICAL TECHNOLOGY
Graduate School, Silpakorn University
Academic Year 2017

Title	Application of microneedles and electroporation for antigen delivery to enhance the efficiency of skin vaccination
By	Boonnada PAMORNPATHOMKUL
Field of Study	(PHARMACEUTICAL TECHNOLOGY)
Advisor	Tanasait Ngawhirunpat

Graduate School Silpakorn University in Partial Fulfillment of the Requirements for the Doctor of Philosophy

..... Dean of graduate school
(Associate Professor Jurairat Nunthanid, Ph.D.)

Approved by

..... Chair person
(Associate Professor Dr. Theerasak Rojanarata)
..... Advisor
(Associate Professor Dr. Tanasait Ngawhirunpat)
..... Co Advisor
(Professor Dr. Praneet Opanasopit)
..... External Examiner
(Associate Professor Dr. Warisada Sila-on)

56354802 : Major (PHARMACEUTICAL TECHNOLOGY)
Keyword : Microneedle, Electroporation, Skin Vaccination, Ovalbumin, Plasmid DNA encoding ovalbumin, Nanocarrier

MISS BOONNADA PAMORNPATHOMKUL : APPLICATION OF MICRONEEDLES AND ELECTROPORATION FOR ANTIGEN DELIVERY TO ENHANCE THE EFFICIENCY OF SKIN VACCINATION THESIS ADVISOR : ASSOCIATE PROFESSOR DR. TANASAIT NGAWHIRUNPAT

In this study, the effect of different transdermal drug delivery methods, including solid microneedles (MNs) patch (poke and patch approach), electroporations (EPs) patch, solid MNs+EPs patch, and hollow MN (poke and flow approach) on ovalbumin (OVA) or plasmid DNA encoding ovalbumin (pOVA) were evaluated to enhance skin permeation and skin immunization. OVA and pOVA, hydrophilic macromolecules, were selected as model antigen because they can generate the immune responses, whereas they have characteristically poor skin permeation. The *in vivo* immune responses of OVA at different concentrations and pOVA complexes with different cationic nanocarriers using the best physical enhancement method compared with subcutaneous injection were also investigated. For enhancing of skin permeation and skin immunization of OVA, different types of MNs and doses of OVA antigen were used for *in vitro* skin permeation and *in vivo* immunization. *In vitro* skin permeation experiments and confocal laser scanning microscopy (CLSM) study revealed that hollow MN had a superior enhancing effect on skin permeation compared with a solid MNs patch and untreated skin by efficiently delivering ovalbumin-fluorescein conjugate (OVA-F) into the deep skin layers. The flux and cumulative amount of OVA-F at 8 h after administering with different types of MNs could be ranked as follows; high dose of OVA-F (500 μg) > medium dose (250 μg) > low dose (100 μg), moreover, the use of hollow MN showed a superior enhancing effect compared with the solid MNs patch. When the hollow MN was used for the delivery of OVA into the skin of BALB/c mice, it was capable of inducing a stronger immunoglobulin G (IgG) immune response than subcutaneous injection at the same antigen dose. IgG levels in the hollow MN group were 5.7, 11.6, and 13.3 times higher than those of the subcutaneous injection group for low, medium, and high doses, respectively. Furthermore, the mice immunized using the hollow MN showed no signs of skin infection or pinpoint bleeding. The results suggest that the hollow MN is an efficient device for delivering the optimal dose of antigen *via* the skin for successful immunization. For a combined approach of hollow MN and cationic nanocarriers for skin immunization with pOVA, the use of different types of MNs and nanocarriers for *in vitro* skin permeation and *in vivo* immunization of pOVA was investigated. *In vitro* skin permeation studies indicated that hollow MN had a superior enhancing effect on skin permeation compared with the combination of MNs and EPs patch, solid MNs patch, EPs patch, respectively. Upon using hollow MN combined with cationic nanocarriers for pOVA delivery, the skin permeation was higher than the delivery of naked pOVA, as evidenced by the increased flux of pOVA. When the hollow MN was used for the delivery of nanocarrier/pOVA complexes into the skin of mice, they induced a stronger IgG immune response than subcutaneous injection. Regarding to safety issues, immunization of mice with the hollow MN are safe. Accordingly, the hollow MN combined with a nanocarrier delivery system is a promising approach for delivering pOVA complexes to the skin for promoting successful skin immunization.

ACKNOWLEDGEMENTS

It would not have been possible to complete this dissertation without the help and support from every people around me. Firstly, I would like to express my sincere gratitude to my thesis advisor, Assoc. Prof. Dr. Tanasait Ngawhirunpat, for the continuous support of my Ph.D study and related research, for his motivation and immense knowledge. His guidance helped me in all the time of research and writing of this thesis. My sincere gratitude also goes to my thesis co-adviser, Prof. Dr. Praneet Opanasopit for her helpful support, invaluable suggestion, and kindness given to me during my study. I am very much indebted to both of them. I could not have imagined having a better advisor and co-advisor for my Ph.D study.

Besides my advisor, I would like to thank the rest of my thesis committee: Assoc. Prof. Dr. Theerasak Rojanarata and Assoc. Prof. Dr. Warisada Sila-on, for their insightful comments and encouragement, but also for the hard question which incented me to widen my research from various perspectives.

My sincere thanks also go to Prof. Ryan F. Donnelly, who provided me an opportunity to join their team as visiting researcher in his laboratory at School of Pharmacy, Queen's University Belfast, UK. I really appreciate his professional and excellent guidance and value everything I have learned from him. My special thanks are extended to the members of Ryan's lab for hugely contributing in my work and personal life. I also wish to thank my friends in Belfast for their helping and caring during my living in the UK.

My next gratitude and appreciation go to the Thailand Research Funds through the Royal Golden Jubilee Ph.D. Program and the National Vaccine Institute (Grant No. PHD/0232/2558), for financial support during my study as well as Faculty of Pharmacy, Silpakorn University for facility support and partial financial support.

My special thanks go to my friends and members of the Pharmaceutical Development of Green Innovation Group (PDGIG), especially Miss Areerut Sripattanaporn, Dr. Samarwadee Plianwong, Dr. Nanthida Wonglertnirant, Dr. Tittaya Suksamran, Dr. Jariya Kowapradit and Mr. Kritamorn Jitrangsri for valuable laboratory techniques and their support.

Last but not the least, I would like to give the greatest appreciation to my parents and my relatives for their spiritual supports, understanding, encouragement, and unconditional love in me, as always, for which my mere expression of thanks likewise does not suffice.

For any mistake or inadequate information that may still in this dissertation, certainly, the responsibility is entirely my own.

Boonnada PAMORNPATHOMKUL

TABLE OF CONTENTS

Page

LIST OF TABLES

Page

LIST OF FIGURES

Page

LIST OF ABBREVIATIONS

ACK lysing buffer	Ammonium-Chloride-Potassium lysing buffer
APCs	antigen presenting cell(s)
ANOVA	analysis of variance
°C	celcius
Cd	donor concentration of the formulations
CLSM	confocal laser scanning microscope
cm^3	cubic centimeter(s)
CO_2	carbon dioxide
CTL	cytolytic T lymphocyte(s)
Da	dalton
DF	dilution factor(s)
DMSO	dimethyl sulfoxide
DNA	deoxyribonucleic acid
dsDNA	double strand deoxyribonucleic acid
E.Coli	*Escherichia coli* DH5-α
ELISA	enzyme-linked immunosorbent assay
EP(s)	electroporation(s)
Eq.	equation
ER	enhancement ratio
et al.	*et alia* (Latin abbreviation of "andothers"; For references with more than two authors)
FBS	fetal bovine serum
10FBS/PBS	10 percent of fetal bovine serum in phosphate buffered saline
FD	fluorescein isothiocyanate-dextran
FDA	Food and Drug Administration
FITC	fluorescein isothiocyanate
h	hour(s)
HCl	hydrochloric acid
HeLa cells	human cervical cancer cell lines

HIV-1	human immunodeficiency virus type 1
HRP	horseradish peroxidase
H_2SO_4	sulfuric acid
HSV	herpes simplex virus malaria
i.e.	*id est* (Latin abbreviation); that is
i.d.	inner diameter
IFN-γ	interferon-gamma
IgG	Immunoglobulin G
IL-4	interleukin-4
J	steady-state flux
KCl	potassium chloride
kDa	kilodalton
kg	kilogram(s)
KH_2PO_4	potassium dihydrogen orthophosphate
Kp	permeability coefficient
kΩ	kiloohm
log P	log partition-coefficient
LTR	localized transport region(s)
m^2	square centimeter(s)
MEM	Minimum essential media
mg	milligram(s)
MHC	major histocompatibility complex
min	minute(s)
mL	milliliter(s)
mm	millimeter(s)
MN(s)	microneedle(s)
MNAE	MN array electrode chip
MOPS	3-(N-morpholino)propanesulfonic acid
ms	millisecond
MTT	3-(4,5-Dimethylthiazol-2-yl)-2,5-Diphenyltetrazolium Bromide
mV	millivolt(s)

MW	molecular weight
N	newton
NaCl	sodium chloride
$NaHCO_3$	sodium bicarbonate
NaOH	sodium hydroxide
ng	nanogram(s)
nm	nanometer(s)
N/P ratio	ratios of moles of the amine groups of cationic polymers to the phosphate groups of deoxyribonucleic acid
OD	optical density
o.d.	outer diameter
OVA	ovalbumin
OVA-F	ovalbumin-fluorescein conjugate
PAA	poly(amino acid)
PAMAM	polyamidoamine
PBS	phosphate buffered saline
pDNA	plasmid deoxyribonucleic acid
PEI	polyethylenimine
pH	potential of hydrogen
PLGA	poly(lactic-coglycolic) acid
pOVA	plasmid DNA encoding ovalbumin
PPI	polypropylenimine
rpm	revolutions per minute
RPMI-1640	Roswell Park Memorial Institute-1640
s	second
SC	*stratum corneum*
SDS	sodium dodecyl sulfate
solid MNs+EPs patch	combination of solid microneedles and electroporations patch
TAE	Tris-acetate-EDTA
TB	tuberculosis

TBE	Tris-Borate-EDTA
Th	T helper
TMB	3,3',5,5'-Tetramethylbenzidine
Tris Cl	Tris chloride
T20/PBS	Tween 20 in phosphate buffered saline
V	volt(s)
v/v	volume by volume
w/w	weight by weight
µA	microampere
µg	microgram(s)
µL	microliter(s)
µm	micrometer(s)
µs	microsecond
Ɛ	extinction coefficient
%	percentage(s)
γ	gamma
λ	lambda
θ	theta
®	registered trademark
™	trademark
×g	gravity at the Earth's surface

CHAPTER 1
INTRODUCTION

1.1 Statement and significance of the research problem

Vaccination is the most cost effective and successful approaches to prevent infectious diseases [1]. Vaccine should be safe, minimally invasive and induces a strong protective immune response. Despite the benefits of vaccination, however, subcutaneous or intramuscular vaccination requires medical staff and can cause pain and stress in vaccine recipients, especially for needle phobic patients. Moreover, healthcare professionals are often time needed to administer these shots, and as a result, are at high risk of needle stick injuries. Additionally, waste disposal and reuse of needles are important issues [2, 3].

Skin immunization is a promising alternative to the conventional intramuscular and subcutaneous injections. The skin is an ideal target tissue for vaccination due to the vaccine's targeting of high density antigen presenting cells (APCs) locating both Langerhans cells within the epidermis and dermal dendritic cells in the dermis. [4-6]. Nevertheless, the most significant challenge in skin immunization are the effective transfer of vaccine into the skin for inducing immunity response. The skin barrier function in the uppermost layer of the skin, *stratum corneum* (*SC*), is a major challenge for delivery vaccine through the skin. This outermost layer consists of corneocytes embedded in lipid-enriched matrix with an approximately 10-20 μm of thickness [7]. DNA vaccines are biological macromolecules, so they do not passively diffuse into skin, because only molecules that are smaller than 500 Da can directly diffuse or permeate through *SC* [8]. Currently, it is hypothesized that skin barrier disruption increases in the transcutaneous permeation of antigens and provides it more readily available to uptake by APCs. Moreover, disruption of skin barrier can stimulate the immune system, which is inducing the pro-inflammatory cytokines secretion by keratinocytes and resulting in dermal dendritic cell activation. According to these reasons, it is attractive to invent and develop useful techniques to overcome the skin barrier, *SC* [9-12].

The location and method of delivery is an important factor in the efficacy of DNA vaccination. Many publications have reported that intradermal injection could induce more immune responses than subcutaneous or intramuscular routes [13-16], because intramuscular and subcutaneous injection cannot effectively target the Langerhans cells and dermal dendritic cells in the skin. Although the intradermal injection is an effective route due to site of injection presence the high density of APCs, the big size of needle can cause pain and stress in vaccine recipients.

To overcome these problematics, the use of microneedles (MNs) for vaccination has been developed. MNs are very promising for the transdermal and intradermal delivery of drugs and vaccines. MNs comprise micron-sized needles with a typically less than 1 mm in length that can pierce the *SC* and upper layers of epidermis. Nevertheless, they do not penetrate through the deeper dermis layer where plenty of nerve ending are located, therefore, little or no pain caused. The strategy of MN involves use of micron-scaled needles to create temporary aqueous microchannels across the skin. These needles are beneficial because they are minimally invasive, mostly pain-free, reduce risk of infections, easy to use, inexpensive, and large scale production [17]. Many publications suggested that using MNs improves protective immunity and simplifies the process for skin vaccination [16, 18-20]. MN can be made of different kinds of materials, such as metals [21-23], silicon [24, 25], plastic [26], glass [27], biodegradable polymer [28-30], sugar [31-33] etc. They can be commonly classified into 4 types of MN; (i) solid MN (ii) drug-coated MN (iii) dissolving MN and (iv) hollow MN [17].

Recently, electroporation (EP) has been shown to successfully deliver different types of macromolecules regardless of their electrical characteristics [34]. EPs is the application of high voltage pulses within very short time (μs-ms) to generate structural rearrangement of the cell membrane resulting in creation of temporary porosity and providing a local driving force for ionic and molecular transport through the pores [35]. In addition, the combination of MN and EP, exhibits a synergistic of physical effect on macromolecules skin permeation. The synergistic effect causes by piercing the *SC* barrier using MNs, resulting in

creating large microchannels. Moreover, an electric current is applied to activate aqueous pore formation in the deeper layers of skin [36, 37].

DNA vaccination is a technique for inducing the immune system in the body to protect against diseases by injection with genetically engineered DNA, which is also called DNA vaccine. DNA vaccine is a novel vaccine technology based on purified plasmid preparations containing a gene encoding an antigen, and a promoter or terminator to trigger an immune response against a wide range of diseases. It is a promising new approach to express antigens *in vivo* for inducing desired immunity, including cytolytic T lymphocytes (CTL), T helper cells and antibodies. While conventional vaccines induce only humoral immune responses, these strategies have been less successful for prophylaxis against many current intruders such as human immunodeficiency virus type 1 (HIV-1), herpes simplex virus (HSV), malaria and tuberculosis (TB) that require a cellular immune response for protection [38-40]. DNA vaccines have been developed to overcome the limitation of traditional vaccines as they can induce cellular immune responses, improve vaccine stability, rapidly be produced in large-scale manufacturing by bacterial culture techniques [41], inexpensive and safe vaccines [42-44]. Many studies have shown the potential of these DNA vaccines in preventing different types of infectious diseases in preclinical stages such as influenza virus [41], rabies virus [45], malaria parasites [46] and mycobacterium tuberculosis [47]. Additionally, it is also used in immunotherapy to treat different types of cancer, allergies and autoimmune diseases.

To deliver DNA vaccine, it is difficult for delivering the naked nucleic acids directly through plasma membrane due to size and physicochemical properties of nucleic acids. Many vectors have been developed for delivering DNA effectively into target cells and protecting it from nuclease degradation. The gene delivery system is divided in two major groups, viral and non-viral system. Although viral system generally has high transfection efficiency, it has several limitations, including carcinogenesis, unpredictable of immunogenicity, inflammation, plasmid size restriction and difficulty of vector production [48, 49]. Non-viral gene system has been developed to avoid these limitations. It shows

desirable properties over viral vectors such as low immune response, less toxicity, unrestricted plasmid size, easy to synthesize and able to modify the function group which targeting to cell [50].

Over the years, non-viral vectors made of polymers [51], lipids [52], dendrimer [53], peptides [54] and nanoparticle-based compounds [55] have been increasingly receiving attention as carriers for *in vitro* and *in vivo* gene delivery. They activate cellular uptake of DNA by complexing nucleic acids into small structure and generating positively charged particles on surfaces via electrostatic interaction. In addition, cationic carriers are able to protect DNA degradation from nuclease and facilitating the endocytosis and endo-lysosomal escape [56, 57].

In this study, ovalbumin (OVA) and plasmid DNA encoding OVA (pOVA), a hydrophilic macromolecules with a high molecular weight (MW), were selected as our model antigen because they can generate the immune response, whereas they have characteristically poor skin permeation [18]. Three commercially transfection reagents, including linear 25 kDa polyethylenimine (PEI), Lipofectamine™ 2000 and SuperFect® were used as the carriers for gene transfection. The particle size and surface charge of pOVA complexes with different transfection reagents were investigated at different weight ratios (w/w). In addition, the transfection efficiency of pOVA complexes with different carriers in the human cervical cancer cell lines (HeLa cells) was investigated at the different weight ratios. The weight ratios of each three commercially carrier that provide the highest transfection efficiency reagents were selected for *in vitro* and *in vivo* study. Moreover, the effect of differentdelivery methods, i.e., solid MNs patch (poke and patch approach), EPs patch, solid MNs+EPs patch, and hollow MN on OVA or pOVA were evaluated in skin permeation. The physical enhancement method resulting in a superior enhancing effect of skin permeation was selected to investigate the effects of carriers complexes with pOVA in *in vivo*. The *in vivo* immune responses of OVA at different concentrations and pOVA complexes with different carriers using the best physical enhancement method compared with subcutaneous injection were evaluated.

1.2 Aims and objectives

1. To evaluate the potential of physical enhancement methods, including solid MNs patch, EPs patch, solid MNs + EPs patch and hollow MN for facilitating the transport of antigens through the skin barrier.
2. To examine the immune responses of antigen alone or antigen complexes with transfection reagents using the best physical enhancement method compare to subcutaneous injection.

1.3 The research hypothesis

1. Physical enhancement methods, including solid MNs patch, EPs patch, solid MNs + EPs patch and hollow MN can enhance the transportation of antigens through the skin barrier.
2. The immune responses of antigen alone or antigen complexes with different carrier using the best physical enhancement method are higher than subcutaneous injection.

CHAPTER 2
LITERATURE REVIEW

2.1 The structure and function of skin

The skin is the largest organ of the body weighing more than 10% of the total body mass with an area of approximately 2 m^2. The skin provides the protection between the body and the external environment, which is composed of two layers, the epidermis or outer skin, and dermis or inner skin, each with a distinct function (Figure 1).

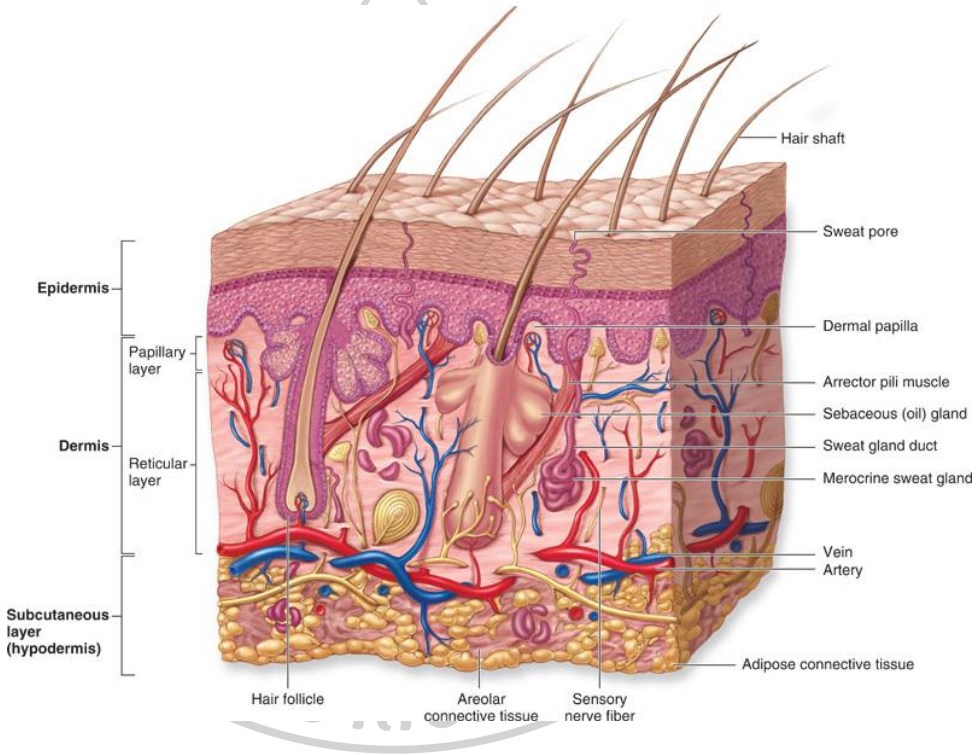

Figure 1 Schematic diagram representing a cross-section of skin showing the skin layers and appendage, including hair follicles and ducts [58].

2.1.1 Epidermis

The epidermis is the outer skin layer that forms a barrier to the outer environment. This barrier prevents the loss of water and the admission of foreign materials. It keeps in fluids, i.e. water and blood, and holds safe minerals, vitamins and heat. The epidermis can be classified into 5 layers indicating steps of keratinocyte differentiation including, *stratum basale*,

stratum spinosum, *stratum granulosum*, *stratum lucidum*, and *stratum corneum* (*SC*) (Figure 2).

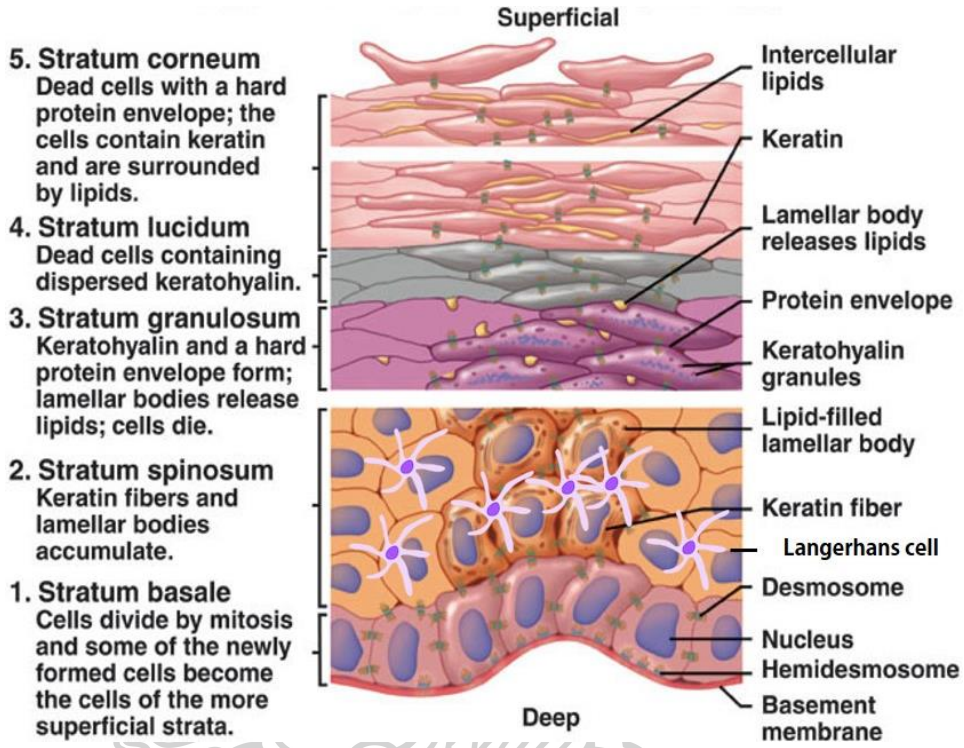

Figure 2 Schematic diagram representing a cross-section of skin showing the different cell layers of epidermis [58].

Considering from inside to outside of the body, first layer, *stratum basale* or basal layer is active growing due to the continual renewal of the epidermis. Proliferation of the stem cells in the *stratum basale* creates new keratinocytes which then propel existing cells towards the surface. Each cell divides under control of a very sophisticated biochemical system. This cycle is being able to replace itself completely in 45-74 days.

The upper layer is *stratum spinosum*. Keratinocytes in this layer maintain a complete set of organelles and membrane-coating granules (or lamellar bodies). The next layer is *stratum granulosum* or granular layer which more flattened keratinocytes are still viable. Lamellar bodies are also found in the upper part of granular cells.

The next layer is *stratum lucidum*, the transitional layer before becoming the *SC*, the cellular organelles are collapsed leaving keratin filaments in the granular layer. The lamellar bodies integrate with cell membrane and release their lipid contents into the intercellular space. These contents can arrange into multilamellar domain.

The *stratum corneum* (*SC*), generally known as the "horny layer", is the non-living specialized uppermost layer of the epidermis that provides a foremost barrier over the body. The whole thickness of epidermis is 0.04-1.5 mm. While the *SC* is very thin (15-150 μm thick), it is also a very tough little tissue. Keratin is a protein that makes up the bulk of the *SC*. Keratin is a helical-shaped protein made up of building blocks, known as polypeptides. The proteins are resistant to water and many chemicals. Hence, it is a complex structure that provides the protections over the skin. The keratins are formed and arranged into cells known as "corneocytes" that are attached together with "lipids". The *SC* can be thought of as a brick wall, with the rich of protein corneocytes as the bricks and the lipids functioning as the mortar (Figure 3). The two major groups of lipids are polar lipids and nonpolar lipids. Polar lipids have an electrical charge, i.e. phospholipids, glycolipids and cholesterol. Nonpolar lipids have no electrical charge. Examples of this types of lipid are triglycerides, squalene and waxes [59]. *SC* is a rate-limiting step to skin permeation as it provides a formidable barrier to permeation [60].

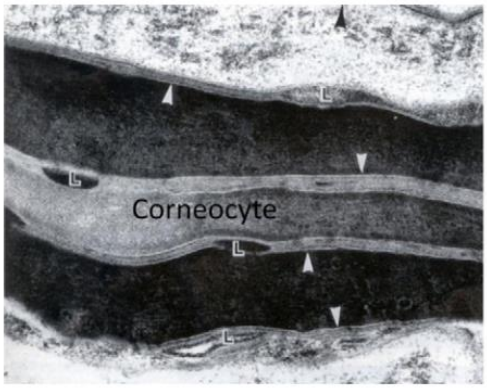

Figure 3 Structure of the SC; corneocytes as brick wall and intercellular lipids (arrowheads) as mortar [61].

2.1.2 Dermis

The dermis is located underlying the epidermis. It accounts for more than 90% of the skin mass. The thickness of dermis is about 1-4 mm. The dermis layer is divided into the papillary dermis and reticular dermis. The upper dermis, the papillary dermis is indirect contact with the undulating epidermis. It contains small and loose fibers. In the papillary dermis, blood vessel is contained to provide nutrition, and lymphatic vessels is contained to drain the wastes of the body. The thicker main part of the dermis, reticular dermis is located under the papillary dermis. It is a fibrous, filamentous and amorphous connective tissue composed of fibroblasts, elastin, collagen and ground substance [62-64]. The main function of reticular dermis is to support the epidermis and embed structures including, blood vessels, nerves, hair follicles, sweat and sebaceous glands, as well as the skin elasticity [65]. Different to the epidermis, dermis tissue is highly vascularised.

2.2 Skin Penetration pathways

Penetration pathways can be divided into 3 pathways including, (a) intercellular, (b) transappendageal pathway, and (c) transcellular as shown in Figure 4. Generally, molecules transverse the *SC* by a combination of these three routes. However, the appendageal pathway does not seem to be important to skin

permeation because it only covers about 0.1% of the skin surface. However, this pathway may facilitate the penetration of ions and large hydrophilic molecules. The relative contributions of these pathways to the total flux will depend on the physicochemical characteristics of the drugs. An additional potential pathway (d) that enabling the large molecular transport via micron-sized holes in skin created by MNs (see Section 2.5) is also displayed in Figure 4.

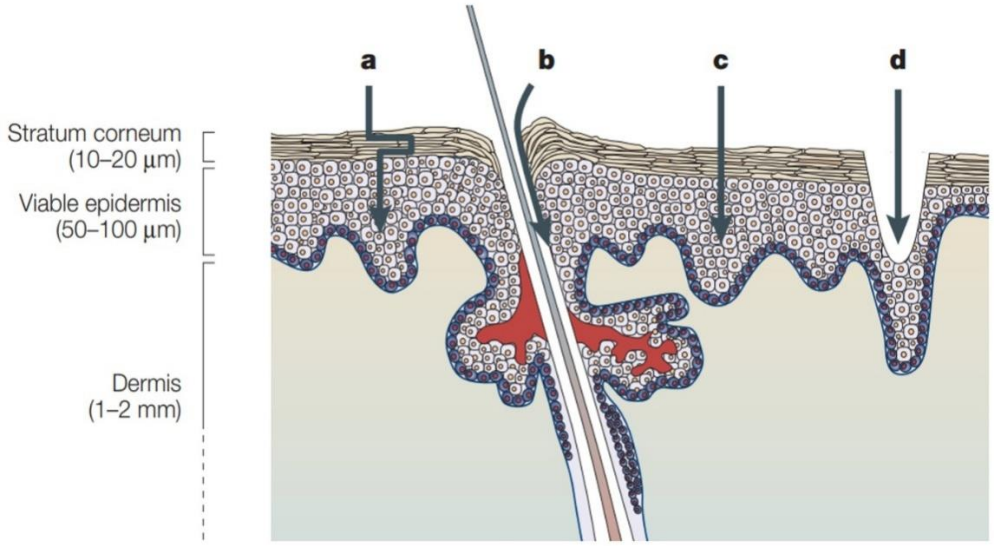

Figure 4 Schematic Skin penetration pathways (a) intercellular, (b) transappendageal, (c) transcellular and, (d) the micron-scaled holes that can be created by MN [66]**.**

2.2.1 Intercellular pathway

The intercellular pathway is a highly tortuous with continuous way through the intercellular lipid domain. The drug diffuses through the continuous lipid matrix present between the corneocytes. It is now accepted that most molecules penetrate through skin via this route [67]. This might be assumed that molecules penetrating via the intercellular route partition into and diffuse through the keratinocyte. For this reason, the intercellular pathway has been the targeted route for improving transdermal drug delivery by manipulating the solubility in the lipid bilayers or using various enhancing techniques aim to disrupt, possibly in the presence of a chemical enhancer, or bypass its well-organized molecular architecture [68].

2.2.2 Transappendageal pathway

The transappendageal route or the shunt route includes penetration across the sweat glands and the hair follicles with their associated sebaceous glands. Because of the low fractional appendageal area (approximately 0.1% of the total skin surface), this pathway usually contributes negligibly to steady state drug flux [67]. Transappendageal route is an important for ionics and hydrophilic molecules that poorly penetrate the intact *SC*. Moreover, these routes are also important for delivering vesicular compounds into the skin and for targeting to the pilosebaceous units.

2.2.3 Transcellular pathway

The transcellular pathway is a pathway that molecules permeate across the *SC* through the keratinized cells. The transportation faces numerous repeating obstacles because the keratinocytes are bound to a lipid envelope that attaches to the intercellular multiply bilayer lipid domain. Therefore, the molecules require not only partitioning into and diffusion through the hydrated keratin but also into and across the intercellular lipids. It is obvious that the multiple partitioning and diffusion processes between hydrophilic and hydrophobic environments are generally undesirable for many drugs. The rate-limiting obstacle for permeation *via* this pathway remains the multiply intercellular lipid bilayers [69]. High-voltage EP has been shown to enhance drug delivery via the transcellular route by disrupting the lipid bilayers [66].

2.3 Basic mathematical principles in skin permeation

All compounds are thought to transfer the skin by a passive diffusion mechanism. It is possible to apply the Fick's laws of diffusion to the data obtained from the skin transport experiments. This law is used to predict the rate at which substances penetrate the skin. The Fick's first laws, equation 1 (Eq. 1), is to presume that the rate of transfer of drug permeating through a unit area is proportional to the concentration gradient;

$$J = -D\frac{\partial C}{\partial x} \quad \text{Eq. 1}$$

Where J is the rate of transfer per unit area, $\partial C/\partial x$ is the concentration gradient, C is the concentration of diffusing substance, x is the space coordinate, and D is the diffusion coefficient.

In real situations steady-state conditions are improbable to be established during the permeation of drugs across the skin. Hence, Fick's second law is used to analyse the flux and concentration profiles as it can be derived from Eq. 1:

$$\frac{\partial C}{\partial t} = D\frac{\partial^2 C}{\partial x^2} \quad \text{Eq. 2}$$

Where t is time. Thus, the rate of change in concentration with time at a given point in a system is proportional to the rate of change in the concentration gradient at that point [70, 71].

2.4 Skin permeation enhancement methods

The achievement of dermatological drugs for systemic or local-targeted drug delivery rely on the potential of the drug to permeate the skin in sufficient amount to achieve the desired therapeutic effect [72]. However, the wide range of drugs that can be self-delivered in therapeutic doses via the skin is limited by an effective foremost skin barrier of the *SC*. To overcome this problem, several permeation enhancement methods were developed to defeat the skin barrier function, which are categorized based on strategies (Figures 5) [67, 73]. Drug permeation across the skin could be enhanced by adapting one or more of the following mechanisms; (1) disruption the structure of *SC* lipid, (2) interaction with intercellular protein and (3) improvement of partition of the drug into the *SC*. According to the proposes of this study, many mechanisms were combined to investigate the synergistic effect. Permeation enhancement methods showing in Figure 5 can be classified roughly into two categories based on type of penetration enhancers, including the chemical penetration enhancers and the physical penetration enhancers.

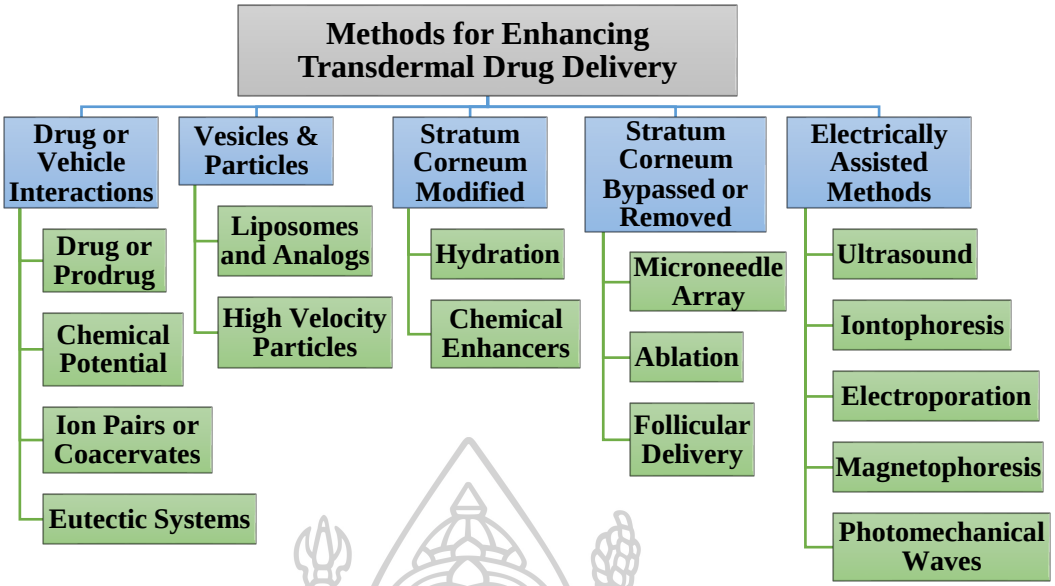

Figure 5 An example of methods for enhancing transdermal drug delivery [67, 73]

2.4.1 Chemical penetration enhancers

Chemical penetration enhancers are compounds or materials that help promoting drugs diffusion through epidermis and/or dermis. The ideal chemical penetration enhancers should have the following these characteristics;

- Pharmacologically and chemically inert and chemically stable
- A high degree of potency with specific activity and reversible effects on the skin properties
- Predictable and reproducible on the activity and duration of action
- Compatible with all components in formulation
- Rapid onset and unidirectionally
- Non-irritating, non-sensitizing, non-allergenic, non-toxic and non-comedogenic
- Odorless, tasteless, colorless, and cosmetically acceptable

Publications reveal several classes of chemical substances that are useful to enhance the permeation of molecules across the skin [74, 75].

2.4.2 Physical penetration enhancers

The unpredictable of the chemical penetration enhancement makes the use of the physical approaches more attractive. Table 1 shows the comparative efficacy of interesting physical enhancement methods, including increase in drug delivery, sustained manner, pain sensation and complexity.

Table 1 Comparison of different approaches to enhance transdermal delivery [66]

Delivery method	Increased transport	Sustained delivery	No pain/ irritation	Low cost/ complexity
Hypodermic needle	+++	++	+	+++
Chemical enhancer	+	+++	++	+++
Iontophoresis	++	+++	+++	+
Electroporation	++	+++	++	+
Ultrasound	++	+++	+++	+
Microneedles (MNs)	++	+++	+++	+
Thermal poration	++	+++	+++	+

+ Low efficacy, ++ Moderate efficacy, +++ high efficacy.

The finding of an inexpensive, safe and reliable technique for transdermal drug delivery without causing painful, led to the development of MNs.

2.5 Microneedles

Microneedles (MNs) are a drug delivery system that is currently used for intradermal and/or transdermal a disparate range of vaccines and drugs delivery. This platform is increasingly interesting for vaccine delivery, as it has proven to be useful for a wide range of vaccines, including diphtheria [76], influenza [16, 77-79], alzheimer's disease [80], hepatitis B [19, 81], HIV [82], Japanese encephalitis [83], Polio [20, 84], Rabies virus [85] and Rotavirus [86]. MN arrays comprise needles typically less than 1 mm in length that can pierce the outer layer

of skin, the *SC*, with minimal invasive the skin. The needles were fabricated in micron-sized which are sufficiently large to deliver drug effectively, but small and short enough to avoid causing pain, as they do not puncture the nerve endings in deeper dermis layer.

2.5.1 Advantages and disadvantages of MN arrays

Table 2 Advantages and disadvantages of using MNs as a physical penetration enhancer [87, 88].

Advantages	- MNs can be fabricated to be long enough to penetrate the *SC* but short enough not to puncture nerve endings. - The technique is minimally invasive and painless administration due to increased patient compliance. - Be able to deliver macromolecules. - Targeting the specific skin area for desired drug delivery. - Micron-sized of MNs could provide highly targeted drug administration to individual cells. - Ease of administration and no need health professional. - Faster healing at injection site than with a hypodermic needle. - Decrease of microbial penetration as compared with a hypodermic needle due to reduced chances of infection. - Enhanced drug efficacy may result in dose reduction and frequent dosage is not required. - Avoidance of first-pass metabolism

	- Bypasses the gastrointestinal tract - Enable rapid drug delivery by coupling with an electrically controlled micropump - Drug can be administered at constant rate for a longer period.
Disadvantages	- Penetration depth could vary due to the thickness variation of the *SC* and other skin layers between individuals. - The external environment, such as hydration of the skin, could affect delivery - Careful use of device may be needed.

2.5.2 Types of MN arrays

MN arrays for delivering vaccines and other pharmaceutical compounds to the skin in minimally invasive way can be commonly classified into 4 types of MN depending on delivery techniques. The limitations, advantages, and disadvantages of each approach are summarized in Table 3.

Table 3 Main features of the different approaches of drug delivery by MNs [17].

Drug delivery approach	Rate-limiting step of drug delivery	Main advantages	Main disadvantages
Poke and Flow	Solvent flow through microneedle bore or at higher volume; Pressure resistance of the skin	Rate of drug delivery can be regulated e.g. via a pump, if solvent flow is rate-limiting Delivery of high volume Integration into lab-on-a-chip systems possible Precise dosing No or limited reformulation of the drug needed	Risk of clogging Impaired microneedle strength Increased risk of leakage for arrays More complex device
Poke and Patch	Diffusion of the drug through the micropores generated by microneedles into the skin, dependent on the pore size and number, and concentration of the drug in the patch	Technically simple No pump or encapsulation/coating process is required Extended release	Low fraction of the drug may be delivered (only of interest for drugs with high potency) Two-step administration process No precise dosing Reformulation of the drug needed
Poke and Release	Dissolving microneedles: dissolution rate Porous microneedles: diffusion of drug from the pores	Small amount of drug may be lost during the encapsulation/absorption process No patch or pump is required No sharp waste (dissolving microneedles) Precise dosing	Impaired microneedle strength (increased fracture and deformation of microneedle geometry) Often less sharp microneedles (decreased penetration ability) Small dose Reformulation of the drug needed
Coat and Poke	Detachment of the coating from microneedle surface or, at thicker coatings: Dissolution rate of the coating	Microneedle strength is retained after coating No patch or pump is required Precise dosing	Requires an efficient coating procedure Small dose Reformulation of the drug needed Reduction of microneedle sharpness/penetration ability

2.5.2.1 Poke and patch approach

To deliver the drug with "poke and patch approach", solid MNs can be used as a pre-treatment in order to first create pore in the skin. Subsequently the MNs are removed, transient microconduits are created in the skin. Then, the drug formulation is applied onto the site of MN application (Figure 6). For this technique, it is important that the micro-sized pores stay open during the drug application period [89]. The drug formulations can be either a conventional formulation, such as cream, ointment, gel, lotion, or transdermal patch [73]. The movement of drug through these microchannels occurs via passive diffusion [17, 90, 91]. Passive transport of drugs through the micropores does not always lead to a high bioavailability of drugs; therefore, this approach has been combined with iontophoresis [92, 93] or EP [36] to further enhance the drug delivery through skin compared to each technique alone.

Solid MN can be fabricated out of various materials such as silicon [94-96], stainless steel [97-99]. Stainless steel displays many advantages, such as providing sufficient mechanical strength, easily cutting using a laser, and FDA-approved safety [100]. Various techniques have been used for fabricating solid MN. For instance, silicon MN with the length of 150 μm was made using a reactive ion etching techniques. The benefit of this technique was that modify the length of needles can be readily modified as required [94].

2.5.2.2 Coat and poke approach

Coat and poke approach involves coating the solid MN arrays (normally made from stainless steel) with an aqueous drug solution using a dip-coating or spraying method and then inserting them into skin. The drug coating is dissolved and diffused into the skin, after which the MN is removed (Figure 6). Coated MN can reduce the step of administration as compared to poke and patch approach, however, the amount of drug coated is limited which is less than 1 mg per coating [44, 73, 101, 102]. Hence, this approach is suitable for very potent drugs or vaccines [17]. The

coating solution usually contains drug, viscosity agent, surfactant, solvent and stabilizing agent [103]. The stability of formulation coated was improved by adding a stabilizing agent, i.e. sugar, in order to protect the drug from degradation during drying process and storage [104]. This approach is also required an extensive optimization for uniform coating.

2.5.2.3 Poke and release approach

Poke and release approach also called "dissolving MN" are fabricated from biodegradable or water-soluble polymers. Drugs or compounds have been encapsulated within the MNs and their drug payload are delivered intradermally when in contact with skin interstitial fluid, with the drug then diffusing to its target tissue within skin or being systemically absorbed (Figure 6) [17, 105]. Dissolving MN arrays can be made of different kinds of materials, such as maltose [106], poly(vinylpyrrolidone) (PVP) [107], starch and gelatin [108], chondroitin sulfate [109], dextran and hyaluronic acid [110]. The advantage of dissolving MN over solid or coated MN is no biohazardous sharp waste after the application and accurate dosing, as only small amounts of the drug are lost during the production process [17]. However, it needs time to completely dissolve, at least 5 min [6, 111].

2.5.2.4 Poke and flow approach

The last type of MN, hollow MNs, deliver drugs via the "poke and flow" approach. Hollow MN containing a hollow bore are similar hypodermic needles, however, the size of hollow MN is much smaller than that of hypodermic needles. Hollow MN permits pressure-driven flow of a liquid formulation through microconduits created by the needles (Figure 6). According to reducing the size of needles into micron scale, pain and tissue trauma occur following hypodermic needle injection was reduced greatly [103]. In addition, an advantage of hollow MN over solid MNs is the possibility to facilitate force-driven fluid flow resulting in increased rates of drug delivery [17, 90, 112-114]. Although, the rate and pressure

for delivering liquid formulation can be adjustable, i.e. making a rapid bolus injection or a slow diffusion, only the formulation in the form of liquid can be applied, solid formulation cannot be used without reconstitution. As a result, the drugs which are unstable in a liquid phase, miss the opportunity to use with hollow MN.

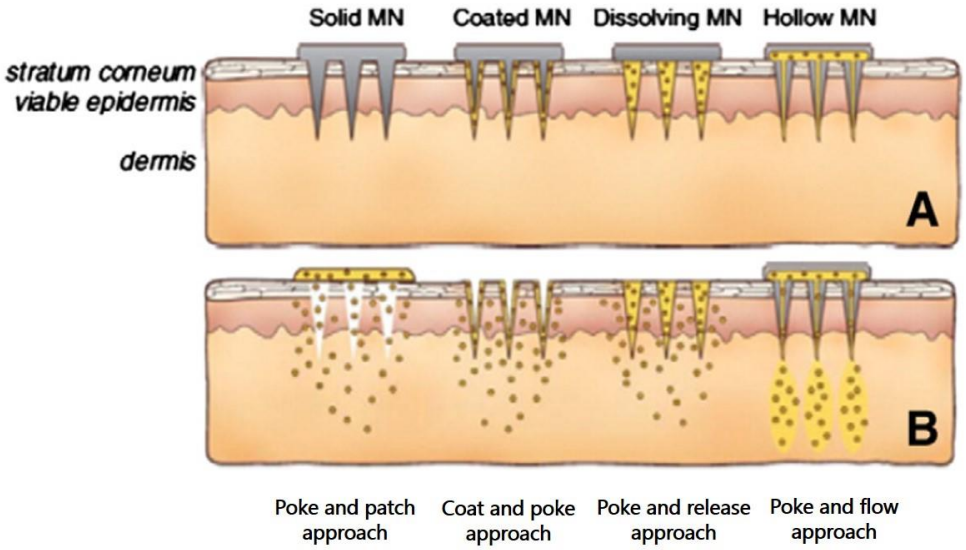

Figure 6 Types of methods for skin drug delivery by MNs. MNs are applied into the skin (A) and then used for drug delivery (B). Solid MNs are used as a pre-treatment, afterward the drug from a formulation can diffuse through microconduits in skin (poke and patch approach). Drug-coated MNs are inserted into the skin, the drug coating dissolves off the MNs in the skin interstitial fluids (coat and poke approach). Drug incorporating MNs are made of biodegradable polymers encapsulating drug that is released in the skin upon MN dissolution (poke and release approach). Hollow MNs are used to inject liquid formulations directly into the skin (poke and flow approach) [115].

2.5.3 Sterility of MNs

If the MN product needs an approval from Food and Drug Administration (FDA), sterility of the MN tends to be required for regulatory approval. This can be done by various methods such as ethylene

oxide gas sterilization, γ-irradiation, and aseptic technique using ethanol [101]. For example, MN made out of stainless steel was firstly assembled into a patch under a laminar flow hood followed by ethylene oxide gas sterilization [116]. The γ-irradiation method may cause oxidation, leading to instability of product which could be reduced by optimizing the irradiation dose and temperature during sterilization process [117].

2.5.4 Safety of MNs

An injury of the skin could cause local or even systemic infection as it allows microorganisms to enter the skin. Several factors affected the risk of infection, including the size, number and depth of breaches, the amounts and nature of microorganisms, and the individual susceptibility of the patient. Indeed, infection rarely occurs during common experiences of minor abrasion, such as routine shaving. According to several studies, MN administration causes minimal risk of infection [118-121]. Prausnitz *et al*. reported that no MN-related infections and no serious adverse events in more than 7,000 human subjects observed following an application of MN devices [122].

2.5.5 Pain

Pain affects patient compliance and the perception of safety. Initial studies reported that using sharp-tipped MNs in 50-200 μm length by human subjects were generally regarded as painless methods [123, 124]. Many studies found that MN length affects pain, an example, a threefold increase in length of MN (from 500 to 1,500 μm) resulted in a sevenfold of pain score increased. Increasing the number of needles from 5 to 50 increased the pain score just two-fold. Varying MN width, thickness, and tip angle did not have a significant effect on pain [98].

2.5.6 Bleeding

The epidermis is lack of blood vessels, and superficial capillary bed is located in the upper dermis close to the dermal-epidermal junction

[125]. Accordingly, MNs could breach capillaries due to penetrating the skin deeper than approximately 100 μm. However, most studies both in animal and human subjects have not found bleeding after MN applications [90]. Generally, bleeding has not found in human subjects from needles sizes ranging from 500 to 1,000 μm. However, a small droplet of blood leave sometimes on the skin after the application of solid MNs with 1,500 μm of the needles height [98].

2.5.7 Skin irritation

No significant skin irritation, including erythema and edema observed in several studies [95, 97, 118, 126-128]. After intradermal vaccinations, skin response has been found in the clinic [13]. Following primary OVA immunization, the average total skin score was just 0.3 at 24 h for all treatment groups (maximum score of 8). However, after booster immunization, the score increased to 2.3 at 24 h [121]. Although mild and transient, these results revealed an immune-mediated skin response. The skin responses might cause insignificant discomfort at the site of vaccination.

2.5.8 Skin vaccination using MNs

MNs provide advantages to deliver vaccines into the skin effectively. The concept of vaccination via the skin has been used since ancient. The word “vaccination” was defined as a result of Edward Jenner’s demonstration that scratching cowpox virus into the skin could prevent smallpox virus infection [129]. Thing not known by the ancient knowledge is the fact that the skin is a very strong immune activating tissue due to the plenty of potent APCs, including Langerhans cells in epidermis layer and dermal dendritic cells in dermis layer [130, 131].

The first device developed comprises of hundreds of needles protruding a few hundred microns from a basement of MN, which are used to pierce holes in the outer layer of skin [132, 133]. Transdermal

permeability has been increased approximately four orders of magnitude following pierced the skin. MN has been shown to deliver macromolecules, including proteins, genetic materials and latex particles of viral dimensions *in vitro* and *in vivo* [97, 128, 134]. MN make microconduits in the skin, which is larger than the size of the protein and vaccines. However, it should be small enough to avoid painful in clinical studies [98, 123, 124].

Intradermal delivery using MNs revealed in many studies to be effective and reduce the dose of antigen required. MNs have not raised safety concerns according to small size and the inert materials of needles used. In addition, MNs provide other advantages over conventional injection and other delivery methods that may also be effective and safe. For instance, the MN patches should facilitate vaccine by patients themselves. The size of MNs is very small, which is easy to storage and rapidly distribute to patients. Combined with the mass production with inexpensive costs, these advantages suggest that MNs are an attractive device for vaccination. Many studies have shown the potential of MN platforms in preventing different types of infectious diseases such as diphtheria [76], influenza [16, 77-79], alzheimer's disease [80], hepatitis B [19, 81], HIV [82], Japanese encephalitis [83], Polio [20, 84], Rabies virus [85] and Rotavirus [86]. Overall, it is obviously seen that MNs can provide a safe and effective method for vaccinations.

2.6 Electroporation (EP)

EP is the application of short, high-voltage electrical pulses (50 to 1,500 V) to enhance transdermal drug delivery. Electrical parameters used are typically 10 to 100 volts (normally higher than 50 V) for microseconds (μs) to milliseconds (ms) with intervals between pulses of a few seconds to a minute. EP of mammalian skin causes reversible phase transition and fluidization of intercellular lipid bilayer in the *SC*, leading to the creation of transient pores. This is due to joule heating and localized temperature that rises over 60°C. The temporary

aqueous pathways are created for enhancing the transport of hydrophilic compounds and macromolecules [35, 101, 135].

2.6.1 Pathways of molecules transport following EP

2.6.1.1 New aqueous pathways or electropores

EP of cell membranes induces a rapid and reversible increase in transmembrane transport and structural changes in membrane barrier [136]. High voltage application created pores or aqueous pathways. Generally, the pores are small (<10 nm), sparse (0.1% of surface area), and short lived between μs to s [136-138].

2.6.1.2 Localization of transport

The transportation of drug following EP application occurs via highly localized transport regions (LTR) of the *SC* which covering between 0.02% and 25% of the skin surface [35]. Size and number of LTR depend on pulsing protocol. The size increases with an increase in pulse duration and number of pulses. Diameter of LTR ranges between 0.1 mm for short pulse and 0.2-2.5 mm for long pulse. In contrast, voltage will affect the number of LTR. Short duration and high voltage pulse will increase the number of LTR more than long duration with medium voltage [35, 139].

2.6.2 Mechanism of molecules transport following EP

The transport of molecules through transiently permeabilized skin by EP results from three mechanisms as follows;

2.6.2.1 Electrophoretic movement

Electrophoretic movement only occurs during pulsing, caused by the electrically driving force. This mechanism is an important for charged molecules [35]. Prausnitz *et al*. revealed that the transport of calcein (-4 charge) was dropped with the reversed electrode polarity which was opposed to the electrophoretic direction [136].

2.6.2.2 Diffusion

Transportation of molecules through the skin highly permeabilized by EP is also due to enhanced passive diffusion. According to publication of Vanbever *et al.*, the transport of mannitol (neutral molecule) after pulsing was similar to that both during and after pulsing. This could be due to prolonged permeabilization of the skin caused by EP after pulsing promoted the molecular transport [140].

2.6.2.3 Electroosmosis

The contribution of electroosmosis during high voltage pulses is low. The short time of current application limits the role of electroosmosis in drug transport by skin EP [35]. Vanbever *et al.* hypothesized that if electroosmosis played an important role in the molecular transport, the higher transport would be obtained when the anode was in the donor compartment. However, the results showed that whether anode or cathode was in the donor compartment, the cumulative amount of mannitol was not different. This confirmed that electroosmosis might have little effect on the molecular transport [140].

2.6.3 Parameters effecting drug delivery by EP

Various parameters of EP can affect and allow control of transdermal drug delivery. These parameters are summarized in Table 4.

2.6.3.1 Electrical parameters: Pulse voltage, pulse number and pulse length

Flux rate increases when electrical conditions strengthen: when the pulse voltage, the number and the duration are increased, the transdermal drug delivery increased [35]. According to these factors, Prausnitz *et al.* reported that the transport of calcein (-4 charge) increased when an increased in pulse voltage from 55 V to 165 V [136]. In addition, the transport of metoprolol increased with an increased in pulse voltage (from 24 V to 250 V) and duration (from 80 ms to 700 ms) [141].

2.6.3.2 Physicochemical properties of drug

2.6.3.2.1 Charge of drug

Charged of drugs can highly pass through electroporated skin since electrophoretic movement is the principal mechanism for skin EP. Hence, an increase in charge of drugs in the formulation results in an increase in the drug transport. Regardless of MW of permeant, at the same condition, the flux of polar molecules could be ranked as follow; calcein (-4 charge) > Lucifer (-2 charge) > erythrosin derivative (-1 charge). Given, pKa of drug molecules as well as pH of formulation are important factors to molecular transport across electroporated skin [136].

2.6.3.2.2 Molecular weight (MW)

MW influences the drug transport through electroporated skin. The higher MW, the lower skin permeation is observed. For example, the cumulative amount of fluorescein isothiocyanate (FITC) and fluorescein isothiocyanate-dextran (FD) across hairless rat skin using 100 V and 150 ms of duration, was decreased with an increase in MW as follow; FITC (MW = 389.4 Da) > FD-4.4 (MW = 4.4 kDa) > FD-12 (MW = 12 kDa) > FD-38 (MW = 38 kDa). It could also be noted that skin penetration of FD which have their MW up to 38kDa could be achieved using EP [34].

2.6.3.2.3 Lipophilicity

EP can enhance the transport of both lipophilic and hydrophilic drugs. However, an increase in lipophilicity of drug such as making prodrug, tends to decrease the enhancement ratio of drug. Sung *et al.* reported that the enhancement ratio of drug decreased with an increased in lipophilicity of prodrug as determined by log P, as follows; nalbuphine (log P = 0.17) > nalbuphine propionate (log P = 1.05) > nalbuphine enanthate (log P = 1.94) [142].

2.6.3.3 Formulation of drug reservoir

2.6.3.3.1 Competitive ions and ionization (pH)

The ions present in the drug reservoir, such as buffer ions, counter ions, ions from the skin, compete with the drug needed to be delivered for the electrophoretic movement. The higher the drug concentration, the higher the transport. The selection and optimization of the reservoir composition must take into account the drug ionization (pH), the pH shift induced with inert electrodes (presence of a buffer required), the presence of competitive ions (ionic strength and composition of the solution) and the conductivity (high conductivity compared to the skin). The optimization of the composition of the reservoir formulation is an important parameter to enhance drug transport [35].

2.6.3.3.2 Viscosity

An increase of the viscosity of the drug solution resulted in decrease of drug transport by EP [141].

Table 4 Parameters affecting drug transport by skin electroporation [35]

Parameters	Increase in	Effect
Electrical parameters	Pulse voltage	+
	Pulse number	+
	Pulse length	+
Physicochemical properties of drug	Charge	+
	Molecular weight	-
	Lipophilicity	-
Formulation of drug reservoir	Competitive ions	-
	Ionization (pH)	+
	Viscosity	-

+, Positive effect; -, negative effect.

2.6.4 Nucleic acid delivery using EP

Nucleic acid delivery without any physical enhancers and cationic nanocarriers has been undesired, with low gene transfection. Cationic nanocarriers and physical methods has been used to enhance gene expression. EP has found to be a successful physical method not only for transdermal drug delivery, but has also been used as an effective gene delivery system both *in vitro* and *in vivo* [143, 144]. It provides physical force to transfer macromolecules, such as DNA and proteins, and drugs from extracellular compartments into cells with temporary increased cell membrane permeability. The electric pulse generated by EP is applied to form small pores across the cell membrane. These pores are open in short periods of time approximately a few seconds to minutes, without causing any significant damage to the cell membrane. During this periods of time, macromolecules or drugs can be easily delivered into the cells by local electrophoretic effect [145-148]. EP is one of the most widely used approaches for nucleic acid delivery because of its flexibility and versatility with different cell types.

Many publications found that EP can increase gene expression by 100- to 1000-fold when compared to naked pDNA injection [149, 150]. Moreover, DNA vaccination using EP provides a promising approach for the prevention of infectious diseases. Several studies revealed that EP has adjuvant-like properties when combined with pDNA injection [151, 152]. The efficiency of nucleic acid delivery by EP is influenced by several physical parameters, as described above, and biological factors, including DNA concentration, DNA conformation, cell size and shape [153].

2.6.5 Safety of transdermal delivery by skin EP

An effect of EP on the skin is an importance issue in the clinical acceptability of transdermal drug delivery using EP. Many studies reported that alterations of the skin following high voltage pulses are mild and

reversible. However, contractions of muscle are usually occurred [154, 155]. An excitation of nerves and muscles was observed during current applied of EP on the skin. Increase in pulse voltage, duration and rate, tends to enhance sensation, such as itching, tingling, pricking, muscle contractions and little pain [156].

2.7 Combinations of enhancing methods

Although many methods have been shown to enhance the transdermal drug delivery, their combinations have been widely studied and found to enhance the transdermal transport more effectively than each of them alone. According to the combination of MN arrays and EP, MNs create additional aqueous pores in the skin through which the applied current is conducted. They can be combined EPs, which are utilized as electrical driving forces to improve drug transport.

Yan *et al*. used the combination of MN and EP (as in-skin EP) as a pre-treatment. A synergistic effect on FD-4 skin permeation compared to MN alone or conventional EP alone was observed. This study showed an approximately 140-fold enhancement in FD-4 delivery over control samples, and an almost 7-fold enhancement over EP alone [36]. Choi *et al*. founded that electrically active MN arrays successfully inserted into human skin and that both red blood cells and DU145 human prostate cancer cells can be efficiently electroporated [157]. Wei *et al*. found that a flexible MN array electrode chip (MNAE) enables efficient low-voltage EP (35 V) and good coverage of the tissue surface together. The MNAE chip provides a promising approach for highly localized and minimally invasive method to deliver nucleic acid *in vivo* for gene therapy or DNA vaccination [158].

2.8 DNA vaccination

Administration of genetically engineered DNA may be considered the next-generation of scientific development for prophylactic vaccines or for therapy. Different to conventional protein or polysaccharide based vaccines, DNA vaccines contain plasmids encoding the vaccine antigen, and a strong promoter/terminator to make the gene express in mammalian cells [159]. DNA vaccination is a new

approach for preventing against diseases by injection with genetically engineered DNA to induce immunological responses. The idea of DNA vaccination has several advantages over traditional vaccination methods, including ability to induce all types of desired immunity (cytolytic T lymphocytes (CTL), T helper cells and antibodies), absence of any infectious agent because it does not contain whole viruses or bacteria, long term persistence of immunogenicity, stability of vaccine for storage and shipping and easy in large-scale production. However, limitation of DNA vaccine is possibility of inducing antibody against DNA and may have a relatively poor immunogenicity [160, 161].

2.8.1 Mechanism of action of DNA vaccines

There are three mechanisms have been found to induce the immune responses of DNA vaccines: (1) Somatic cells (e.g. myocytes or keratinocytes) present DNA-encoded antigens through major histocompatibility complex (MHC) class I pathway to $CD8^+$ T cells; (2) Immunization by DNA vaccine occurs via direct transfection of professional APCs such as dendritic cells; and (3) Cross-priming results from transfected somatic cells being phagocytosed by professional APCs which then present the antigens to T cells. Muscle cells (myocytes) are inefficient to present antigens via MHC class I due to lack of the costimulatory signals in conjunction with MHC class I molecules that are required for the expansion of naïve APCs $CD8^+$ T cells [38, 159]. Therefore, the second and the third mechanism may be more important for DNA vaccinations [159]. It was found that professional APCs play an important role in the induction of immune responses by presenting short peptides on the cell surface of MHC class I molecules, following direct transfection or cross-presentation, and MHC class II molecules after antigen capture and processing within the endocytic pathway. The level of immune responses depends on several factors, including the method of vaccination, vaccine regimen and exist of adjuvants. In addition, the efficacy of DNA vaccination also relies on the interaction between

peptides and APCs, or lymphocytes, which are the important cells that mediate immunity at the cellular level [38].

2.8.2 Cationic nanocarriers used in DNA vaccine delivery

The ability of non-professional APCs to present antigens on the MHC class II molecules for inducing $CD4^+$ T helper cells is very limited. Strategies for DNA vaccination have been developed to deliver DNA vaccines to professional APCs, such as dendritic cells. Skin and lymph nodes contain high density of professional APCs than muscle, and therefore are useful tissues in which to target dendritic cells. According to immunization using naked DNA vaccine, it was found that inefficient, with only a small amount of DNA vaccine being taken up by cells and expressed. An alternative approach is to deliver DNA vaccines in coated nanocarriers, which protect DNA from degradation and increase phagocytic uptake by professional APCs [162]. Synthetic nanocarriers are more commonly used to protect pDNA from degradation, which include compaction of negatively charged nucleic acid by polycationic carriers, belonging to cationic polymers and cationic liposome.

Nanocarriers are nanomaterial being used as a drug and gene delivery to the target tissues. Nanocarriers are currently being studied for use in wide range of drug and macromolecules delivery. Cationic nanocarriers/DNA complexes used in gene transfer are relied on the hypothesis that the cationic complexes adsorb more effectively to the anionic plasma cell membranes via electrostatic interactions. The electrostatic interaction between positively charged groups on nanocarriers (cationic polymers or cationic lipids) and the negatively charged phosphate backbone of the nucleic acid leading to positive complexes called polyplex or lipoplex, respectively [163]. The mechanisms of gene delivery using cationic nanocarriers involve the following steps [164]: cationic polymers or liposomes combined with anionic DNA in aqueous buffer solution to form polyplex or lipoplex nanoparticles. The positively charged complexes

bind to the negatively charged cell surface of mammalian cells by non-specific, electrostatic interactions [165-167], and then enter cells by endocytosis. Inside the endosome compartments, the pH of the endosome decreases from pH 7 to 5.5 and part of the complexes escapes from endosomes into the cytosol. The lipoplexes or polyplexes then dissociate and release pDNA into the nucleus [168].

2.8.2.1 Cationic polymers

Cationic polymers have been widely used as non-viral vectors for gene delivery. These polymers form particulate complexes with pDNA, generally termed as polyplexes. They contain a hydrophilic moiety and are completely soluble in water. They can condense pDNA molecules to a small size. This is an important for gene delivery as their help improving transfection efficacy [169]. The structures of cationic polymers are very different, including linear polymers such as chitosan and PEI, branched polymers such as branched PEI, circle-like polymers such as cyclodextrin, network (crosslinked) type polymers such as crosslinked poly(amino acid) (PAA), and dendrimers. Examples of these cationic polymers include PEI, poly(lactic-coglycolic) acid (PLGA), chitosan and dendrimers.

2.8.2.1.1 Polyethylenimine (PEI)

Among various cationic polymers, PEI has been one of the most potent non-viral polymeric for gene delivery due to its pH buffering capacity [170], which is superior transfection efficiency in different types of cells. PEI contains 25% of primary amine, 50% of secondary amine and 25% of tertiary amines, which is two-thirds of the amines are protonated in a physiological pH. The unprotonated amines with different pKa values confer a buffering effect over a wide range of pH. The buffering property provides an opportunity for PEI to escape from the endosome avoiding lysosomal degradation (proton sponge effect), which is an essential step to achieve high gene transfection [171]. PEI exists both linear and branched PEI. Branched PEI showed stronger electrostatic interaction with pDNA

than linear PEI, resulting in higher DNA condensing capability and zeta potential and smaller particle size [172]. Corresponding to the results from Dunlap *et al*., linear PEI is less effective compared with the branched PEI for similar MW [173]. The low MW linear or branched PEI has low cytotoxicity compared to their high MW PEI. God bey *et al*. found that transfection efficiency of PEI complexes increases when MW increased from 600 to 70,000 Da [174]. The optimal MW of PEI for complexes formation is generally between 5 and 25 kDa [175, 176]. Choosakoonkriang *et al*. found that 25 kDa of branched and linear PEI complexes showed the highest transfection efficiencies at an N/P ratio of 6:1 in COS-7 and CHO-K1 cells [177]. Apart from MW, the degree branching of PEI has been found to affect complex formation and stability.

2.8.2.1.2 Dendrimers

Polycationic dendrimers are a particular class of cationic polymers. The term "dendrimer" is derived from its tree-like branching structure. Dendrimers consist of an alkyl-diamine central core and tertiary amine branched [53]. Dendrimers interact with cell membranes by creating small, transient pores near the contact site. The ability of dendrimer to form pores relies on the charge density and generation of dendrimers. The higher in charge density or generation increases the transfection efficiency [53]. Nevertheless, large molecules with high generation commonly increase cytotoxicity [178]. Generally, dendrimers showed lower toxicity than that of PEI [179]. The most popularly used dendrimers are poly(amidoamine) (PAMAM) and poly(propylenimine) (PPI) dendrimers.

PAMAM dendrimers are hyperbranched polymers (Figure 7), which are now one of the most important types in dendrimer family due to safe, nonimmunogenic, and effective for delivering genetic material into cells [180]. PAMAM dendrimers are synthesized starting from a central core (ethylenediamine or ammonia) and esterizing the core with methylacrylate following amidation of the ester with ethylenediamine

[181]. PAMAM dendrimers can compact pDNA with electrostatic interaction to form nano-sized complexes for the cell uptake and release DNA in the cell *via* "sponge effect" [182, 183]. Buffering occurs when the low pH inside the endosome promotes the uptake and accumulation of choride ions, resulting in endosomal swelling/lysis and release of the nucleic acid [184]. Many studies have been reported in improving characteristics of PAMAM for decreasing cytotoxicity [185, 186]. Therefore, fractured dendrimers were developed to help compact and release nucleic acid easier upon pH alteration. Currently, Superfect®, a fractured PAMAM dendrimer is commercially available as a standard for *in vivo* gene transfection studies [187]. Main properties for potential use of dendrimer in nucleic acid delivery are defined by the high density of terminal groups. These provide many attachment sites for conjugation of targeting moieties, and determine the molecular mass, which is important for the ability to isolate other molecules inside the dendrimer core [53].

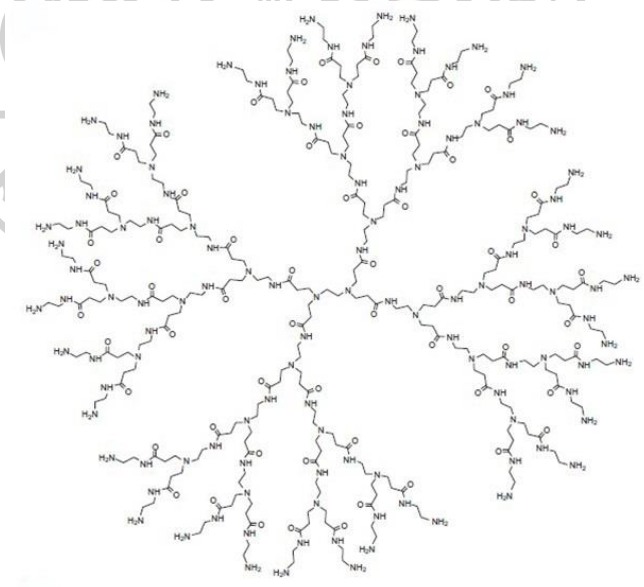

Figure 7 Structural characteristics of polyamidoamine (PAMAM) dendrimers [180]

2.8.2.2 Cationic lipids

Cationic lipids are amphiphilic molecules with positively charged made of three basic components, a cationic head group (usually amino groups), a linker connecting the polar head group with the non-polar tail and a hydrophobic tail (contain alkyl chains or cholesterol) (Figure 8 and 9a) [181]. The cationic head group electrostatically interacts with nucleic acids and condenses into nanoparticles called “lipoplexes” (Figure 9) [188]. It is hypothesized that lipoplexes entering cells via endocytosis followed by destabilization of endosomal membrane and flip-flop reorganization of phospholipids, which is resulting in the release of DNA into the cytoplasm [188]. Therefore, the positively charge of cationic liposomes improves cells uptake by macrophages and dendritic cells and consequently, the uptake of the antigen and its presentation to responder cells [189-192].

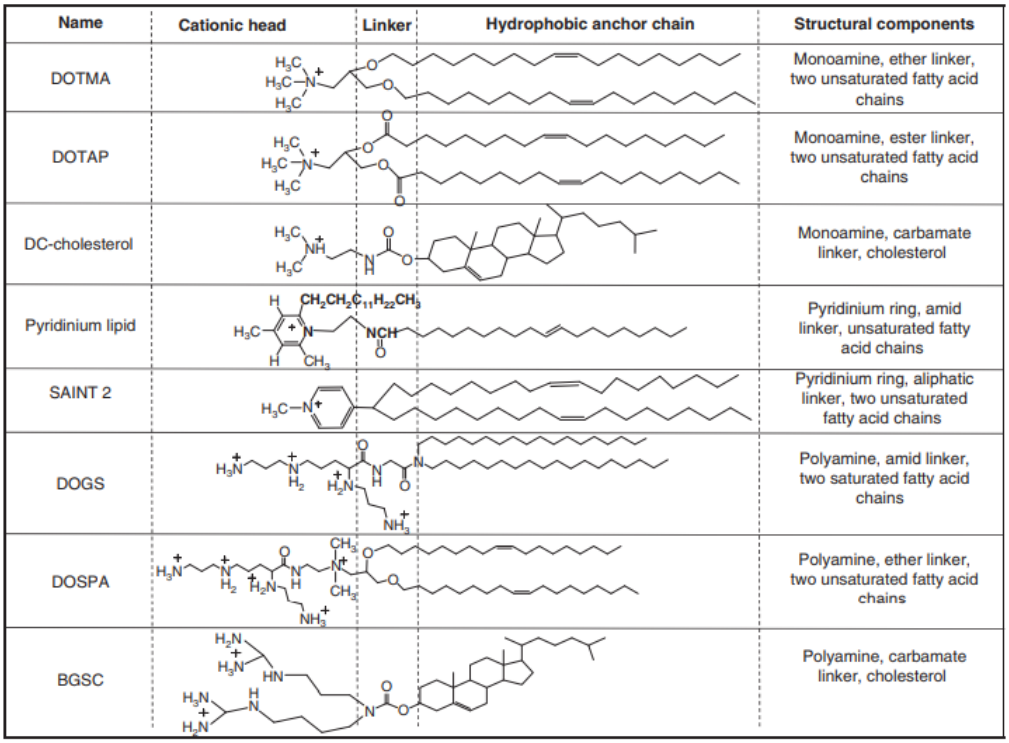

Figure 8 The structures of commonly used cationic lipids [181]

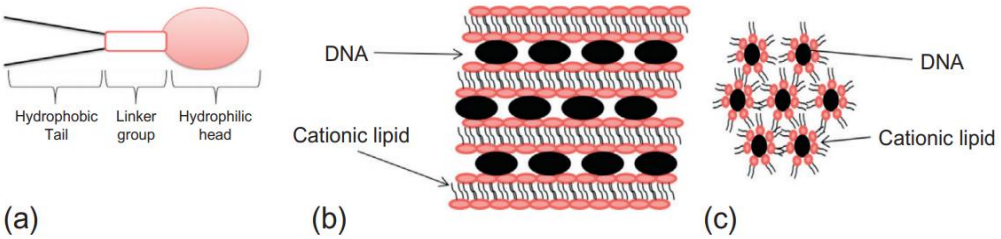

Figure 9 (a) Basic components of cationic lipids, (b) schematic representation of lamellar or inverted phase and (c) generally structure of lipoplexes [188]

Cationic liposomes interact with nucleic acid to form lipoplexes via a multistep mechanism. DOSPA (Figure 8) have been developed as a very effective cationic liposome in improving cellular uptake of nucleic acids for nucleic acid delivery [193]. It is a commercially available called Lipofectamine™. In addition, cationic liposomes destabilize endosomes to deliver antigens into the cytoplasm of the APCs and the eliciting of $CD8^+$cytotoxic lymphocytes responses [194]. According to these reasons, cationic lipid formulations are widely used *in vivo* for immunization studies. Transfection efficiency of cationic lipid bases on many factors including, degree of positive charge from head group and the distance between hydrophilic head and hydrophobic tail groups. Generally, cationic lipid with multiple cationic head group and long distance between head and tail groups has a higher transfection efficiency compared to single-charged head group and short distance between head and tail groups, respectively. The limitation of cationic liposomes, is high protein binding efficiency, resulting in rapidly cleared from plasma [188].

CHAPTER 3
MATERIALS AND METHODS

3.1 Material

- Albumin from chicken egg white (ovalbumin; OVA, Grade V, MW 44.3 kDa) (Sigma-Aldrich, St. Louis, U.S.A.)
- Monoclonal anti-chicken egg albumin antibody produced in mouse (Sigma-Aldrich, St. Louis, U.S.A.)
- Rabbit anti-goat IgG peroxidase (Sigma-Aldrich, St. Louis, U.S.A.)
- Ovalbumin-fluorescein conjugate (OVA-F, MW 45 kDa; Molecular Probes Inc., Oregon, U.S.A.)
- 3,3',5,5'-Tetramethylbenzidine (TMB) (Zymed, Invitrogen,San Francisco, U.S.A.)
- Tween 20 (BDH, Poole dorset, England)
- Dimethyl sulfoxide (DMSO; Sigma-Aldrich, St. Louis, U.S.A.)
- Sulfuric acid (H_2SO_4, 98%w/w) (BDH, Poole dorset, England)
- The goat anti-mouse IgG horseradish peroxidase (HRP) conjugate (ZyMax™ Grade, Invitrogen, New York, U.S.A.)
- Sodium bicarbonate ($NaHCO_3$) (Fisher Scientific, Leicestershire, England)
- Plasmid DNA encoding ovalbumin (pOVA; Addgene plasmid #31598, Massachusetts, U.S.A.)
- Plasmid Maxi Kits (Qiagen®, California, U.S.A.)
- Branched polyethylenimine (PEI, MW 25,000) (Aldrich, Wisconsin, U.S.A.)
- Lipofectamine™ 2000 (Invitrogen, Carlsbad, U.S.A.)
- Superfect (Qiagen®, California, U.S.A.)
- Quant-iT™ PicoGreen®dsDNA reagent and kits (Molecular Probes, Inc., Oregon, U.S.A.)
- Human cervical cancer cell lines (HeLa cells) (American Type Culture Collection, Maryland, U.S.A.)
- Fetal bovine serum (FBS) (GIBCO™, New York, U.S.A.)
- Minimum essential media (MEM) (GIBCO™, New York, U.S.A.)

- L-glutamine (GIBCO™, New York, USA)
- MEM non-essential amino acids (100X) (GIBCO™, New York, U.S.A.)
- Kanamycin (GIBCO™, New York, U.S.A.)
- RPMI-1640(Roswell Park Memorial Institute-1640) medium (GIBCO™, New York, U.S.A.)
- ACK (Ammonium-Chloride-Potassium) lysing buffer (GIBCO™, New York, U.S.A.)
- Potassium dihydrogen orthophosphate (KH_2PO_4, Ajax Finechem, Australia)
- Sodium chloride (NaCl; QReC Chemical, New Zealand)
- Potassium chloride (KCl; Ajax Finechem, Australia)
- Sodium hydroxide (NaOH; Ajax Finechem, Australia)
- 37% Hydrochloric acid (HCl; QReC Chemical, New Zealand)
- High-sensitive enzyme-linked immunosorbent assay (ELISA) kits for ovalbumin (Biomatik, Ontario, Canada).
- Mouse IFN-γ Platinum ELISA kits (eBioscience®, California, U.S.A.)
- Mouse IL-4 High SensitivityELISA kits (eBioscience®, California, U.S.A.)
- All other chemicals were of molecular biology quality

3.2 Equipments

- Pulse generator (ECM 830 Electro Cell Manipulator; BTX, California, U.S.A.)
- Inverted Zeiss LSM 510 META confocal microscope (Carl Zeiss, Jena, Germany)
- Fluorescence spectrophotometer (RF 5300PC; Shimadzu, Kyoto, Japan)
- Fluoroskan Ascent™ Microplate Fluorometer (Massachusettes, U.S.A)
- Zetasizer Nano ZS (Malvern Instruments Ltd., Malvern, UK)
- Centrifuge (Sorvall® Biofuge Stratos)
- Stereo zoom microscopes (SMZ-171 series, Motic®, Hong Kong)
- Digital multimeter (Fluke 177; Everett, Washington, U.S.A.)
- Hollow MN (33-gauge hypodermic needle (i.d., 0.20 mm) connected to a 27-gauge hypodermic needle (i.d., 0.22 mm; o.d., 0.40 mm) (Nanopass™, Terumo Co., Tokyo, Japan)

- Acupuncture needle (0.25×30 mm) (DongBang Acupuncture Inc., Chung Nam, Korea)
- Silicone sheet; thickness 2 mm
- Copper wire; surface area 0.5 mm^2
- Suction Catheter (diameter 2.67 mm, length 50 cm; Suzhou Yudu Medical, China)
- Thermo-regulated water bath
- Franz diffusion cell; volume of receiver 6 mL
- Magnetic stirrer and magnetic bar
- Micropipette (2-20 μL, 20-200 μL, 100-1,000 μL, 1-5 mL)
- Micropipette tips (Corning®, Corning Incorporated, New York, U.S.A.)
- pH meter (Horiba compact-B212)
- Parafilm (Bemis®, Wisconsin, U.S.A.)
- Vortex mixer (VX100, Labnet)
- Microcentrifuge tube 1.7 mL; Costar® tubes (Corning®, Corning Incorporated, New York, U.S.A.)
- Analytical balances (Satorious CP224S, Scientific promotion Co., Ltd.)
- Autoclave (Model: LS-2D; Scientific promotion Co., Ltd.)
- Cell culture flask, 25 cm^3, 75 cm^3 (Corning®, Corning Incorporated, New York, U.S.A.)
- Centrifuge (Sorvall® Biofuge Stratos)
- Conical centrifuge tube (15, 50 mL) (Corning®, Corning Incorporated, New York, U.S.A.)
- Electronic pipette controller (Powerpette Plus; Bio-Active Co., Ltd.)
- Fluorescence microscope (Model: GFP-B, wavelengths: excitation filter 480/40 and emission filter 535/50)
- Gel electrophoresis apparatus (MyRUN intelligent electrophoresis unit, Cosmobio Co., Ltd., Japan)
- GelDoc system (Multi Genus Bio-imaging system, Syngene™)
- GeneRay UV-Photometer (Biometra® $\lambda_{260/280}$ nm)
- Hot air oven

- Humid CO_2 Incubator (37°C, 95% RH, 5% CO_2) (HERA Cell 240 Hereaus)
- Laminar air flow (BIO-II-A)
- Microplate reader (Universal Microplate Analyzer, Model AOPUS01 and AI53601, Packard Bio-Science, Connecticut, U.S.A.)
- Electronic multichannel pipette with 8 channel aspiration manifold 20-200 µL (Eppendorf, Hamburg, Germany)
- UV cabinet
- UV spectrophotometer (NanoVue™, GE Healthcare, UK)
- Vacuum filtration pump and filter set (Sartorius BORO 3.3 Goettingen, Germany)
- Filter membrane, 0.22 micron (Sartorius AG. 37070 Goettingen, Germany)
- Flat clear-bottom, 24 well plate (Corning®, Corning Incorporated, New York, U.S.A.)
- Flat clear-bottom, 48 well plate (Corning®, Corning Incorporated, New York, U.S.A.)
- Flat clear-bottom, 96 well plate (Nunc MaxiSorp®, Thermo Fisher Scientific Inc., New York, U.S.A.)
- Black clear-bottom, 96 well plate (Corning®, Corning Incorporated, New York, U.S.A.)
- Hypodermic needle 27 gauge×1/2 inches (Terumo Co., Tokyo, Japan)
- Glass syringe 100 µL (Hamilton®, Nevada, U.S.A.)
- Cell Strainers (Corning Falcon™, New York, U.S.A.)
- Stopwatch
- Adhesive tape
- Medical scissor
- Fine forceps
- Freezer/refrigerator at -20°C and -80°C
- Aluminium foil
- Thermometer
- Glass slide and cover slip
- Gloves

3.3 Methods

3.3.1 Fabrication of the solid MNs patch

Acupuncture needles (32 gauges, 0.25×30 mm) were cut and punctured into a silicone sheet (15×15×2 mm) vertically [37]. To anchor the needles in the silicone sheet, the other ends of the acupuncture needles were bent to obtain a perpendicular shape. The tips of the acupuncture needles extended out of the sheet approximately 900 μm (Figure 10A). The MN patch comprised 5×5 needles, with a center-to-center distance of 2.5 mm. To assure that the needles remained stationary, an adhesive tape was then attached to the MN patch. The MN patch was imaged under stereo zoom microscopes to confirm the length of needles (Figure 10B-C).

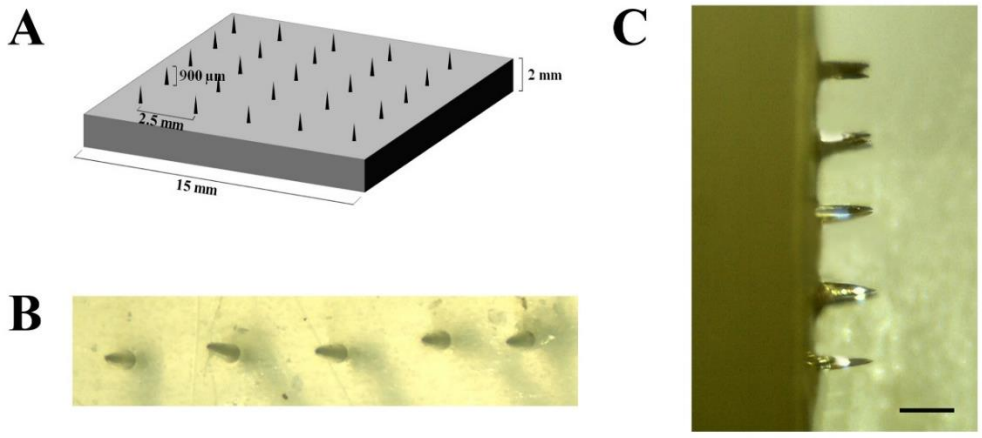

Figure 10 (A) Schematic representation of a solid MNs patch, (B) top-down view of a solid MNs (0.5X) and (C) side view, each needle with a height of approximately 900 μm (bar = 1 mm).

3.3.2 Fabrication of the combination of the solid MNs and EPs (MNs + EPs) patch and EPs patch

To investigate the combinatorial effect of the MNs + EPs patch, the needles were prepared as described above. Nevertheless, the copper wires, the positive and negative line, were inserted under the perpendicular part of the needle before fixing the needles with the silicone sheet so that the

MNs+EPs array could be used as an electrode in the EP experiments (Figure 11). To determine the effect of EPs alone and to avoid the effect of the MNs array, the tip of the needles was cut and filed until dull; these needles are referred as blunted MNs (Figure 12A and B) and were used to prepare the blunted-MN arrays following a method similar to that used to prepare the MNs+EPs patch.

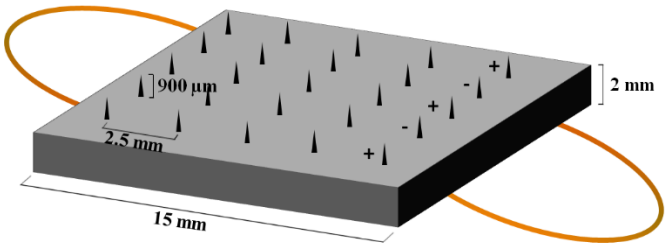

Figure 11 Schematic representation of the combined solid MNs and EPs patch

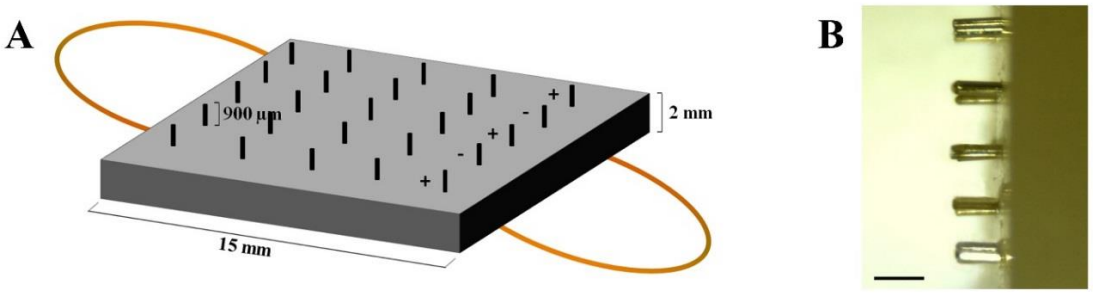

Figure 12 (A) Schematic representation of an EPs patch and (B) Photographs (0.5X) an EPs patch, each with a blunted array as an electrode

3.3.3 Preparation of Hollow MN

The hollow MN was assured to a triangular shape silicone sheet to fix an angle of insertion (θ) of 40° and constant insertion depth of approximately 300 µm in the skin tissue (Figure 13). The hollow MN was then connected to a Hamilton® glass syringe, volume 100 µL, to attain intradermal injection.

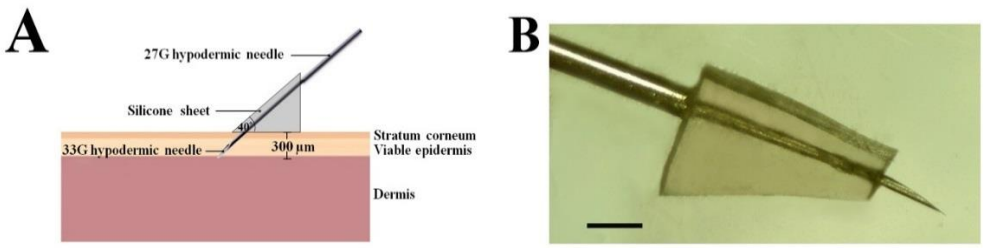

Figure 13 (A)Schematic representation of a hollow MN and (B) photographs (1X) of a hollow MN (bar = 1 mm).

3.3.4 Preparation of skin

Female Sprague Dawley rats, 5-6 weeks old, were obtained from the National Laboratory Animal Center, Mahidol University, Thailand. All animal studies were approved by the ethics committee for the use of laboratory animals, Faculty of Pharmacy, Silpakorn University (Approval Number: 002/2015). All of the animal experiments were conducted in accordance with the Animals for Scientific Purposes Act, 2015, provided by the Animal Care and Use Committee of National Research Council of Thailand. All rats were acclimatised to laboratory conditions for 7 days. The rats were anesthesia with sodium pentobarbital (100 mg/kg) by intraperitoneal injection. Before the collection of the dorsal skin, the hair of rat was fine shaved. The full-thickness skin was excised from the dorsal region of the rats. The subcutaneous and connective tissues were carefully removed from the skin using scissor. The skin was then washed with phosphate buffered saline (PBS; pH 7.4), wrapped in aluminium foil and stored at -20°C. The skin sample was thawed in PBS (pH 7.4) at room temperature for 1 h immediately prior to use.

Before starting an experiment, the integrity of skin membrane was determined by measurement an electrical resistance a multimeter with Ag and Ag/AgCl electrodes when < 80 µA of electric current was applied through the skin sample. The electrical resistance of skin was calculated using the voltage and current readings. The selection criterion of rat skin

samples with intact barrier function was skin electrical resistance ≥ 3 kΩ [195].

3.3.5 Effect of MNs and doses of OVA on skin permeation and skin immunization

3.3.5.1 *In vitro* skin permeation study

Delivery of OVA-F across the skin were examined using a vertical Franz diffusion cell. The skin was obtained as described above. The prepared skin sample was placed between the donor and the receptor compartments with the *SC* upward the donor compartment, and the cell was affixed using clamps. The receptor compartment was filled with 6 mL of degassed PBS (pH 7.4) and continuously stirred at 400 rpm using a magnetic stirrer to maintain constant stirring of the receptor solution. To achieve occlusive condition, the top of the donor compartment was then covered with Parafilm® sheet. The temperature of the system was controlled at 32 ± 1ºC using a circulating water jacket. To determine the cumulative permeation profiles, a 500 µL of sample solution was collect at designated time points: 0.5, 1, 2, 4, 6 and 8 h, followed by replacement with fresh PBS to maintain a constant volume. The skin used for this experiment can be divided into three groups, as follows: 1) untreated skin, 2) skin treated with a solid MNs patch, and 3) skin treated with a hollow MN.

For untreated skin, OVA-F at doses of 100 µg (low dose), 250 µg (medium dose), 500 µg (high dose), and 0 µg (without OVA-F) in PBS was added in the donor compartment.

For skin treated with the solid MNs patch, solid MNs patch was applied perpendicularly onto the skin. A plastic container filled with water was placed on the solid MNs patch to provide force of 10 N per patch for 2 min [37]. The amount of OVA-F added into the donor compartment was 100, 250, or 500 µg.

For the hollow MN group, OVA-F 100, 250, or 500 μg was directly delivered into the skin using hollow MN. It was manually injected by applying gentle pressure at a plunger of syringe. The volume of OVA-F delivered into the skin was kept constant at 100 μL with a single needle.

Quantification of OVA-F was carried out using fluorescence spectrophotometry with an excitation wavelength of 494 nm and emission wavelength of 520 nm. The sample solutions of untreated skin at designated time points: 0.5, 1, 2, 4, 6 and 8 h were used as controls. The cumulative amounts of OVA-F permeated across the skins were plotted against time. From the slope of the linear portion of the plot, the steady-state flux was acquired. The skin permeation of OVA-F was calculated using a mathematical model based on Fick's law of diffusion;

$$K_p = J / C_d \qquad \text{Eq. 3}$$

where K_p is the permeability coefficient, J is the steady-state flux, and C_d is the donor concentration of the formulations.

The enhancement ratio (ER) was calculated as follow;

$$ER = \frac{Flux\ of\ different\ conditions}{Flux\ of\ untreated\ skin\ with\ 100\ \mu g\ of\ OVA{-}F} \qquad \text{Eq. 4}$$

3.3.5.2 Accumulation of OVA-F in full-thickness skin

The accumulation of OVA-F in full-thickness skin was also evaluated. After the *in vitro* skin permeation study, skin samples were washed with PBS (pH 7.4). A piece of skin was then carefully placed on a glass slide with the *SC* facing upward and examined using the inverted Zeiss LSM 510 META confocal microscope (10X) of equipped with a green helium-neon laser at an excitation wavelength of 543 nm. The OVA-F across the skin was measured using Carl Zeiss AIM Version 3.2 Application Software.

3.3.5.3 *In vivo* immunization study

Female BALB/c mice (6-8 weeks old) were purchased from the National Laboratory Animal Center, Mahidol University, Thailand. All of the animal experiments were conducted in accordance with the Animals for Scientific Purposes Act, 2015, provided by the Animal Care and Use Committee of National Research Council of Thailand. Mice were acclimatised to laboratory conditions (25 ± 2°C) for 7 days. The mice (n=6 per group) were divided into seven groups as described in Table 5. The mice in all groups were immunized on days 0 and 14.

Table 5 OVA immunization groups for the *in vivo* study in mice

Mice groups	Formulation	Route of administration
Naïve	100 µL of sterile normal saline	Subcutaneous injection
Hollow MN 1	100 µg of OVA in PBS, pH 7.4	Hollow MN
Hollow MN 2	250 µg of OVA in PBS, pH 7.4	Hollow MN
Hollow MN 3	500 µg of OVA in PBS, pH 7.4	Hollow MN
Subcutaneous 1	100 µg of OVA in PBS, pH 7.4	Subcutaneous injection
Subcutaneous 2	250 µg of OVA in PBS, pH 7.4	Subcutaneous injection
Subcutaneous 3	500 µg of OVA in PBS, pH 7.4	Subcutaneous injection

For vaccination using the hollow MN, mice were anesthetized with sodium pentobarbital (40 mg/kg) by intraperitoneal injections. The dorsal skin of mice was shaved using electric clippers and then with an electric razor. The application site was gently swabbed with 70% ethanol and allowed to dry. One-hundred microliters of different doses of OVA were injected into the skin layer at a fixed 40º as described above. Regarding to safety issues, mice were observed for skin bleeding and infection over the experiment.

For the subcutaneous immunization, one-hundred microliters of different doses of OVA were subcutaneously injected at the neck region of mice using a 27 gauge of hypodermic needle.

3.3.5.4 Blood samples collection

Blood samples (200 µL per mouse) were obtained from the cut tail tip at day 0. At the end of the study, on day 21, blood collection (600-1,000 µL per mouse) from mice euthanized using diethyl ether was performed via cardiac puncture. For tail bleeds of control groups, the blood was collected and pooled for each group of mice. For blood collected via cardiac puncture, the blood sample from each mouse was stored separately. Plasma separation was carried out by centrifuging the blood at 8,000×g for 5 min at 4°C. The plasma was then stored at -20°C until assayed.

Control mouse blood for assay method development was acquired from healthy female BALB/c mice. Blood collection from mice euthanized using CO_2 at different time points (2, 3, 6, 24 and 48 h) was performed *via* cardiac puncture. Plasma separation was carried out by centrifuging the blood at 8,000×g for 5 min at 4°C. The plasma was then stored at -20°C until assayed.

3.3.5.5 Determination of immune responses

Quantifications of OVA-specific serum immunoglobulin G (IgG) antibodies was carried out using a standard enzyme-linked immunosorbent assay (ELISA). Briefly, MaxiSorp NUNC-Immuno^{TM} flat bottom 96-well plates were coated with 100 µg/mL of OVA in the coating solution (0.1 M $NaHCO_3$, pH 8.2) for 50 µL per well at 4°C overnight. The solution was aspirated from the plates; the plates was then washed with 0.05% (v/v) Tween 20 in PBS (T20/PBS). The remaining solution was removed by snapping the plate onto absorbent paper. This process was repeated for 3 times. Following the last wash, all of remaining Wash Buffer were removed by aspirating or decanting. The plate was inverted and blotted it

against absorbent paper. The plate was blocked using 200 µL of 10% (v/v) FBS in PBS (10FBS/PBS) for 2 h at 25ºC. After washing the plates with T20/PBS for 6 times, plates were incubated with 200 µL serially diluted plasma samples in 10FBS/PBS at 25ºC for 1 h. For the standard curve, the OVA-specific monoclonal antibody at a concentration of 100 ng/mL was diluted with 10FBS/PBS in the ELISA plates, resulting in a series of concentrations ranging from 100-1.56 ng/mL. The plate was then washed 6 times with T20/PBS and incubated with goat anti-mouse IgG HRP conjugate (1:4000 dilution) for 45 min at 25ºC. Following the washing step, bound antibody was detected using TMB, and the reaction was stopped by adding 100 µL per well of 1 N sulfuric acid. The optical absorbance was measured at 450 nm using a microplate reader.

3.3.6 Effect of delivery devices and nanocarriers on skin permeation and skin immunization with pOVA

3.3.6.1 Preparation of pOVA

The plasmids DNA encoding OVA (pOVA; Figure 14) were amplified from previously transformed stocks of *Escherichia coli* DH5-α (*E.Coli*) with ampicillin. After amplification of the *E.Coli*, the plasmids were then isolated and purified using QIAGEN® Plasmid Maxi Kits. Briefly, *E.Coli* cells were harvested by centrifuged at 6,000 g for 15 min at 4ºC. The bacterial pellets were then resuspended in 10 ml of buffer P1 (50 mM Tris Cl pH 8.0, 10 mM EDTA and 100 µg/mL RNase A). The cells were lysed using buffer P2 (200 mM NaOH, 1% w/v SDS, Lyseblue reagent). The solutions were neutralized by chilled buffer P3 (3.0 M potassium acetate, pH 5.5) and then centrifuged at 20,000×g for 30 min at 4ºC. The supernatant was collected. The supernatant was then filtered using QIAGEN®-tip and washed with QC buffer (1.0 M NaCl; 50 mM MOPS, pH 7.0; 15% v/v isopropanol). Plasmid was then eluted using buffer QF (1.25 M NaCl; 50 mM TrisCl, pH 8.5; 15% v/v isopropanol) and then precipitated by adding isopropanol and centrifuged at 15,000×g

for 30 min at 4ºC. The supernatant was carefully removed and the pellets were washed with 70% ethanol following centrifugation at 15,000xg for 10 min at 4ºC. The pellets were dried at room temperature and dissolved in TE buffer (pH 8.0). The quantity and quality of purified pOVA were determined by the optical density (OD) at 260 and 280 nm. The OD_{260}/OD_{280} value of plasmid solution was used to evaluate the purity of plasmid, which is usually in the range of 1.8 to 2.0. The concentration of purified pOVA was calculated by the following equation.

$$pOVA\ concentration\ (\mu g/mL) = \varepsilon_{260} \times OD_{260} \times DF \qquad Eq.\ 5$$

Where; ε_{260} is an extinction coefficient of double stand DNA at 260 nm which is equal to 50 µg/mL

OD_{260} is an optical density from the measurement

DF is a dilution factor

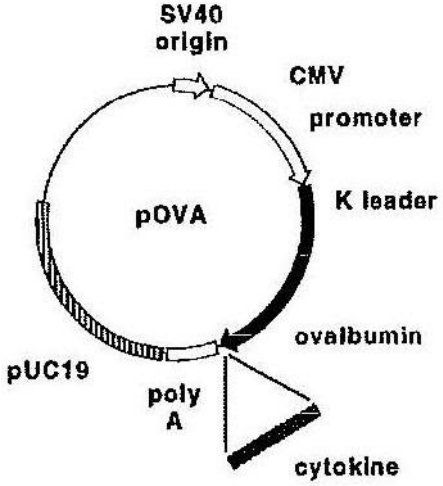

Figure 14 Plasmid map of pOVA
(Available from: http://www.addgene.org/31598/)

3.3.6.2 Preparation of cationic nanocarrier/pOVA complexes

Commercially transfection reagents i.e., linear 25 kDa PEI, Lipofectamine™ 2000 and SuperFect® were used as the model of cationic polymer, cationic lipid and cationic dendrimer, respectively. The

PEI/pOVA complexes were prepared by mixing the solution of branced PEI (25 kDa) (stock solution 1 mg/mL) to the plasmid solution in 1.5 mL microcentrifuge tubes at different weight ratios of 0.25:1, 0.5:1, 1:1, 2:1 and 3:1. For Lipofectamine™ 2000/pOVA, lipoplexes were prepared at weight ratios of 1:1, 2:1, 3:1, 4:1 and 5:1. For SuperFect®/pOVA were prepared at weight ratios of 2:1, 3:1, 4:1, 6:1 and 15:1. The mixture was gently mixed by pipetting and further incubated at 25°C for the appropriate time according to the manufacturer's instructions to initiate the formation of complexes.

3.3.6.2 Characterization of cationic nanocarrier/pOVA complexes

3.3.6.2.1 Particle size and zeta potential analysis

The particle size and surface charge of the complexes were investigated by photon correlation spectroscopy using a Zetasizer Nano ZS. The pOVA (2 μg) were mixed with different types of cationic nanocarriers at various weight ratios as described above. The complexes were diluted with sterile water to obtain 1 mL of mixture (pH 7.4) at the time of measurement. The measurement of each sample was performed in triplicate at room temperature.

3.3.6.2.2 Agarose gel retardation

The complexes were prepared by mixing 0.25 μg of pOVA with different nanocarriers at various weight ratios as described above. Agarose gel electrophoresis was performed using 1% agarose in 1X Trisacetate-EDTA (TAE) buffer. Before loading into the gel, the complex solutions were mixed with 50% glycerol. Electrophoresis was carried out in TAE running buffer (pH 8.3) at 100 V for 45 min. The pOVA on agarose gel were then stained with ethidium bromide for 30 min, following de-stained in sterile water to remove remaining ethidium bromide. The bands of pOVA were visualized and imaged by a UV transilluminator using a GelDoc system.

3.3.6.3 *In vitro* transfection efficiency

Transfection efficiency of the complexes were determined in human cervical carcinoma cell (HeLa cell) lines. HeLa cells were seeded in 48-well plates to obtain 1×10^5 cells per well and incubated with 5% CO_2 at 37°C for 24 h. The cells were then transfected with complexes at various weight ratios in serum-free medium, the complexes containing pOVA 0.5 μg per well. After 4 h, the transfection media were replaced with fresh medium, and the cells were then incubated overnight. The media were collected, and the cells were trypsinized with a cell lysis buffer (50 mM Tris, 150 mM NaCl, 1 mM EDTA, 1% Triton X-100) and then frozen and thawed for 3 cycles. Insoluble substances were removed by centrifugation at 14,000 rpm for 10 min at 4°C, and the supernatant was then collected. The amounts of OVA expressed were determined both in the medium and the supernatant from cells lysis using a ELISA kit for OVA.

3.3.6.4 Cytotoxicity of cationic nanocarrier/pOVA complexes

The cytotoxicity of complexes was carried out using an MTT (3-(4,5-Dimethylthiazol-2-yl)-2,5-Diphenyltetrazolium Bromide) assay. HeLa cells were seeded into a 96-well plate to obtain 8,000 cells/well and incubated with 5% CO_2 at 37 °C for 24 h prior to transfection. The cells were then treated with the different complexes formulations under the same conditions and the weight ratios as *in vitro* transfection study. Following 4 h of transfection, the media were removed and the cells were then washed with PBS and continually incubated in the complete medium for 24 h. To obtain the final concentration of 1 mg/mL per well, MTT solution (5 mg/mL in PBS) were added and incubated in laboratory condition for 4 h. The media were then removed and the formazan crystals formed in the living cells were dissolved in 100 μL per well of DMSO. The optical density (OD) was measured at 550 nm using a microplate reader. Percentage of relative viability was calculated according to Eq. 6.

$$Relative\ viability\ (\%) = \frac{OD_{treated\ cells}}{OD_{non-treated\ cells}} \times 100 \qquad \text{Eq. 6}$$

The viability of non-treated cells is defined as 100 %.

3.3.6.5 Stability study of pOVA in the presence of serum

To evaluate the stability against nuclease digestion, serum stabilities of pDNA in the complexes was examined as previously described [196]. Our previous study found that pDNA without cationic nanocarriers were completely degraded in the presence of 10% BALB/c serum for 6 h [197]. According to our previous study, the different complexes formulations were incubated with 10% serum from female BALB/c mice (6-8 weeks old) for 6 h and examined with agarose gel electrophoresis. Different complexes formulations (0.25 μg of pOVA) at the most suitable weight ratios were incubated with 10% serum at 37°C for 6 h. For the samples containing the nanocarriers, pOVA were extracted from the nanocarriers by adding 10% sodium dodecyl sulfate solution into the samples and incubating at room temperature for 30 min. All samples were loaded into 1% agarose gel. The electrophoresis was performed at 100 V for 45 min. The bands of pOVA were visualized under a UV transilluminator using a GelDoc system. Naked pOVA with and without serum were performed under the same conditions as control.

3.3.6.6 *In vitro* skin permeation study

In vitro skin permeation studies of pOVA were carried out using vertical Franz diffusion cells as described above. A 500 μL aliquot was withdrawn from the receptor compartment at the time points of 0.5, 1, 2, 4, 6, 8 and 24 h.

3.3.6.6.1 Effect of delivery devices

To investigate the effect of the solid MNs patch, the EPs patch, the MNs+EPs patch, 1 mL of naked pOVA (pOVA without cationic nanocarriers; 50 μg/mL) was pipetted into the donor compartment. In skin permeation experiments using the hollow MN, the same concentration of naked pOVA solution was injected into the skin. The experiments were

performed in five parallel groups: (1) passive delivery, (2) solid MNs patch, (3) EPs patch, (4) MNs+EPs patch, (5) hollow MN.

For the skin permeation experiments of the solid MNs patch, the skin was pre-treated with the solid MNs patch at 10 N force for 2 min using a plastic container filled with water as described above.

For the skin permeation experiments of the EPs patch, an EP was applied using a square-wave pulse generator. The skin was pre-treated with the EPs patch at pulse voltages of 150 V. The pulse duration and number of pulses were fixed at 1 msec and 99 pulses, respectively.

For the skin permeation experiments of the MNs + EPs patch, a patch comprised 25-acupuncture needles connected with copper wire was used as an electrode. The skin was pierced with the MNs+EPs patch at a force of 10 N for 2 min. Pulse voltages at 150 V were applied to the skin using a pulse generator via conditions similar to those described above.

For the skin permeation experiments of the hollow MN, one-hundred microliters of pOVA was injected into the skin with 10 injections per skin sample and manually delivered by applying gentle finger pressure to the end of the syringe plunger.

3.3.6.6.2 Effect of cationic nanocarriers

To investigate the effect of cationic nanocarriers to deliver pOVA through the skin, hollow MN was chosen as it was the best technique for skin permeation of naked pOVA. The effects of the various cationic nanocarriers were also evaluated, including PEI/pOVA at the weight ratio (w/w) of 1:1, Lipofectamine™ 2000/pOVA at a ratio of 2:1 and SuperFect®/pOVA at a ratio of 6:1, as these weight ratios provided the highest transfection efficiency in the HeLa cells. The pOVA complexes with different cationic nanocarriers were injected directly into the skin using hollow MN. The volume of solution injected was fixed at 100 μL with 10 injections per sample.

The amount of pOVA diffused into the receiver compartment was quantified using a Quant-iT™ PicoGreen assay and Fluoroskan Ascent™ Microplate Fluorometer with an excitation wavelength of 480 nm and an emission wavelength of 520 nm. For the sample solutions containing the nanocarriers, 10% sodium dodecyl sulfate was added to the samples for extracting pOVA from the nanocarriers, and the mixture was then incubated at 25ºC for 30 min before being stained using a Quant-iT™ PicoGreen. Fora control group, the skin permeation of naked pOVA at the time intervals of 0.5, 1, 2, 4, 6, 8, 12 and 24 h was also evaluated. The concentrations of pOVA were calculated using a calibration curve.

3.3.6.7 *In vivo* immunization study

Female BALB/c mice (6-8 weeks old) were obtained and acclimatised to laboratory conditions as described above in 3.3.5.3. The mice were divided into 10 groups (n=6), including naïve group (received sterile normal saline as a negative control), and the other groups were immunized with different pOVA formulations and routes as described in Table 6. The mice in all groups were immunized on days 0 and 14.

Table 6 Immunization groups of pOVA for the *in vivo* study in mice

Mice groups	Formulations	Route of administrations
Naïve 1	100 µL sterile normal saline	Hollow MN
Naïve 2	100 µL sterile normal saline	Subcutaneous injection
Hollow MN 1	10 µg of pOVA in PBS, pH 7.4	Hollow MN
Hollow MN 2	PEI/10 µg of pOVA (1:1) in PBS, pH 7.4	Hollow MN
Hollow MN 3	Lipofectamine™ 2000/10 µg of pOVA (2:1) in PBS, pH 7.4	Hollow MN
Hollow MN 4	SuperFect®/10 µg of pOVA (6:1) in PBS, pH 7.4	Hollow MN
Subcutaneous 1	10 µg of pOVA in PBS, pH 7.4	Subcutaneous injection
Subcutaneous 2	PEI/10 µg of pOVA (1:1) in PBS, pH 7.4	Subcutaneous injection
Subcutaneous 3	Lipofectamine™ 2000/10 µg of pOVA (2:1) in PBS, pH 7.4	Subcutaneous injection
Subcutaneous 4	SuperFect®/10 µg of pOVA (6:1) in PBS, pH 7.4	Subcutaneous injection

For the hollow MN immunization, the mice were anesthetized with sodium pentobarbital (40 mg/kg) by intraperitoneal injection. The dorsal region of the mice was finely shaved with electric clipper following an electric razor. The shaved skin was gently swabbed with 70% ethanol and allowed to dry. The mice were twice immunized with 100 µL of different pOVA formulations (100 µg/mL of pOVA) into the superficial dermal layer using hollow MN fixed at a 40º angle, as described above. According to the safety issues, mice were assessed for signs of skin bleeding and infection [122].

For the subcutaneous immunization, conscious mice were subcutaneously injected with different pOVA formulations at the neck region using a 27 gauge of hypodermic needle.

3.3.6.7.1 Blood sample collection

The blood samples were collected on day 0 and day 14 as described above. Plasma separation was then carried out by centrifuging the blood as described above (see section 3.3.5.4). The plasma was then stored at -20°C until assayed.

3.3.6.7.2 Determination of serum antibody responses

The levels of OVA-specific serum IgG antibody were analysed using ELISA assay. Briefly, 96-well microplate was coated with 50 µL of 100 µg/mL OVA in coating solution (0.1 M $NaHCO_3$, pH 8.2) at 4°C overnight. The plates were then washed three times with 0.05% (v/v) Tween 20 in PBS (T20/PBS) and blocked with 200 µL of 10% (v/v) FBS in PBS (10FBS/PBS) for 2 h incubation at 25ºC. After washing 6 times with T20/PBS, the plates were incubated with 200 µL serially diluted serum samples in 10FBS/PBS for 1 h. For the standard curve, an OVA-specific monoclonal antibody at a concentration of 100 ng/mL was diluted with 10FBS/PBS in the ELISA plates, resulting in a series of concentrations ranging from 1.56-100 ng/mL. The plate was then washed 6 times with T20/PBS and incubated with goat anti-mouse IgG HRP conjugate diluted to 1:4000 for 45 min. After washing, bound antibody was detected using a TMB, and 100 µL/well of 1 N H_2SO_4 was added to stop the reaction. The optical absorbance was measured at 450 nm using a microplate reader.

3.3.6.8 *In vivo* cytokine release study

Following blood sample collection in mice, spleens were then removed aseptically. The spleen was mashed through the cell strainer into 50 mL centrifuge tube using black rubber end of the plunger from 3 mL syringe. The cell strainer was rinsed with 5mL of complete RPMI-1640 medium (RPMI-1640 supplemented with 10% heat-inactivated FBS). After centrifugation at 1,000 rpm for 10 min at 4ºC, erythrocytes were lysed by ACK lysing buffer and cell pellets were washed twice with

RPMI-1640 medium. Cells were resuspended in completed medium and the cell number was adjusted to $2x10^6$ cells/mL. Viability of splenocytes was investigated using trypan-blue dye exclusion technique. For stimulating cytokine release, splenocytes were cultured in clear flat bottom 96-well plate, and 100 µL/well of OVA (2 mg/mL) was then added and incubated at 37°C with 5% CO_2 for 3 days. Cells were then collected and centrifuged at 1,500 rpm for 10 min at 4°C. The supernatant was collected and stored at -20 ºC until assayed. IFN-γ and IL-4 cytokines were then analysed using Mouse IFN-γ Platinum ELISA kits and Mouse IL-4 High Sensitivity ELISA kits, respectively.

3.3.7 Statistical analysis

In vitro experiments were analysed using Student's t-test and one-way analysis of variance (ANOVA), with Tukey's HSD post-hoc test. Comparisons for animal studies were made using the Mann-Whitney U-test. A value of $p<0.05$ was considered statistically significant.

CHAPTER 4
RESULTS AND DISCUSSION

4.1 Effect of MNs and doses of OVA on skin permeation and skin immunization

4.1.1 Solid MNs patch and hollow MN characterization

Figure 10B-C show a successfully produced solid MNs patch with a total of 25 needles per array (5×5 needles). Each needle was cone shaped with a height of approximately 900 μm. The hollow MN was approximately 300 μm of insertion depth into the upper skin layer (Figure 13B).

4.1.2 *In vitro* skin permeation study

In vitro skin permeation profiles of OVA-F following pre-treatment with the solid MNs patch and hollow MN are presented in Figure 15A and B, respectively. The permeation parameters following application of the different types of MNs and doses of OVA-F are shown in Table 7. The rate of absorption, or flux (*J*), of any compound across a skin is proportional to its concentration difference across that skin; the proportionality constant relating the flux to the concentration is the permeability coefficient (*Kp*) [198]. The flux and cumulative amount of OVA-F at 8 h after administering various doses with different types of MNs could be ranked as follows: hollow MN; OVA-F 500 μg (high dose) > hollow MN; OVA-F 250 μg (medium dose) > hollow MN; OVA-F 100 μg (low dose) > MN patch; OVA-F 500 μg > MN patch; OVA-F 250 μg > MN patch; OVA-F 100 μg > untreated skin; OVA-F 500 μg > untreated skin; OVA-F 250 μg > untreated skin; OVA-F 100 μg > untreated skin without OVA-F (Figure 15C and Table 7). For the solid MNs patch, skin permeability to OVA-F following pre-treatment using the solid MNs patch significantly increased as the dose of OVA-F increased from 100 μg to 250 μg and from 250 μg to 500 μg (Figure 15A and Table 7). Similarly, the OVA-F skin permeabilities using the hollow MN were significantly

different among the different doses. When the dose of OVA-F was increased, the cumulative amount increased (Figure 15B and Table 7). In addition, treatment of the skin with the solid MNs patch or hollow MN resulted in a significant increase in the cumulative amount of OVA-F compared to the untreated skin with or without OVA-F (Figure 15C and Table 7). Overall, the use of the hollow MN had the highest enhancing effect on the skin permeation of OVA-F, followed by the MN patch and then untreated skin. Although the length of a hollow MN was 3 times shorter than that of the needles on the solid MNs patch and the antigen delivery took place via a single needle, its performance was superior to that of the solid MNs patch.

The mechanism of the solid MNs patch for intradermal or transdermal drug delivery is via the "poke and patch" approach, i.e., following removal of the solid MNs patch, transient microchannels are created in the skin and OVA formulations, which are applied to a specific site, moved through these microchannels via passive diffusion. In contrast, the hollow MN delivered drugs *via* the "poke and flow" approach, where a liquid formulation containing the antigen is directly injected through the hollow needle bore-opening in the skin. These results were consistent with those of a previous study [199], which found that macromolecules delivered into rat skin using a hollow MN were distributed throughout the dermis. Although the injection was at a specific site within the dermis layer, the large volume of fluid injected expanded throughout the dermis. As we compared the mechanisms, the results may be attributed to a key advantage of the hollow MN over the solid MNs patch in that the former facilitates pressure-driven fluid flow, hence allowing rapid rates of drug delivery [2, 199, 200].

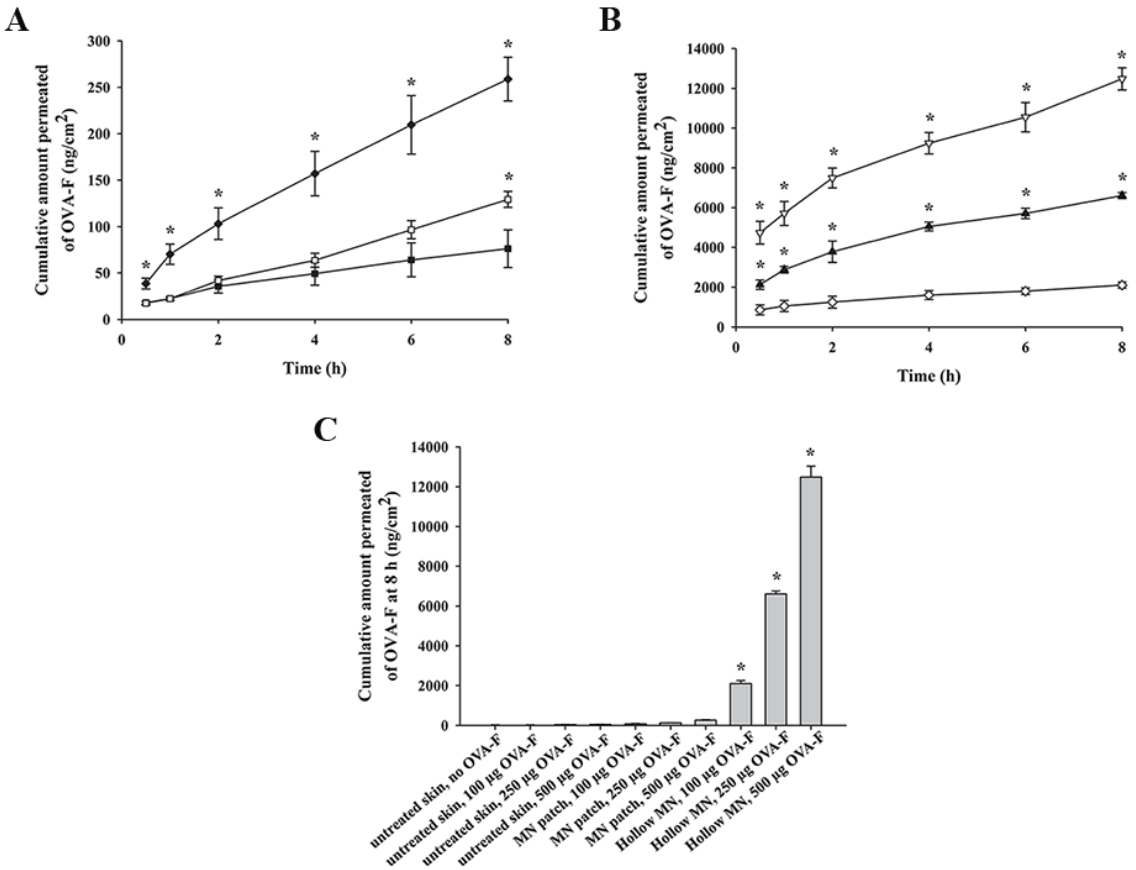

Figure 15 *In vitro* permeation profiles of OVA-F following pre-treatment with (A) the solid MNs patch: (■) 100 µg of OVA-F, (□) 250 µg of OVA-F, (◆) 500 µg of OVA-F, (B) hollow MN: (◇) 100 µg of OVA-F, (▲) 250 µg of OVA-F, and (▽) 500 µg of OVA-F and (C) the cumulative amount of OVA-F at 8 h of untreated and pre-treated skin. *Statistically significant ($p<0.05$).

Table 7 The permeation parameters from the different types of MNs and various doses of OVA-F *Statistically significant (p<0.05).

Delivery techniques, formulations	Flux (μg/cm^2·h)	ER	K_p (×10^{-2}) (cm/h)
Untreated skin, OVA-F 100 μg	0.0017 ± 1.71	-	1.68 ± 0.00
Untreated skin, OVA-F 250 μg	0.0032 ± 0.60	1.88	1.30 ± 2.40
Untreated skin, OVA-F 500 μg	0.0036 ± 0.51	2.12	0.72 ± 0.01
Solid MNs patch, OVA-F 100 μg	0.0077 ± 3.53	4.53	7.74 ± 3.53
Solid MNs patch, OVA-F 250 μg	0.0148 ± 2.05	8.71	5.92 ± 8.21
Solid MNs patch, OVA-F 500 μg	0.0283 ± 3.26	16.65	5.66 ± 6.51
Hollow MN, OVA-F 100 μg	0.1576 ± 27.51*	92.71	15.57 ± 27.51*
Hollow MN, OVA-F 250 μg	0.5678 ± 28.69*	334	22.71 ± 11.48*
Hollow MN, OVA-F 500 μg	1.1024 ± 92.31*	648.47	22.05 ± 11.46*

4.1.3 Accumulation of OVA-F in full-thickness skin

Fluorescence imaging of a full thickness skin, isolated from a Sprague-Dawley rat that had been treated with different types of MNs, confirmed the enhancement of skin permeation. As shown in Figure 16A-J, images of the skin in vertical depth sections were observed after the permeation of OVA-F. Figure 17 shows fluorescence intensity of OVA-F at different penetration depths. It was known from the previously described *in vitro* skin permeation studies that the flux and cumulative amount of OVA-F permeation is very low in untreated skin. For the untreated skin (control group) exposed to various doses of OVA-F, minimal fluorescent signal was observed in the *SC* and lower epidermal tissue (Figure 16B-D and 17). However, when untreated skin was exposed to the high dose of OVA-F (500 μg), the green fluorescence intensity increased in the depth range of 40-160 μm (Figure 16D). As compared untreated skin and skin treated with the solid MNs patch at the same dose of OVA-F, more OVA-F was clearly visible in the skin treated with the solid MNs patch at depths of up to 100 μm, 140 μm, and 260 μm for the

low, medium and high doses, respectively (Figure 16E-G and 17). In addition, strong fluorescence intensity was also detected in the ranges of 20-100 μm, 0-140 μm and 0-260 μm for the low, medium and high doses of OVA-F, respectively. The fluorescence signal in the skin following a treatment with the hollow MN at the same dose of OVA-F was observed in the dermal region deeper than that the skin treated with the solid MNs patch, at depths of 140 μm, 220 μm and 340 μm, with stronger fluorescence intensity detected in the ranges of 20-140 μm, 0-220 μm and 0-340 μm for the low, medium and high doses, respectively (Figure 16H-J and 17). Therefore, it could be assumed that higher doses of OVA-F correlated with increasing in skin permeation.

As expected, both types of MNs created the pore channels underneath the skin surface, as seen by the dark circular region, around which the green fluorescence signal was localized (Figure 16E-J). As a result, these pores are considered an effect of the MNs' piercing the *SC* barrier and acted to enhance the antigen permeation. It can be clearly observed in Figure 16 and 17 from the fluorescence intensity of OVA-F at the same doses that the hollow MN had the highest enhancing effect on skin permeation, followed by the solid MNs patch and untreated skin, respectively. These results confirmed the effect of the hollow MN, which resulted in increased driving force to deliver the antigen into the skin similar to a conventional injection, and the solid MNs patch, which created aqueous pores in the skin, resulting in enhanced skin permeation of the antigens. Therefore, the hollow MN was selected for further use in an *in vivo* immunization study.

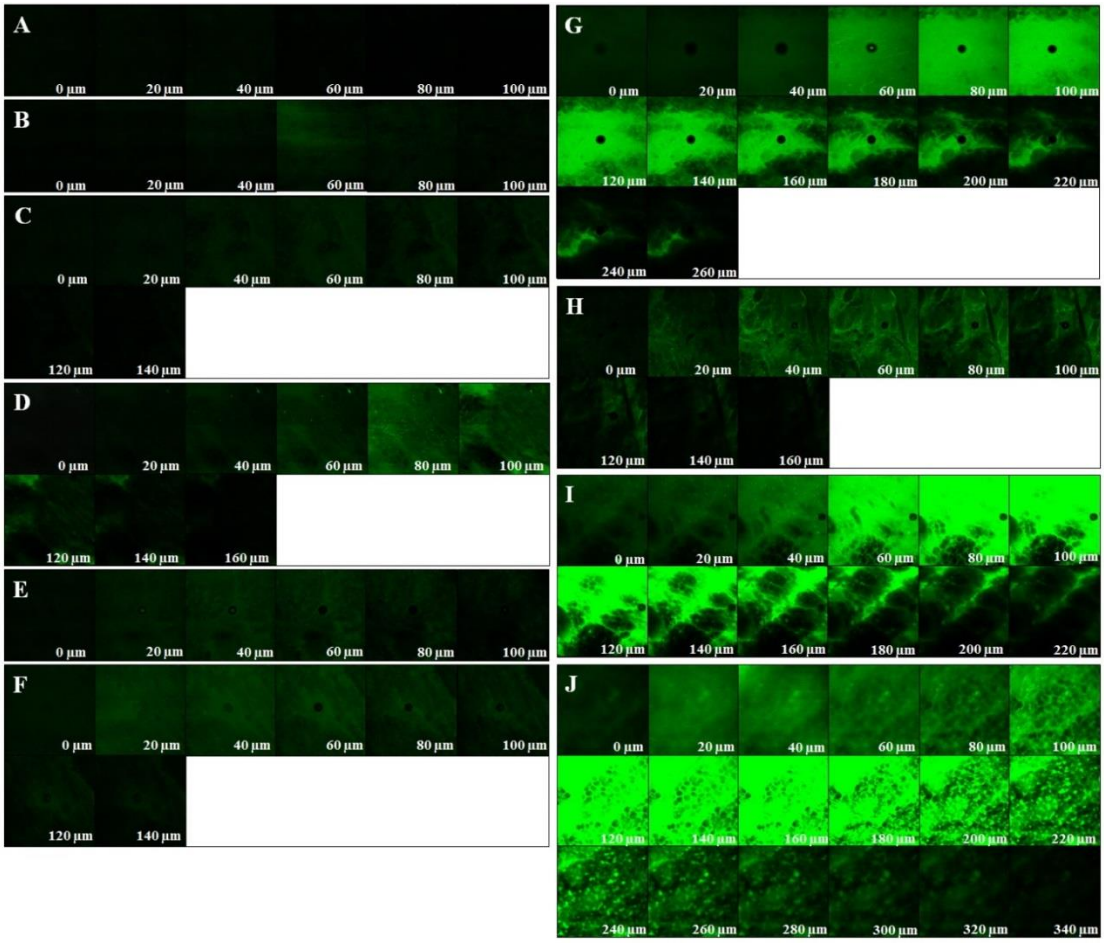

Figure 16 Fluorescence confocal laser scanning microscopy (CLSM) images of OVA-F at various doses after *in vitro* permeation of untreated and treated skin. (A) untreated skin without OVA-F; (B) untreated skin, 100 µg of OVA-F; (C) untreated skin, 250 µg of OVA-F; (D) untreated skin, 500 µg of OVA-F; (E) solid MNs patch, 100 µg of OVA-F; (F) solid MNs patch, 250 µg of OVA-F; (G) solid MNs patch, 500 µg of OVA-F; (H) hollow MN, 100 µg of OVA-F; (I) hollow MN, 250 µg of OVA-F; and (J) hollow MN, 500 µg of OVA-F.

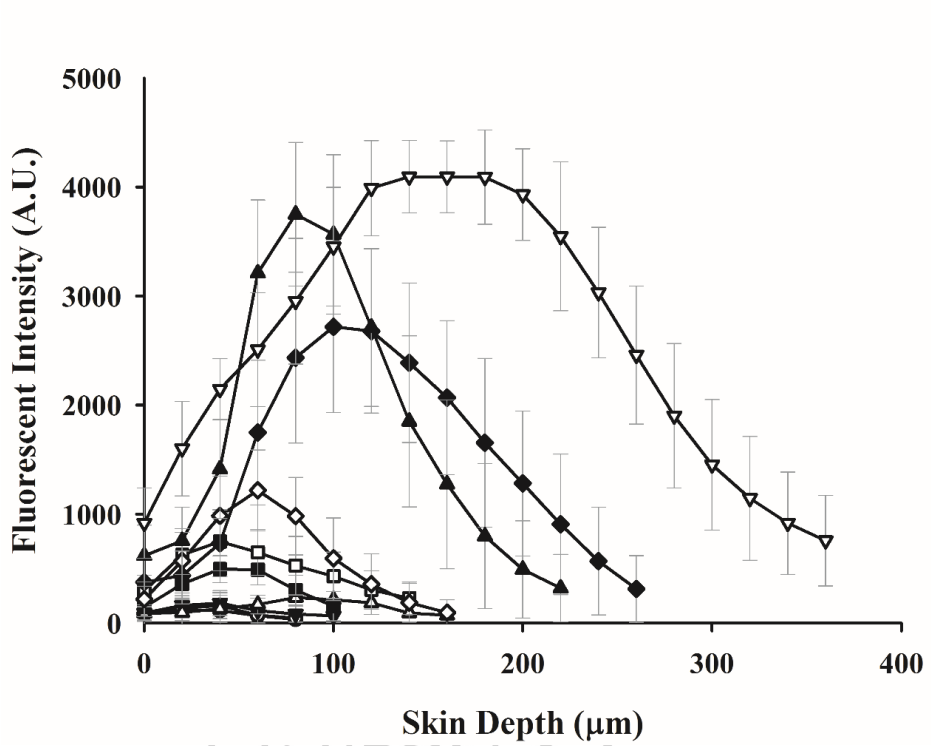

Figure 17 Fluorescent intensity of OVA-F in Sprague Dawley rat skin with various doses after *in vitro* permeation of untreated and treated skin. Untreated skin: (●) without OVA-F, (○) 100 μg of OVA-F, (▼) 250 μg of OVA-F, (△) 500 μg of OVA-F; Solid MNs patch: (■) 100 μg of OVA-F, (□) 250 μg of OVA-F, (◆) 500 μg of OVA-F; Hollow MN: (◇) 100 μg of OVA-F, (▲) 250 μg of OVA-F, and (▽) 500 μg of OVA-F.

4.1.4 *In vivo* immunization study

Serum IgG antibody responses after immunization were examined in BALB/c mice after a second immunization of OVA (100, 250 and 500 μg) with the hollow MN, by measuring the plasma concentration of OVA-specific antibodies. One week after the second immunization, the levels of IgG in the mice immunized using the hollow MN were significantly higher than those in the subcutaneous immunization and naïve groups, as shown in Figure 18. IgG levels in the hollow MN group were 5.7, 11.6 and 13.3 times higher than those of the subcutaneous group for low, medium and high dose, respectively. Moreover, no significant difference was observed

in the levels of IgG antibody responses specific to OVA after vaccination using subcutaneous injection with various doses of OVA, including 100μg, 250μg and 500 μg. For the hollow MN, when the dose of OVA antigen increased, the immune responses also increased. It was found that the serum IgG levels were significantly stronger at the medium dose of OVA than at the low dose. Although a high dose of OVA slightly improved the antibody titers in comparison with the medium dose, there were no significant differences between IgG levels after vaccination. These results were probably due to saturation of the immune response when an adequately high concentration of antigen was provided [201, 202]. The immune responses were clearly observed to be dose dependent. According to the results, 250 μg of OVA was selected as an optimal dose. From these results, in addition to the method of antigen administration, the dose delivered is also an important factor for effective induction of immune responses.

Regarding the safety of this vaccination method, none of the mice immunized using the hollow MN showed signs of skin infection or pinpoint bleeding at the administration sites. From many human and animal studies, there have been no reports on skin infection due to the use of MNs [115] because the skin has defended mechanisms to protect itself from pathogens[203]. Generally, MN arrays with needles length of less than 1 mm do not cause bleeding [98, 122]. These results were consistent with the findings of a previous study that showed that 30-gauge needles caused less bleeding and bruising than 27-gauge needles [204]. According the results, the hollow MNs could potentially induce a stronger immune response than subcutaneous injection of the same dose of the OVA antigen, which confirmed that the skin is a very suitable target site for vaccination. Similar results have been observed in previous studies, intradermal injection with the hollow MN (MicronJet™) eliciting significantly higher antibody responses than intradermal injection using a conventional needle (Mantoux technique) with same dose of Inflexal® V (3

μg) and resulting in stronger immune responses than intramuscular injection with a full dose (15 μg) of Inflexal® V [16]. Consequently, the hollow MN delivered the antigen in the proximity of Langerhans cells and dendritic cells, professional APC, allowing potential uptake of the antigen by these cells for the efficient induction of immune responses.

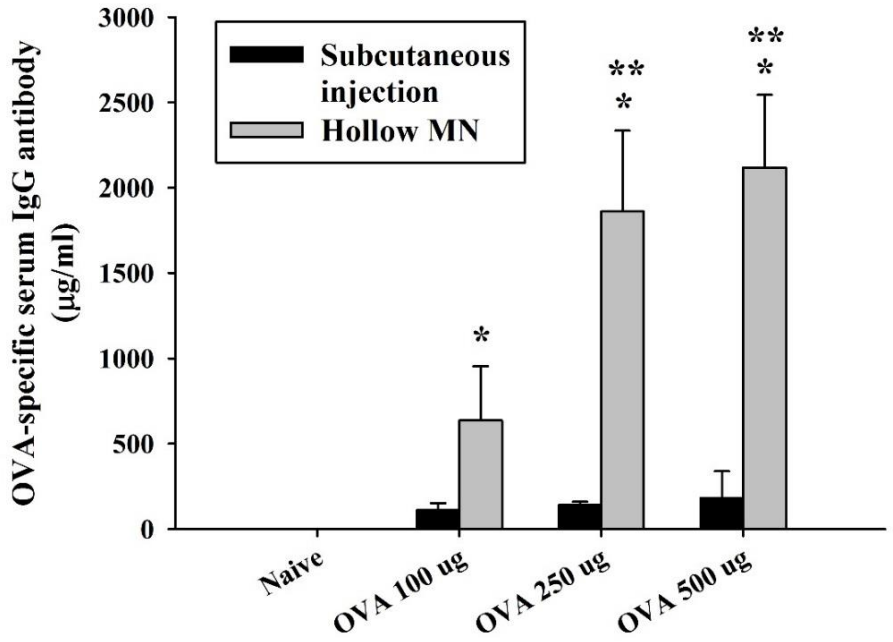

Figure 18 Antibody titers of serum IgG obtained from mice 21 days after vaccination with OVA by (▒) a hollow MN or (■) subcutaneous injection. The serum IgG level was measured by ELISA one week after the second immunization. *p<0.05 compared to naïve group. **p<0.05 compared to OVA 100 μg.

4.2 Effect of delivery devices and nanocarriers on skin permeation and skin immunization with pOVA

4.2.1 The morphology of delivery devices

The morphology of the solid MNs patch, EPs patch and the MNs+EPs patch used in this study was evaluated. The solid MNs patches were approximately 900 μm in length and were arranged in 5 rows as previously described (see section 4.1.1 and Figure 10B and C). The blunted EPs patch is shown in Figure12B. The hollow MNs with a triangular silicone sheet were approximately 300 μm of insertion depth into the skin layer (Figure13B).

4.2.2 Characterization of cationic nanocarrier/pOVA complexes

The particle size and zeta potential were plotted against the weight ratios of the different cationic nanocarriers/pOVA complexes (Figure 19). The PEI/pOVA complexes were performed at the weight ratios of 0.25, 0.5, 1, 2 and 3. As shown in Figure 19A, the size of the PEI/pOVA complexes was dependent on the concentration of PEI used. The smallest particle size of the PEI/pOVA complexes was observed at the weight ratio of 1. Then, the particle sizes dramatically increased when the weight ratio increased from 2 to 3. Increasing the weight ratio of PEI resulted in higher positive charges, and the surface of complexes were positive at a weight ratio of 0.5 to 3 (Figure 19A). Because the weight ratio of the Lipofectamine™ 2000/pOVA complexes increased from 1 to 5, the particle size of the complexes increased from 300 to 600 nm, and the zeta potential of the complexes were also increased from -10 to 60 mV. The positive charge of the lipoplex was observed at the weight ratio of 2 to 5 (Figure19B). In addition, increasing in the concentrations of SuperFect® from 2 to 15 resulted in larger complexes between 180 to 890 nm, and the zeta potential of the complexes increased from 25 to 55 mV, as shown in Figure19C. Although, the size of the SuperFect®/pOVA complexes was in

the nanoscale range, there were very large sizes due to the dendrimer structure (hyperbranched macromolecules) or “tree-like” structure of SuperFect® [205].

The zeta potential of the complexes is an important factor for DNA delivery because the zeta potential controls their DNA binding ability and the interaction between positive charges of the complexes and negative charges of the cell membranes. To confirm the positive charge of the complexes, the complete complex formation was determined by agarose gel retardation (Figure 20). The result showed the complete complex formation of the PEI/pOVA complexes at the weight ratio of 1 to 3 (Figure 20A), the Lipofectamine™ 2000/pOVA complexes at a weight ratio of 2 to 5 (Figure 20B), and the SuperFect®/pOVA complexes at a weight ratio of 2 to 15 (Figure 20C). As a result, these weight ratios of the different nanocarrier complexes showed that the particle size was in the nanoscale range with a highly positive charge. The correlation of the charge and the weight ratios demonstrated that the cationic nanocarriers were able to bind and neutralize the negative charge of pOVA. Therefore, it can be assumed that the optimal weight ratio of the PEI/pOVA complexes was between 1 to 3, the Lipofectamine™ 2000/pOVA complexes at a weight ratio of 2 to 5, and the SuperFect®/pOVA complexes at a weight ratio of 2 to 15. However, the best weight ratio must be chosen in the next study to yield the highest transfection efficiency for further study.

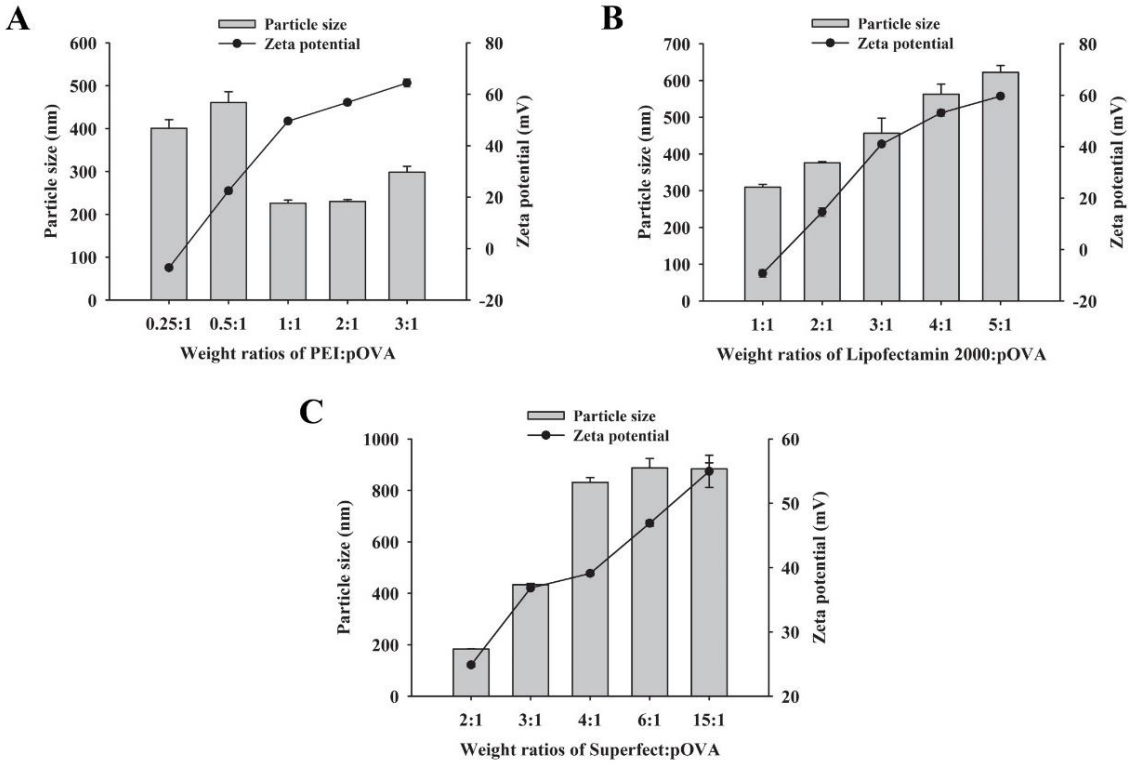

Figure 19 The particle size and zeta potential at various weight ratios of (A) PEI/pOVA complexes, (B) Lipofectamine™ 2000/pOVA complexes and (C) SuperFect®/pOVA complexes.

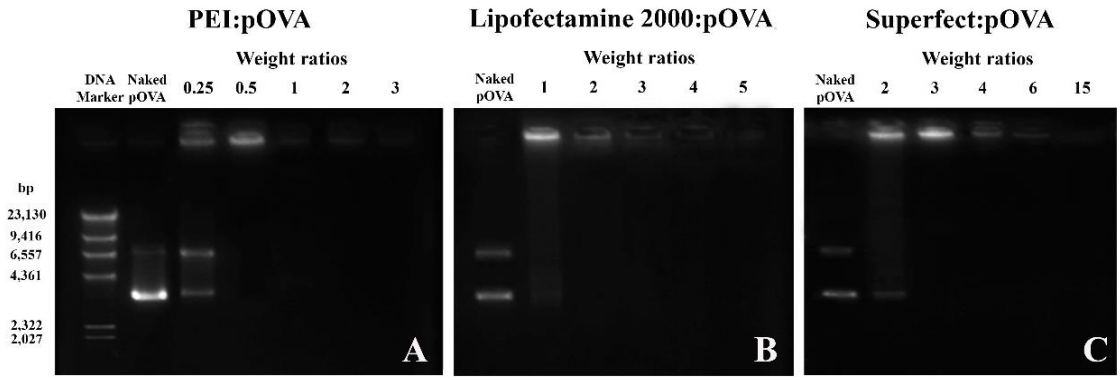

Figure 20 Gel retardation of (A) PEI/pOVA complexes, (B) Lipofectamine™ 2000/pOVA complexes and (C) SuperFect®/pOVA complexes to confirm the positive charges of the complexes at different weight ratios.

4.2.3 *In vitro* transfection efficiency

An effective gene delivery system should provide high transfection efficiency. To investigate the *in vitro* transfection efficiency, the complexes with different cationic nanocarriers at various weight ratios were transfected into HeLa cells. It was found that the transfection efficiency of the complexes (pOVA with cationic nanocarriers) at all of the weight ratios was significantly higher than naked pOVA (pOVA without cationic nanocarriers) transfection. The highest transfection efficiency of PEI, Lipofectamine™ 2000 and SuperFect® was observed for weight ratios of 1, 2 and 6, respectively (Figure 21). In comparison, the transfection efficiency was ranged as follows: PEI (850±433 ng/mL) > Lipofectamine™ 2000 (354 ± 172 ng/mL) > SuperFect® (43 ± 9 ng/mL). For PEI, the highest transfection efficiency was obtained for a weight ratio of 1, while the transfection efficiency showed very low ovalbumin protein expression for increased PEI/pOVA weight ratios (Figure21A). These results suggested that the decreasing transfection efficiency may be due to the toxicity of high amounts of PEI. In addition, the results indicated that SuperFect® has the lowest transfection efficiency, which may be due to the large size of SuperFect®/pOVA when compared with PEI/pOVA and Lipofectamine™ 2000/pOVA, as described above (see section 4.2.2).

To provide a high transfection efficiency, the size of the complexes should be approximately 200 nm, which may have restricted their ability to enter cells *via* receptor-mediated endocytosis [206, 207]. As a result, the PEI/pOVA complexes at a weight ratio of 1, the Lipofectamine™ 2000/pOVA complexes at a weight ratio of 2 and the SuperFect®/pOVA complexes at a weight ratio of 6 were selected to study the effect of different cationic nanocarriers using the best device (evaluated in the following study), the hollow MN, in an *in vitro* skin permeation study and *in vivo* immunization study in mice.

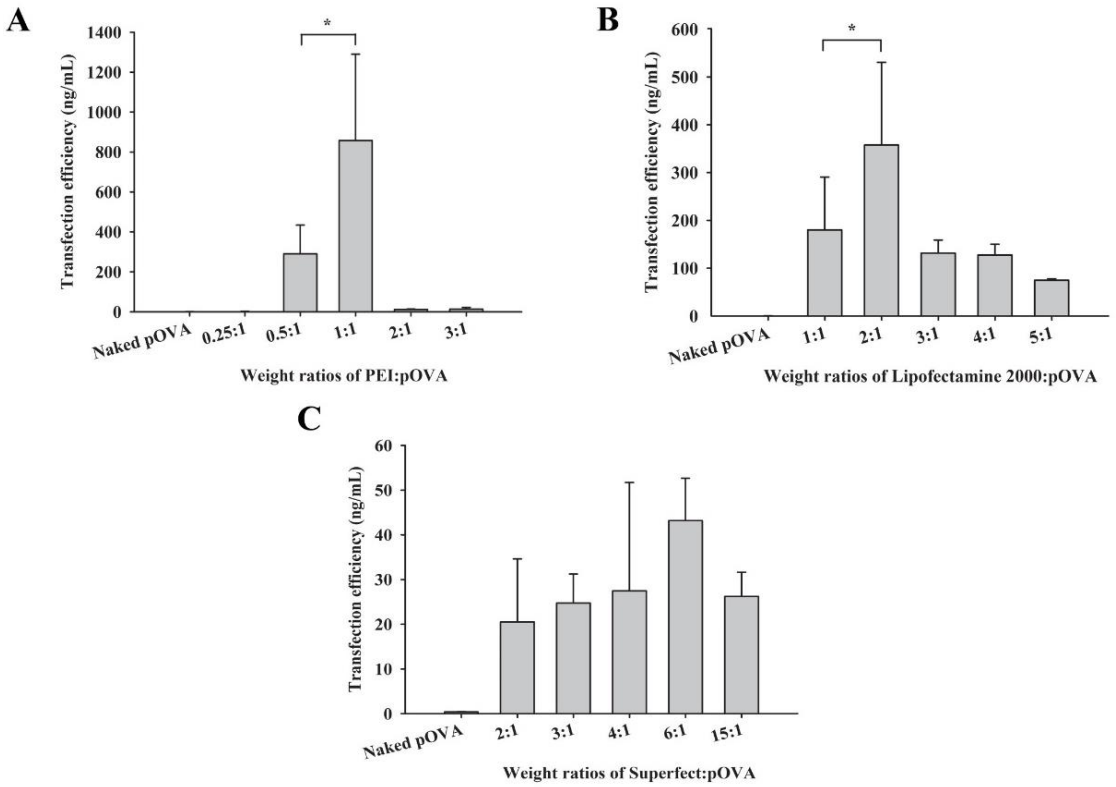

Figure 21 *In vitro* transfection efficiency in HeLa cells at varying weight ratios of (A) PEI/pOVA complexes, (B) Lipofectamine™ 2000/pOVA complexes and (C) SuperFect®/pOVA complexes. *p<0.05 compared between two groups.

4.2.4 Cytotoxicity of cationic nanocarriers/pOVA complexes

Apart from the efficiency of nanocarriers for delivering DNA, cytotoxicity was one of the most important factors for DNA delivery. To ensure the safety of the complexes, an MTT assay was determined in HeLa cells culture (Figure 22). The cell viability of the nanocarriers/pOVA complex-treated cells was compared with the untreated cells. Safe formulations should exhibit cell viabilities similar to those of untreated cells. As shown in Figure 22A, the viability of the cells transfected with PEI/pOVA complexes was observed to be concentrations-dependent. The cell viability significantly decreased when transfecting with lower (0.25:1) and higher weight ratios of complexes (2:1 and 3:1). The cell viabilities of PEI/pOVA complexes at the weight ratios of 3:1 were less than 80%. The

transfection efficiency of PEI/pOVA complexes decreased at high weight ratio due to the increase in cytotoxicity of the complexes. In addition, the cell viabilities of Lipofectamine™ 2000/pOVA complexes were significantly decreased when increasing the weight ratios of Lipofectamine™ 2000 (4:1 and 5:1) as shown in Figure 22B. For SuperFect®/pOVA complexes, there were no significant differences between cell viabilities at any weight ratios as compared with control (Figure 22C). As a result, PEI/pOVA complexes were safe for use at the weight ratios of 0.5:1 and 1:1; Lipofectamine™ 2000/pOVA complexes were safe at the weight ratios of 1:1, 2:1 and 3:1, whereas SuperFect®/pOVA complexes were safe at all of the weight ratios.

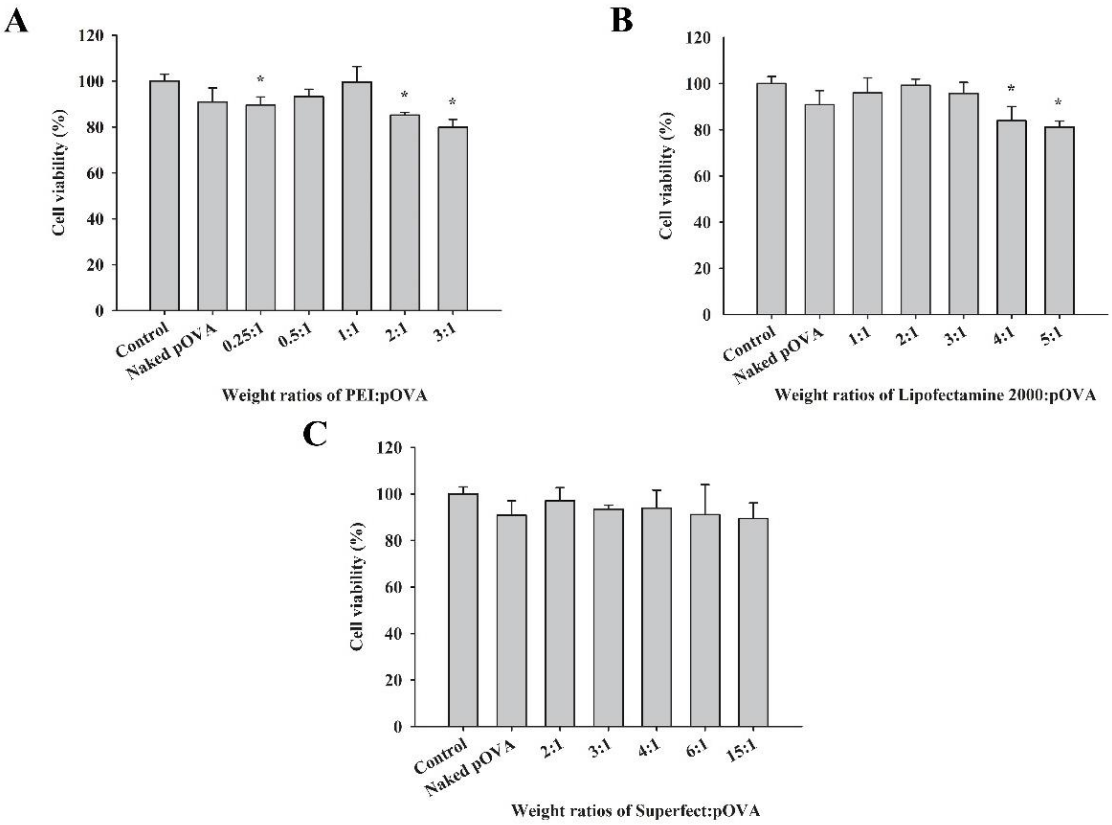

Figure 22 *In vitro* cell viability of HeLa cells after transfected with (A) PEI/pOVA complexes, (B) Lipofectamine™ 2000/pOVA complexes and (C) SuperFect®/pOVA complexes at pH 7.4. Each value was presented as mean ± SD of triplicate samples. *p<0.05 compared to control.

4.2.5 Stability study of pOVA in the presence of serum

The degradation of DNA by serum has been reported, and cationic nanocarriers have been used to protect DNA from degradation [196, 208]. According to this issue, the stability of naked pOVA and different cationic nanocarriers/pOVA complexes in the present of 10% serum of BALB/c mice was investigated. As shown in Figure 23, the DNA band of naked pOVA and Lipofectamine™ 2000/pOVA complexes in the present of 10% serum were almost completely disappeared due to degradation of pOVA. This result revealed that the serum composition may interfere the property of Lipofectamine™ 2000/pOVA complexes [209]. In contrast, the bands of DNA from the PEI/pOVA and SuperFect®/pOVA complexes in the present of 10% serum were slightly faded; this may be because the nanocarriers can protect the pOVA from degradation by nuclease in the serum.

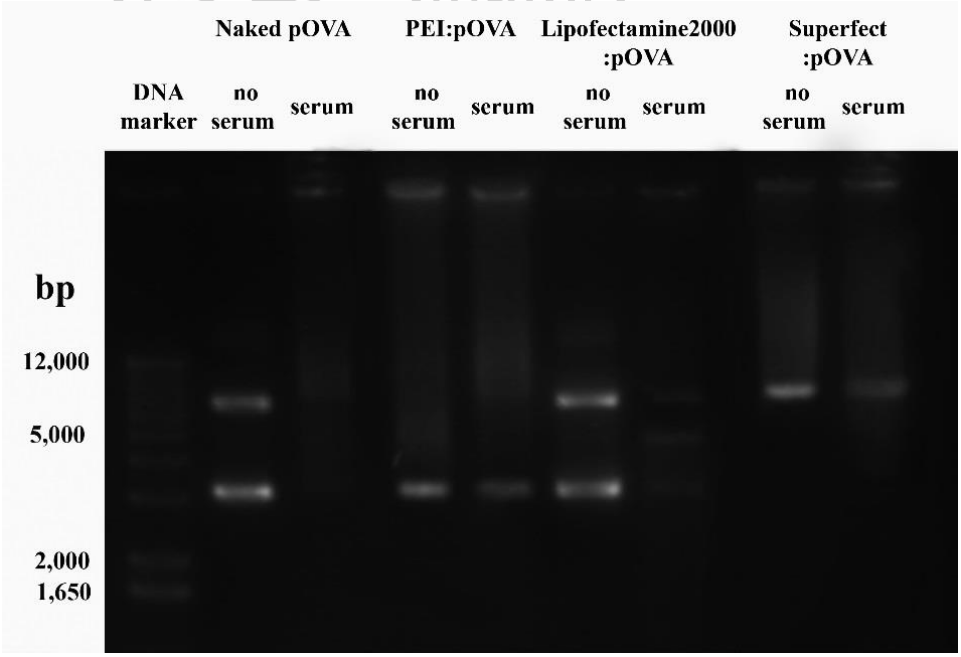

Figure 23 Gel retardation assay: Lane 1DNA marker; lane 2 naked pOVA without serum; lane 3 naked pOVA in the presence of 10% serum of BALB/c mice for 6 h; lane 4 PEI/pOVA complexes (1:1) without serum; lane 5 PEI/pOVA complexes (1:1) in the presence of 10% serum; lane 6

Lipofectamine™ 2000/pOVA complexes (2:1) without serum; lane 7 Lipofectamine™ 2000/pOVA complexes (2:1) in the presence of 10% serum; lane 8 SuperFect®/pOVA complexes (6:1) without serum; lane 9 SuperFect®/pOVA complexes (6:1) in the presence of 10% serum.

4.2.6 *In vitro* skin permeation studies

4.2.6.1 Effect of delivery devices

The *in vitro* skin permeation profiles of naked pOVA (pOVA without cationic nanocarriers) using the different delivery devices are illustrated in Figure 24A and 24C. The permeation parameters following application of the different types of MNs and formulations of pOVA are shown in Table 8. The most enhanced effect on the skin permeation of naked pOVA was found for use of the hollow MN, followed by MNs+EPs patch, the solid MNs patch, and the EPs patch. The cumulative amounts of naked pOVA permeated through the skin over 24 h after using the EPs patch, the solid MNs patch, the MNs+EPs patch, and hollow MN were 10-, 25-, 36-, and 64-fold greater than that of untreated skin (passive diffusion), respectively. The cumulative amount of naked pOVA in the treated skin using the MNs+EPs patch was 3-fold higher than the EPs patch-treated skin and 1.5-fold higher than the solid MNs patch-treated skin. These results suggested that the combined MNs and EPs patch had a synergistic effect for the transdermal delivery of pOVA because MNs and EPs exhibit different mechanisms of action for enhancing skin permeation. The combination of both methods can enhance the skin permeation of pOVA by first breaking the *SC* barrier due to use of the solid MNs patch to create large microchannels. Then, an electric current stimulates aqueous pore formation by rearranging the lipid bilayer in the cell membranes resulting in a temporary increase in porosity and prolonging the duration of pore opening [37]. Moreover, it can provide a local driving force for pOVA through the pores [35, 36]. Therefore, the combination of MNs and EPs was more effective than using each device alone. These results were

consistent with the findings of previous studies by Yan *et al*. and Petchsangsai *et al*., which indicated that the combined devices significantly enhanced the skin permeation of macromolecules compared with individual methods [36, 37].

In addition, the cumulative amount of pOVA using the hollow MN was 2.6-fold and 2-fold higher than that of the solid MNs patch and the MNs+EPs patch, respectively. The mechanism of hollow MN depends on the "poke and flow" approach [200]; similar to conventional injection, it can improve the transdermal delivery of pOVA by providing the pressure to push the pOVA solution into the skin. In addition, an important advantage of hollow MN over solid MNs patches is the possibility to facilitate force-driven fluid flow, thereby allowing faster rates of drug delivery [2, 16, 200, 210]. Compared to the MNs+EPs patch, the hollow MN had a significantly superior enhancing effect. Therefore, hollow MN was chosen to study the effect of various types of cationic nanocarriers on *in vitro* skin permeation, as they showed a superior enhancing effect.

4.2.6.2 Effect of cationic nanocarriers

The effects of cationic nanocarriers, including PEI, Lipofectamine™ 2000 and SuperFect® complexed with 50 µg of pOVA, on skin permeation using the hollow MN device were investigated. Although the nanocarrier/pOVA complexes slightly improved skin permeation in comparison with naked pOVA (pOVA without a cationic nanocarrier), there were no significant differences between the cumulative amounts at 24 h (Figure 24B and 24C). Although the partical size of the PEI/pOVA complexes at the weight ratio of 1:1 was the smallest (230 ± 7 nm), following by Lipofectamine™ 2000/pOVA complexes at the weight ratio of 2:1 (380 ± 3 nm) and the SuperFect®/pOVA complexes at the weight ratio of 6:1 (890 ± 37 nm), respectively, all of the complexes could pass through the skin into the receiver solution in the similar amount. These might be because the pOVA complexes had already existed in the

dermis by using hollow MN, therefore, there was no significant effect of the particle size of the complexes on the skin permeability.

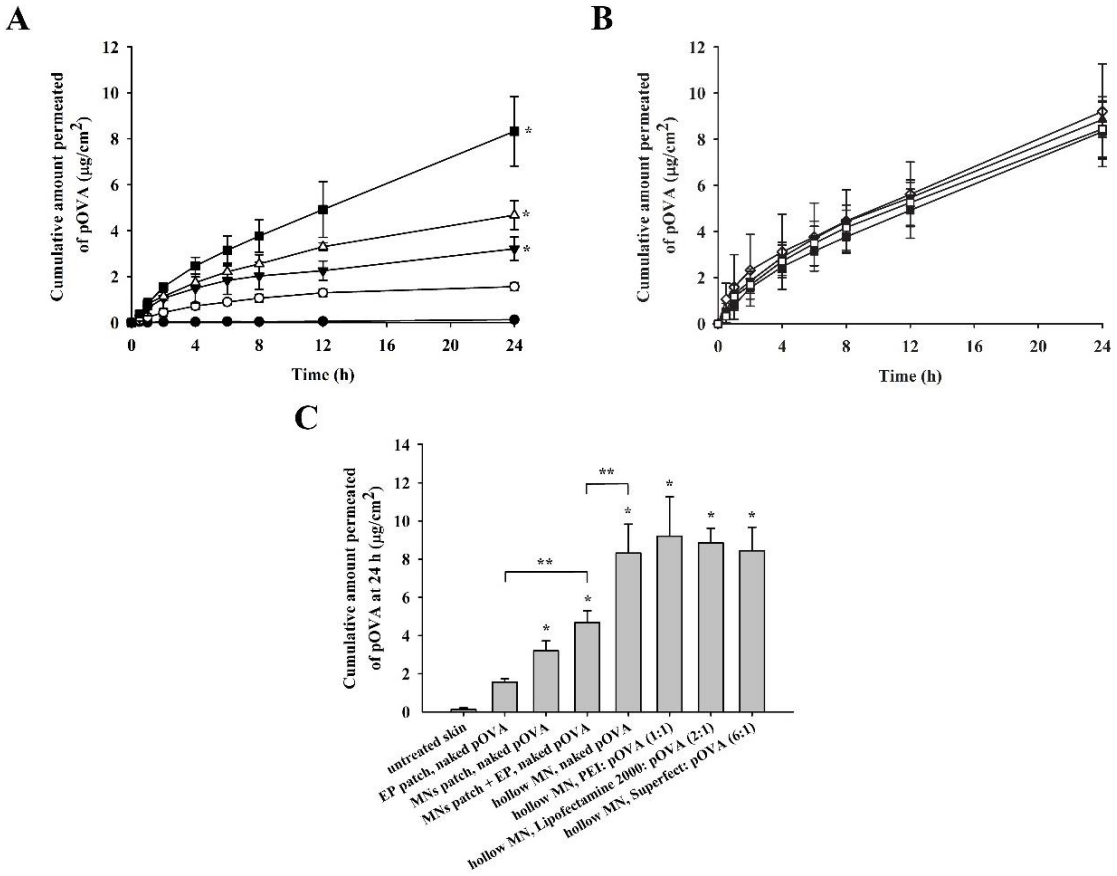

Figure 24 *In vitro* permeation profiles of pOVA across the skin with (A) various delivery devices: (●) untreated skin, (○) EPs patch, (▼) solid MNs patch, (△) combined solid MNs and EPs patch, (■) hollow MN (B) hollow MN: (■) naked pOVA, different cationic nanocarriers, including (◇) PEI/pOVA complexes, (▲) Lipofectamine™ 2000/pOVA complexes and (□) SuperFect®/pOVA complexes, (C) The cumulative amount of pOVA permeated at 24 h. *p<0.05 compared to untreated skin. **p<0.05 compared between two groups.

Table 8 The permeation parameters from the different types of MNs and formulations of pOVA *p<0.05 compared to untreated skin.

Delivery techniques, formulations	Flux (μg/cm^2·h)	ER	K_p (×10^{-2}) (cm/h)
Untreated skin	0.0047 ± 0.00	-	0.01 ± 0.00
EPs patch, naked pOVA	0.0564 ± 0.10	12	0.11 ± 0.01
MNs patch, naked pOVA	0.1243 ± 0.02	26.45	0.25 ± 0.03
MNs+EPs patch, naked pOVA	0.1888 ± 0.03*	40.17	0.38 ± 0.05*
Hollow MN, naked pOVA	0.3370 ± 0.07*	71.70	0.67 ± 0.15*
Hollow MN, PEI/pOVA (1:1)	0.3521 ± 0.07*	74.91	0.70 ± 0.15*
Hollow MN, Lipofectamine™ 2000/pOVA (2:1)	0.3525 ± 0.04*	75	0.70 ± 0.08*
Hollow MN, SuperFect®/pOVA (6:1)	0.3426 ± 0.04*	72.89	0.68 ± 0.08*

4.2.7 *In vivo* immunization study

To confirm the effect of cationic nanocarriers on improving skin immunization, IgG antibody responses were investigated in mice after a second immunization with different pOVA formulations and routes (Table 6) by measuring the plasma concentration of OVA-specific antibodies. The results revealed that the levels of IgG in the mice immunized via a hollow MN were significantly higher than the levels for the subcutaneous immunization, as shown in Figure 25. The highest IgG responses were observed in the PEI/pOVA complexes followed by the SuperFect®/pOVA complexes, Lipofectamine™ 2000/pOVA complexes and naked pOVA, respectively. Compared to naked pOVA, cationic nanocarriers/pOVA complexes significantly increased the immune responses. Upon injection of naked pDNA to activate protein expression *in vivo*, it was found that within 90 min of injection, 99% of the injected naked pDNA was degraded by endonuclease in the skin [211]. As a result, naked pDNA may be

rapidly degraded by endonuclease in the skin before transcription and translation to induce protein expression in the cells.

The IgG levels in the PEI/pOVA complexes were 2.6 and 1.4 times significantly higher than the Lipofectamine™ 2000/pOVA complexes and SuperFect®/pOVA complexes, respectively. PEI with a high molecular weight (branched PEI, 25 kDa) was used in this study, as it exhibited high transfection efficiency due to efficient endosomal escape [212]. It had a ratio of primary to secondary to tertiary amines of 1:2:1, which it could be protonated in a physical environment. PEI has a strong buffering effect over a wide physiological pH range (the proton sponge effect) because PEI escapes from the endosome and facilitates the intracellular trafficking of pDNA [213]. In contrast with Lipofectamine™ 2000/pOVA complexes, the results showed the lowest level of IgG responses, which were likely due to the major disadvantages of cationic lipids in *in vivo* use. This result corresponds to the finding from the serum stability study, Lipofectamine™ 2000/pOVA complexes were degraded in the presence of 10% BALB/c mice serum. The lipoplexes were unstable upon aggregation in the *in vivo* environments, especially in serum-containing environments due to the destabilization of vesicles, resulting in pDNA leakage from the carriers before reaching the target cells [214, 215]. For dendrimers, although the *in vitro* transfection efficiency of SuperFect® at 24 h corresponded to the lowest level, there was a higher IgG level than Lipofectamine™ 2000. Pojo *et al.* found that 48 h of exposure of the cell lines dendrimers corresponded to approximately 100 % internalization efficiency of the tested concentrations [216]. Moreover, the accumulation of radiolabeled dendrimers in mice was evaluated by Roberts *et al.*, and dendrimers accumulated in several organs over 48 h [217]. These findings suggested that accumulation might occur because the expression process of dendrimer complexes did not complete within 24 h, and thus, transfection durations more than 24 h may be required. As a result, superior immune responses were clearly observed using PEI. In addition to the method of

antigen administration, the type of nanocarrier is also an important factor for the effective induction of immune responses.

Regarding the safety issue, no skin infection or pinpoint bleeding at the site of injection was observed in any of the mice immunized with hollow MN. These results showed that using hollow MNs could induce a stronger immune response than subcutaneous injection of pOVA, which revealed that the skin is a very suitable target site for immunization.

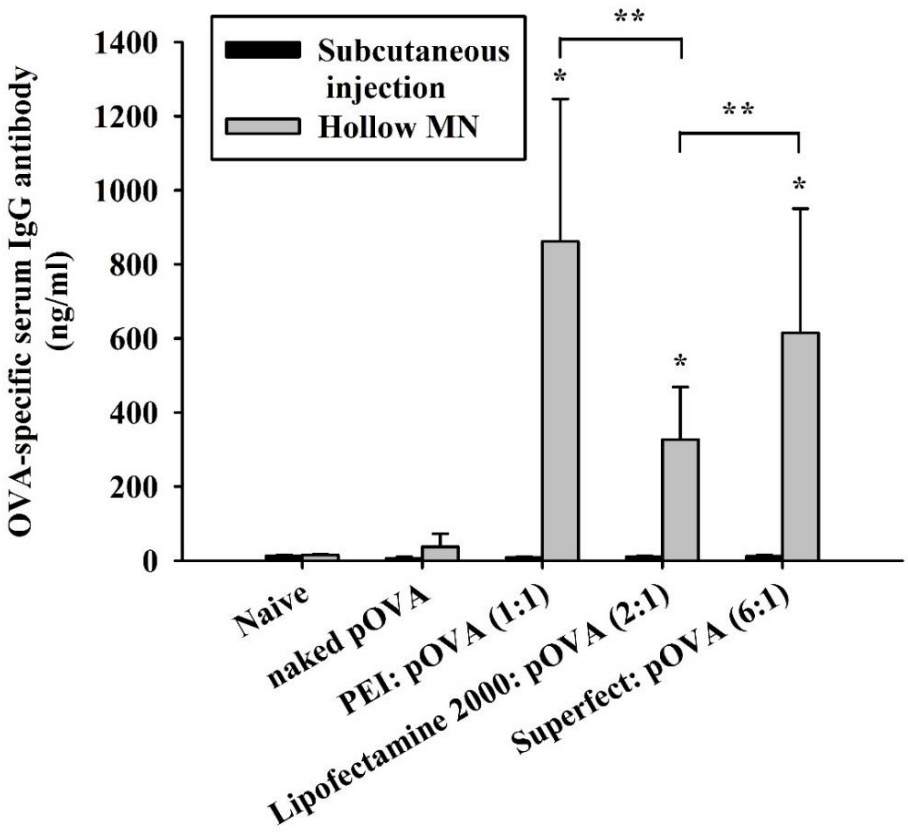

Figure 25 Antibody titers of serum IgG obtained from mice 21 days after vaccination with pOVA using (▒) a hollow MN or (■) subcutaneous injection (n=6). *p<0.05 compared to naïve group. **p<0.05 compared between two groups.

4.2.8 *In vivo* cytokine release study

To achieve potent immunization by DNA vaccination using hollow MN, activation of Th1&Th2 immunity with high immune responses are important. Th1 cells produce IFN-γ and predominantly induce cell-mediated immune responses [218]. Production of IFN-γ by Th cells is often induced by IL-12 which is secreted by APCs [219]. In contrast to Th1 cells, Th2 cells secrete IL-4 and promote the proliferation and differentiation of B-cells [218]. The balance between Th1 and Th2 cells plays a major role in immunity and pathogenesis for several infectious diseases [220]. The effect of cationic nanocarriers/pOVA complexes injections on cytokine release was assessed by measuring the cytokine levels excreted from splenocytes. The levels of IFN-γ (Th1 cytokines) and IL-4 (Th2 cytokines) secreted in the mice immunized via a hollow MN were significantly higher than the levels for the subcutaneous injected mice (Figure 26 and 27). The highest observed levels of IFN-γ and IL-4 were present in the PEI/pOVA complexes. With regards to IFN-γ and IL-4, the PEI/pOVA complexes slightly improved the IFN-γ and IL-4 cytokine release compared to naked pOVA, however, there were no significant differences. (Figure 26 and 27). The results suggest that skin immunization by hollow MN significantly enhances the differentiation of helper T cells to both Th1 and Th2 cells, which are pivotal cells for the activation of cytotoxic T lymphocytes (CTL) and B cells, respectively. Also, DNA vaccine potency is enhanced by helper T cells towards differentiation to Th1 and Th2 cells when DNA vaccine is administered with cationic nanocarrier, indicating the usefulness of cationic nanocarrier as a DNA vaccine carrier. Thus, targeted delivery of DNA vaccine using the combination of PEI and hollow MN to APCs is an effective approach for enhancing the potency of DNA vaccination.

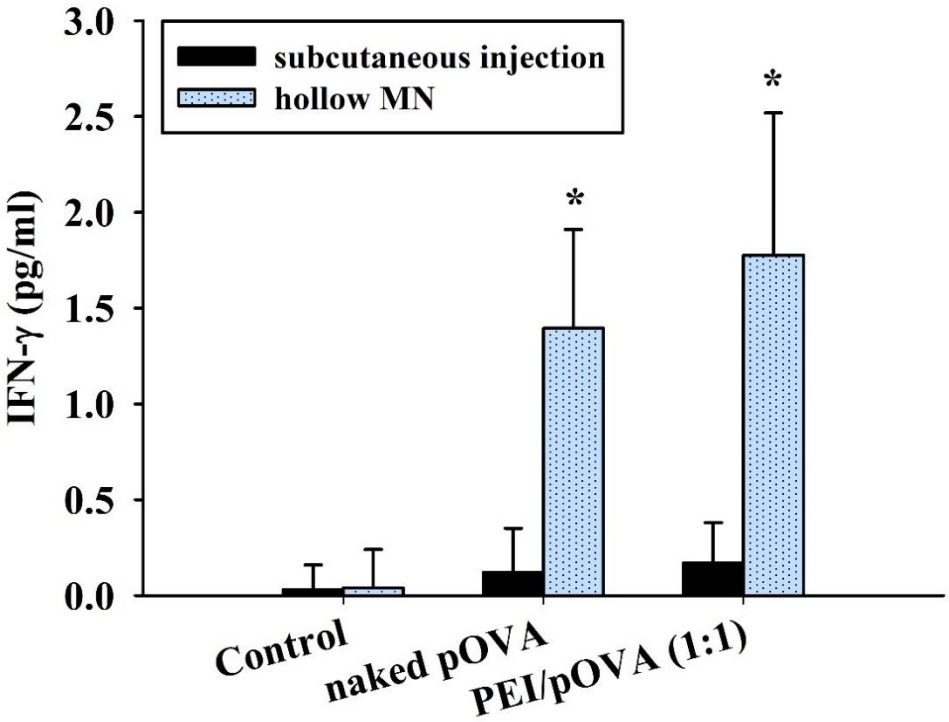

Figure 26 IFN-γ cytokine release obtained from splenocytes of mice 21 days after vaccination with different formulations of pOVA by (□) a hollow MN or (■) subcutaneous injection (n=6). *p<0.05 compared to naïve group.

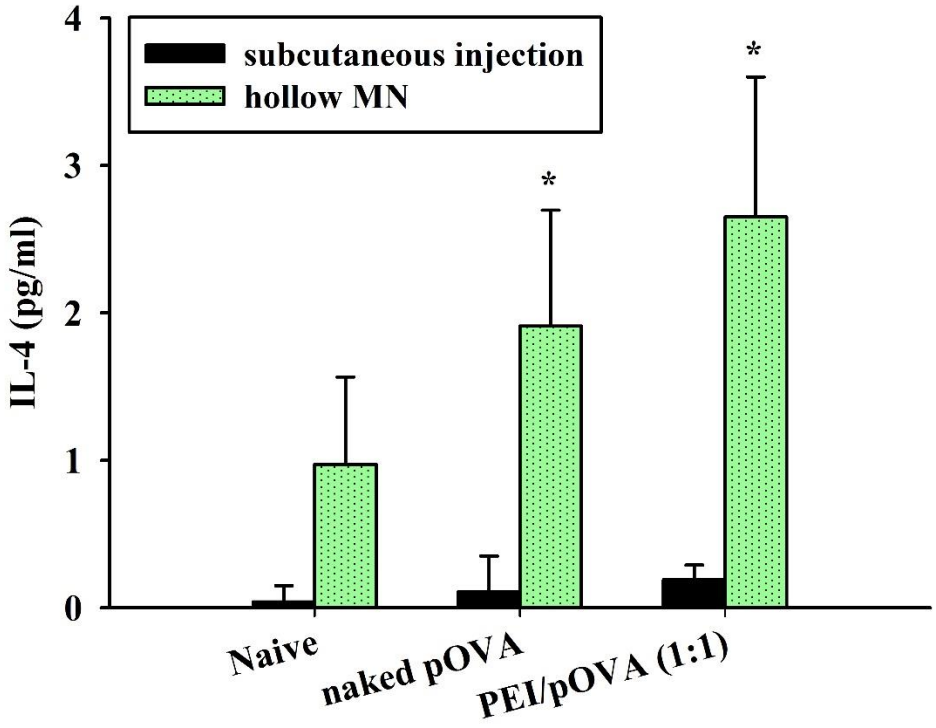

Figure 27 IL-4 cytokine release obtained from splenocytes of mice 21 days after vaccination with different formulations of pOVA by (▩) a hollow MN or (■) subcutaneous injection (n=6). *p<0.05 compared to naïve group. **p<0.05 compared to naked pOVA.

CHAPTER 5
CONCLUSION

In this study, ovalbumin (OVA) and plasmid DNA encoding OVA (pOVA), hydrophilic macromolecules, were selected as our model antigen because they can generate the immune response, whereas they have characteristically poor skin permeation. Three commercially transfection reagents, including linear 25 kDa PEI, Lipofectamine™ 2000 and SuperFect® were used as the carriers for pOVA transfection. Moreover, the effect of different delivery methods, i.e., solid MNs patch (poke and patch approach), EPs patch, solid MNs+EPs patch, and hollow MN (poke and flow approach) on OVA or pOVA are evaluated in skin permeation. The *in vivo* immune responses of OVA at different concentrations and pOVA complexes with different cationic nanocarriers using the best physical enhancement method compared with subcutaneous injection are also evaluated. The results of this study could be concluded as follow:

5.1 Effect of MNs and doses of OVA on skin permeation and skin immunization

In this study, a hollow MN and solid MNs patch were evaluated for delivery of OVA antigen at different doses into the skin. It was observed that the skin permeation and immune response to the OVA antigen were dependent on the type of MN and the antigen dose. The hollow MN successfully enhanced skin permeation and induced strong IgG immune responses. Skin permeation and the immune response were dose-dependent, but at a high concentration of the antigen, saturation of the immune response was observed. Hence, a medium dose (250 μg) of OVA-F was chosen as an optimal dose. Immunization of mice with OVA antigen using the hollow MN elicited significantly higher levels of serum IgG antibody responses compared to subcutaneous immunization, and no skin infection or pinpoint bleeding was observed. Given the clear advantages of hollow MN, this method represents a minimally invasive and safe alternative to hypodermic injections for immunization.

5.2 Effect of delivery devices and nanocarriers on skin permeation and skin immunization with pOVA

The skin permeation and immune responses to pOVA relied on the type of MN and nanocarriers. In conclusion, hollow MNs combined with PEI/pOVA complexes successfully enhanced skin permeation and induced the strongest IgG immune responses. Skin immunization with naked pOVA induced very low levels of IgG level. Immunization of mice with nanocarrier/pOVA complexes using the hollow MN elicited significantly higher levels of serum IgG antibody responses compared to subcutaneous immunization, and no skin infection or pinpoint bleeding was observed. The highest observed levels of IFN-γ and IL-4 were present in the PEI/pOVA complexes, indicating the usefulness of cationic nanocarrier as a DNA vaccine carrier. Thus, targeted delivery of DNA vaccine using the combination of PEI and hollow MN to APCs is an effective approach for enhancing the potency of DNA vaccination. These immunologic advantages, combined with safety benefits, revealed that hollow MN delivery of pOVA to the skin may offer an alternative method of skin immunization in the future.

All the results indicated that the hollow MN device could have a great potential role in promoting successful skin immunization both OVA and pOVA. Among the nanocarriers, PEI showed the highest transfection efficiency and skin immunization of pOVA.

REFERENCES

1. Hilleman, M.R., *Vaccines in historic evolution and perspective: a narrative of vaccine discoveries.* Vaccine, 2000. **18**(15): p. 1436-47.
2. Bal, S.M., et al., *Advances in transcutaneous vaccine delivery: do all ways lead to Rome?* J Control Release, 2010. **148**(3): p. 266-82.
3. Jacobson, R.M., et al., *Making vaccines more acceptable--methods to prevent and minimize pain and other common adverse events associated with vaccines.* Vaccine, 2001. **19**(17-19): p. 2418-27.
4. Berman, B., et al., *Anatomical mapping of epidermal Langerhans cell densities in adults.* Br J Dermatol, 1983. **109**(5): p. 553-8.
5. Babiuk, S., et al., *Cutaneous vaccination: the skin as an immunologically active tissue and the challenge of antigen delivery.* J Control Release, 2000. **66**(2-3): p. 199-214.
6. Kim, Y.-C., J.-H. Park, and M.R. Prausnitz, *Microneedles for drug and vaccine delivery.* Advanced Drug Delivery Reviews, 2012. **64**(14): p. 1547-1568.
7. Fuchs, E. and S. Raghavan, *Getting under the skin of epidermal morphogenesis.* Nat Rev Genet, 2002. **3**(3): p. 199-209.
8. Glenn, G.M., et al., *Transcutaneous immunization: a human vaccine delivery strategy using a patch.* Nat Med, 2000. **6**(12): p. 1403-6.
9. Kock, A., et al., *Human keratinocytes are a source for tumor necrosis factor alpha: evidence for synthesis and release upon stimulation with endotoxin or ultraviolet light.* J Exp Med, 1990. **172**(6): p. 1609-14.
10. Wood, L.C., et al., *Cutaneous barrier perturbation stimulates cytokine production in the epidermis of mice.* J Clin Invest, 1992. **90**(2): p. 482-7.
11. Fluhr, J.W., et al., *Additive impairment of the barrier function by mechanical irritation, occlusion and sodium lauryl sulphate in vivo.* Br J Dermatol, 2005. **153**(1): p. 125-31.
12. Romani, N., et al., *Langerhans cells - dendritic cells of the epidermis.* Apmis, 2003. **111**(7-8): p. 725-40.
13. Belshe, R.B., et al., *Serum antibody responses after intradermal vaccination against influenza.* N Engl J Med, 2004. **351**(22): p. 2286-94.
14. Kenney, R.T., et al., *Dose sparing with intradermal injection of influenza vaccine.* N Engl J Med, 2004. **351**(22): p. 2295-301.
15. Quan, F.S., et al., *Intradermal vaccination with influenza virus-like particles by using microneedles induces protection superior to that with intramuscular immunization.* J Virol, 2010. **84**(15): p. 7760-9.
16. Levin, Y., E. Kochba, and R. Kenney, *Clinical evaluation of a novel microneedle device for intradermal delivery of an influenza vaccine: are all delivery methods the same?* Vaccine, 2014. **32**(34): p. 4249-52.
17. van der Maaden, K., W. Jiskoot, and J. Bouwstra, *Microneedle technologies for (trans)dermal drug and vaccine delivery.* Journal of Controlled Release, 2012. **161**(2): p. 645-655.
18. Kim, Y.C., et al., *Formulation and coating of microneedles with inactivated influenza virus to improve vaccine stability and immunogenicity.* J Control Release, 2010. **142**(2): p. 187-95.
19. Qiu, Y., et al., *DNA-based vaccination against hepatitis B virus using dissolving*

microneedle arrays adjuvanted by cationic liposomes and CpG ODN. Drug Deliv, 2016. **23**(7): p. 2391-2398.
20. Edens, C., et al., *Inactivated polio vaccination using a microneedle patch is immunogenic in the rhesus macaque.* Vaccine, 2015. **33**(37): p. 4683-90.
21. Kalluri, H., C.S. Kolli, and A.K. Banga, *Characterization of Microchannels Created by Metal Microneedles: Formation and Closure.* The AAPS Journal, 2011. **13**(3): p. 473-481.
22. Li, J., et al., *Fabrication of a Ti porous microneedle array by metal injection molding for transdermal drug delivery.* PLOS ONE, 2017. **12**(2): p. e0172043.
23. Vinayakumar, K.B., et al., *A hollow stainless steel microneedle array to deliver insulin to a diabetic rat.* Journal of Micromechanics and Microengineering, 2016. **26**(6): p. 065013.
24. Chen, B., et al., *Silicon microneedle array with biodegradable tips for transdermal drug delivery.* Microsystem Technologies, 2008. **14**(7): p. 1015-1019.
25. Ashraf, M.W., et al., *Design, fabrication and analysis of silicon hollow microneedles for transdermal drug delivery system for treatment of hemodynamic dysfunctions.* Cardiovasc Eng, 2010. **10**(3): p. 91-108.
26. Duan, D., et al., *Enhanced delivery of topically-applied formulations following skin pre-treatment with a hand-applied, plastic microneedle array.* Curr Drug Deliv, 2011. **8**(5): p. 557-65.
27. Ayittey, P.N., et al., *Glass microneedles for force measurements: a finite-element analysis model.* Pflugers Arch, 2009. **457**(6): p. 1415-22.
28. Hong, X., et al., *Dissolving and biodegradable microneedle technologies for transdermal sustained delivery of drug and vaccine.* Drug Des Devel Ther, 2013. **7**: p. 945-52.
29. Park, J.-H., M.G. Allen, and M.R. Prausnitz, *Biodegradable polymer microneedles: Fabrication, mechanics and transdermal drug delivery.* Journal of Controlled Release, 2005. **104**(1): p. 51-66.
30. Kyoung Je, C., et al., *Simple and cost-effective fabrication of solid biodegradable polymer microneedle arrays with adjustable aspect ratio for transdermal drug delivery using acupuncture microneedles.* Journal of Micromechanics and Microengineering, 2014. **24**(11): p. 115015.
31. Nguyen, H.X. and A.K. Banga, *Fabrication, characterization and application of sugar microneedles for transdermal drug delivery.* Ther Deliv, 2017. **8**(5): p. 249-264.
32. Miyano, T., et al., *Sugar micro needles as transdermic drug delivery system.* Biomed Microdevices, 2005. **7**(3): p. 185-8.
33. Loizidou, E.Z., et al., *Structural characterisation and transdermal delivery studies on sugar microneedles: experimental and finite element modelling analyses.* Eur J Pharm Biopharm, 2015. **89**: p. 224-31.
34. Lombry, C., N. Dujardin, and V. Preat, *Transdermal delivery of macromolecules using skin electroporation.* Pharm Res, 2000. **17**(1): p. 32-7.
35. Denet, A.R., R. Vanbever, and V. Preat, *Skin electroporation for transdermal and topical delivery.* Adv Drug Deliv Rev, 2004. **56**(5): p. 659-74.
36. Yan, K., H. Todo, and K. Sugibayashi, *Transdermal drug delivery by in-skin electroporation using a microneedle array.* Int J Pharm, 2010. **397**(1-2): p. 77-

83.
37. Petchsangsai, M., et al., *The combination of microneedles with electroporation and sonophoresis to enhance hydrophilic macromolecule skin penetration.* Biol Pharm Bull, 2014. **37**(8): p. 1373-82.
38. Shedlock, D.J. and D.B. Weiner, *DNA vaccination: antigen presentation and the induction of immunity.* J Leukoc Biol, 2000. **68**(6): p. 793-806.
39. Tang, D.C., M. DeVit, and S.A. Johnston, *Genetic immunization is a simple method for eliciting an immune response.* Nature, 1992. **356**(6365): p. 152-4.
40. Pereira, V.B., et al., *DNA Vaccines Approach: From Concepts to Applications.* World Journal of Vaccines, 2014. **Vol.04No.02**: p. 22.
41. Perdue, M.L., et al., *The future of cell culture-based influenza vaccine production.* Expert Rev Vaccines, 2011. **10**(8): p. 1183-94.
42. Arturo, R.-S. and C.J.E. Hildegund, *DNA Vaccines.* Current Molecular Medicine, 2001. **1**(2): p. 217-243.
43. Kutzler, M.A. and D.B. Weiner, *DNA vaccines: ready for prime time?* Nat Rev Genet, 2008. **9**(10): p. 776-88.
44. Mumper, R.J. and H.C. Ledebur, Jr., *Dendritic cell delivery of plasmid DNA. Applications for controlled genetic immunization.* Mol Biotechnol, 2001. **19**(1): p. 79-95.
45. Xiang, Z.Q., et al., *Vaccination with a plasmid vector carrying the rabies virus glycoprotein gene induces protective immunity against rabies virus.* Virology, 1994. **199**(1): p. 132-40.
46. Sedegah, M., et al., *Protection against malaria by immunization with plasmid DNA encoding circumsporozoite protein.* Proceedings of the National Academy of Sciences of the United States of America, 1994. **91**(21): p. 9866-9870.
47. Tascon, R.E., et al., *Vaccination against tuberculosis by DNA injection.* Nature Medicine, 1996. **2**: p. 888.
48. Yin, H., et al., *Non-viral vectors for gene-based therapy.* Nature Reviews Genetics, 2014. **15**: p. 541.
49. Schaffer, D.V., J.T. Koerber, and K.I. Lim, *Molecular engineering of viral gene delivery vehicles.* Annu Rev Biomed Eng, 2008. **10**: p. 169-94.
50. Leong, K.W., et al., *DNA-polycation nanospheres as non-viral gene delivery vehicles.* J Control Release, 1998. **53**(1-3): p. 183-93.
51. Midoux, P., et al., *Polymer-based gene delivery: a current review on the uptake and intracellular trafficking of polyplexes.* Curr Gene Ther, 2008. **8**(5): p. 335-52.
52. Lonez, C., M. Vandenbranden, and J.M. Ruysschaert, *Cationic liposomal lipids: from gene carriers to cell signaling.* Prog Lipid Res, 2008. **47**(5): p. 340-7.
53. Dufès, C., I.F. Uchegbu, and A.G. Schätzlein, *Dendrimers in gene delivery.* Advanced Drug Delivery Reviews, 2005. **57**(15): p. 2177-2202.
54. Vázquez, E., N. Ferrer-Miralles, and A. Villaverde, *Peptide-assisted traffic engineering for nonviral gene therapy.* Drug Discovery Today, 2008. **13**(23): p. 1067-1074.
55. Ravi Kumar, M., et al., *Nanoparticle-mediated gene delivery: state of the art.* Expert Opin Biol Ther, 2004. **4**(8): p. 1213-24.
56. Al-Dosari, M.S. and X. Gao, *Nonviral Gene Delivery: Principle, Limitations, and Recent Progress.* The AAPS Journal, 2009. **11**(4): p. 671.

57. Park, T.G., J.H. Jeong, and S.W. Kim, *Current status of polymeric gene delivery systems.* Adv Drug Deliv Rev, 2006. **58**(4): p. 467-86.
58. Mescher, A.L., *Chapter 18. Skin*, in *Junqueira's Basic Histology, 13e*. 2013, The McGraw-Hill Companies: New York, NY.
59. Draelos, Z.D., Z.K. Draelos, and P.T. Pugliese, *Physiology of the Skin*. 2011: Allured Business Media.
60. Hadgraft, J., *Skin, the final frontier.* Int J Pharm, 2001. **224**(1-2): p. 1-18.
61. Menon, G.K., G.W. Cleary, and M.E. Lane, *The structure and function of the stratum corneum.* International Journal of Pharmaceutics, 2012. **435**(1): p. 3-9.
62. Bachinger, H.P., et al., *The relationship of the biophysical and biochemical characteristics of type VII collagen to the function of anchoring fibrils.* J Biol Chem, 1990. **265**(17): p. 10095-101.
63. Goldsmith, L.A., et al., *Fitzpatrick's Dermatology in General Medicine, Eighth Edition, 2 Volume set*. 2012: McGraw-Hill Education.
64. Sandberg, L.B., N.T. Soskel, and T.B. Wolt, *Structure of the elastic fiber: an overview.* J Invest Dermatol, 1982. **79 Suppl 1**: p. 128s-132s.
65. Schaefer, H. and T.E. Redelmeier, *Skin barrier: principles of percutaneous absorption*. 1996: Karger.
66. Prausnitz, M.R., S. Mitragotri, and R. Langer, *Current status and future potential of transdermal drug delivery.* Nat Rev Drug Discov, 2004. **3**(2): p. 115-24.
67. Barry, B.W., *Novel mechanisms and devices to enable successful transdermal drug delivery.* Eur J Pharm Sci, 2001. **14**(2): p. 101-14.
68. Benson, H.A., *Transdermal drug delivery: penetration enhancement techniques.* Curr Drug Deliv, 2005. **2**(1): p. 23-33.
69. Williams, A., *Transdermal and Topical Drug Delivery from Theory to Clinical Practice*. 2003: Pharmaceutical Press.
70. Watkinson, A.C. and K.R. Brain, *Basic Mathematical Principles In Skin Permeation.* Journal of Toxicology: Cutaneous and Ocular Toxicology, 2002. **21**(4): p. 371-402.
71. Yamashita, F. and M. Hashida, *Mechanistic and empirical modeling of skin permeation of drugs.* Adv Drug Deliv Rev, 2003. **55**(9): p. 1185-99.
72. Kanikkannan, N., et al., *Structure-activity relationship of chemical penetration enhancers in transdermal drug delivery.* Curr Med Chem, 2000. **7**(6): p. 593-608.
73. Alexander, A., et al., *Approaches for breaking the barriers of drug permeation through transdermal drug delivery.* J Control Release, 2012. **164**(1): p. 26-40.
74. Smith, E.W. and H.I. Maibach, *Percutaneous Penetration Enhancers, Second Edition*. 2005: CRC Press.
75. Lopes, L.B., M.T. Garcia, and M.V. Bentley, *Chemical penetration enhancers.* Ther Deliv, 2015. **6**(9): p. 1053-61.
76. Ding, Z., et al., *Microneedle arrays for the transcutaneous immunization of diphtheria and influenza in BALB/c mice.* J Control Release, 2009. **136**(1): p. 71-8.
77. Hirobe, S., et al., *Clinical study and stability assessment of a novel transcutaneous influenza vaccination using a dissolving microneedle patch.* Biomaterials, 2015. **57**: p. 50-8.

78. Song, J.M., et al., *DNA vaccination in the skin using microneedles improves protection against influenza.* Mol Ther, 2012. **20**(7): p. 1472-80.
79. Norman, J.J., et al., *Microneedle patches: usability and acceptability for self-vaccination against influenza.* Vaccine, 2014. **32**(16): p. 1856-62.
80. Matsuo, K., et al., *Vaccine efficacy of transcutaneous immunization with amyloid beta using a dissolving microneedle array in a mouse model of Alzheimer's disease.* J Neuroimmunol, 2014. **266**(1-2): p. 1-11.
81. Hirschberg, H., et al., *A combined approach of vesicle formulations and microneedle arrays for transcutaneous immunization against hepatitis B virus.* Eur J Pharm Sci, 2012. **46**(1-2): p. 1-7.
82. Ma, Y., et al., *Vaccine delivery to the oral cavity using coated microneedles induces systemic and mucosal immunity.* Pharm Res, 2014. **31**(9): p. 2393-403.
83. Dean, C.H., et al., *Cutaneous delivery of a live, attenuated chimeric flavivirus vaccine against Japanese encephalitis (ChimeriVax)-JE) in non-human primates.* Hum Vaccin, 2005. **1**(3): p. 106-11.
84. van der Maaden, K., et al., *Novel hollow microneedle technology for depth-controlled microinjection-mediated dermal vaccination: a study with polio vaccine in rats.* Pharm Res, 2014. **31**(7): p. 1846-54.
85. Laurent, P.E., et al., *Safety and efficacy of novel dermal and epidermal microneedle delivery systems for rabies vaccination in healthy adults.* Vaccine, 2010. **28**(36): p. 5850-6.
86. Moon, S., et al., *Dose sparing and enhanced immunogenicity of inactivated rotavirus vaccine administered by skin vaccination using a microneedle patch.* Vaccine, 2013. **31**(34): p. 3396-402.
87. Birchall, J.C., *Microneedle array technology: the time is right but is the science ready?* Expert Rev Med Devices, 2006. **3**(1): p. 1-4.
88. Escobar-Chávez, J.J., et al., *Microneedles: A Valuable Physical Enhancer to Increase Transdermal Drug Delivery.* The Journal of Clinical Pharmacology, 2011. **51**(7): p. 964-977.
89. Kalluri, H. and A.K. Banga, *Formation and closure of microchannels in skin following microporation.* Pharm Res, 2011. **28**(1): p. 82-94.
90. Prausnitz, M.R., et al., *Microneedle-Based Vaccines*, in *Vaccines for Pandemic Influenza*, R.W. Compans and W.A. Orenstein, Editors. 2009, Springer Berlin Heidelberg. p. 370-389.
91. van der Maaden, K., et al., *Impact-insertion applicator improves reliability of skin penetration by solid microneedle arrays.* Aaps j, 2014. **16**(4): p. 681-4.
92. Chen, H., et al., *Iontophoresis-driven penetration of nanovesicles through microneedle-induced skin microchannels for enhancing transdermal delivery of insulin.* J Control Release, 2009. **139**(1): p. 63-72.
93. Wu, X.-M., H. Todo, and K. Sugibayashi, *Enhancement of skin permeation of high molecular compounds by a combination of microneedle pretreatment and iontophoresis.* Journal of Controlled Release, 2007. **118**(2): p. 189-195.
94. Henry, S., et al., *Microfabricated microneedles: a novel approach to transdermal drug delivery.* J Pharm Sci, 1998. **87**(8): p. 922-5.
95. McAllister, D.V., et al., *Microfabricated needles for transdermal delivery of macromolecules and nanoparticles: fabrication methods and transport studies.* Proc Natl Acad Sci U S A, 2003. **100**(24): p. 13755-60.

96. Pearton, M., et al., *Gene delivery to the epidermal cells of human skin explants using microfabricated microneedles and hydrogel formulations.* Pharm Res, 2008. **25**(2): p. 407-16.
97. Martanto, W., et al., *Transdermal delivery of insulin using microneedles in vivo.* Pharm Res, 2004. **21**(6): p. 947-52.
98. Gill, H.S., et al., *Effect of microneedle design on pain in human subjects.* The Clinical journal of pain, 2008. **24**(7): p. 585-594.
99. Verbaan, F.J., et al., *Improved piercing of microneedle arrays in dermatomed human skin by an impact insertion method.* J Control Release, 2008. **128**(1): p. 80-8.
100. Gill, H.S. and M.R. Prausnitz, *Coated microneedles for transdermal delivery.* J Control Release, 2007. **117**(2): p. 227-37.
101. Kalluri, H. and A.K. Banga, *Transdermal Delivery of Proteins.* AAPS PharmSciTech, 2011. **12**(1): p. 431-441.
102. Bariya, S.H., et al., *Microneedles: an emerging transdermal drug delivery system.* J Pharm Pharmacol, 2012. **64**(1): p. 11-29.
103. Kulkarni, V.S., *Handbook of Non-Invasive Drug Delivery Systems: Science and Technology*. 2009: Elsevier Science.
104. Pearton, M., et al., *Microneedle delivery of plasmid DNA to living human skin: Formulation coating, skin insertion and gene expression.* J Control Release, 2012. **160**(3): p. 561-9.
105. Lutton, R.E., et al., *Microneedle characterisation: the need for universal acceptance criteria and GMP specifications when moving towards commercialisation.* Drug Deliv Transl Res, 2015. **5**(4): p. 313-31.
106. Lee, K., C.Y. Lee, and H. Jung, *Dissolving microneedles for transdermal drug administration prepared by stepwise controlled drawing of maltose.* Biomaterials, 2011. **32**(11): p. 3134-40.
107. Ronnander, P., et al., *Dissolving polyvinylpyrrolidone-based microneedle systems for in-vitro delivery of sumatriptan succinate.* Eur J Pharm Sci, 2018. **114**: p. 84-92.
108. Ling, M.H. and M.C. Chen, *Dissolving polymer microneedle patches for rapid and efficient transdermal delivery of insulin to diabetic rats.* Acta Biomater, 2013. **9**(11): p. 8952-61.
109. Ito, Y., et al., *Application of dissolving microneedles to glucose monitoring through dermal interstitial fluid.* Biol Pharm Bull, 2014. **37**(11): p. 1776-81.
110. Ito, Y., et al., *Two-layered dissolving microneedles for percutaneous delivery of sumatriptan in rats.* Drug Dev Ind Pharm, 2011. **37**(12): p. 1387-93.
111. Chu, L.Y. and M.R. Prausnitz, *Separable arrowhead microneedles.* J Control Release, 2011. **149**(3): p. 242-9.
112. McCrudden, M.T., et al., *Microneedle applications in improving skin appearance.* Exp Dermatol, 2015. **24**(8): p. 561-6.
113. Indermun, S., et al., *Current advances in the fabrication of microneedles for transdermal delivery.* J Control Release, 2014. **185**: p. 130-8.
114. Tuan-Mahmood, T.M., et al., *Microneedles for intradermal and transdermal drug delivery.* Eur J Pharm Sci, 2013. **50**(5): p. 623-37.
115. Kim, Y.C., J.H. Park, and M.R. Prausnitz, *Microneedles for drug and vaccine delivery.* Adv Drug Deliv Rev, 2012. **64**(14): p. 1547-68.

116. Wermeling, D.P., et al., *Microneedles permit transdermal delivery of a skin-impermeant medication to humans.* Proceedings of the National Academy of Sciences of the United States of America, 2008. **105**(6): p. 2058-2063.
117. Ameri, M., X. Wang, and Y.F. Maa, *Effect of irradiation on parathyroid hormone PTH(1-34) coated on a novel transdermal microprojection delivery system to produce a sterile product--adhesive compatibility.* J Pharm Sci, 2010. **99**(4): p. 2123-34.
118. Cormier, M. and P. Daddona, *Macroflux Technology for Transdermal Delivery of Therapeutic Proteins and Vaccines*, in *Modified-Release Drug Delivery Technology*, M.J. Rathbone, J. Hadgraft, and M.S. Roberts, Editors. 2002, Taylor & Francis. p. 589-598.
119. Cormier, M., et al., *Transdermal delivery of desmopressin using a coated microneedle array patch system.* J Control Release, 2004. **97**(3): p. 503-11.
120. Matriano, J.A., et al., *Macroflux microprojection array patch technology: a new and efficient approach for intracutaneous immunization.* Pharm Res, 2002. **19**(1): p. 63-70.
121. Widera, G., et al., *Effect of delivery parameters on immunization to ovalbumin following intracutaneous administration by a coated microneedle array patch system.* Vaccine, 2006. **24**(10): p. 1653-64.
122. Prausnitz, M.R., et al., *Microneedle-Based Vaccines*, in *Vaccines for Pandemic Influenza*, R.W. Compans and W.A. Orenstein, Editors. 2009, Springer Berlin Heidelberg: Berlin, Heidelberg. p. 369-393.
123. Kaushik, S., et al., *Lack of pain associated with microfabricated microneedles.* Anesth Analg, 2001. **92**(2): p. 502-4.
124. Mikszta, J.A., et al., *Improved genetic immunization via micromechanical disruption of skin-barrier function and targeted epidermal delivery.* Nat Med, 2002. **8**(4): p. 415-9.
125. Barker, J.H. and T.J. Ryan, *Skin microcirculation*, in *Clinically Applied Microcirculation Research*, J.H. Barker, G.L. Anderson, and M.D. Menger, Editors. 1995, Taylor & Francis. p. 315-338.
126. Martanto, W., et al., *Transdermal Delivery of Insulin Using Microneedles in Vivo.* Pharmaceutical Research, 2004. **21**(6): p. 947-952.
127. Gardeniers, H.J.G.E., et al., *Silicon micromachined hollow microneedles for transdermal liquid transport.* Journal of Microelectromechanical Systems, 2003. **12**(6): p. 855-862.
128. Lin, W., et al., *Transdermal delivery of antisense oligonucleotides with microprojection patch (Macroflux) technology.* Pharm Res, 2001. **18**(12): p. 1789-93.
129. Ellner, P.D., *Smallpox: Gone but not forgotten.* Infection, 1998. **26**(5): p. 263-269.
130. Huang, C.M., *Topical vaccination: the skin as a unique portal to adaptive immune responses.* Semin Immunopathol, 2007. **29**(1): p. 71-80.
131. Larregina, A.T. and L.D. Falo, Jr., *Changing paradigms in cutaneous immunology: adapting with dendritic cells.* J Invest Dermatol, 2005. **124**(1): p. 1-12.
132. Bronaugh, R.L. and H.I. Maibach, *Percutaneous Absorption: Drugs--Cosmetics--Mechanisms--Methodology: Drugs--Cosmetics--Mechanisms--Methodology,*

Third Edition. 1999: CRC Press.
133. Prausnitz, M.R. and R. Langer, *Transdermal drug delivery.* Nature biotechnology, 2008. **26**(11): p. 1261-1268.
134. Birchall, J., et al., *Cutaneous DNA delivery and gene expression in ex vivo human skin explants via wet-etch micro-fabricated micro-needles.* J Drug Target, 2005. **13**(7): p. 415-21.
135. Wong, T.W., *Electrical, magnetic, photomechanical and cavitational waves to overcome skin barrier for transdermal drug delivery.* J Control Release, 2014. **193**: p. 257-69.
136. Prausnitz, M.R., et al., *Electroporation of mammalian skin: a mechanism to enhance transdermal drug delivery.* Proc Natl Acad Sci U S A, 1993. **90**(22): p. 10504-8.
137. Weaver, J.C., *Electroporation: a general phenomenon for manipulating cells and tissues.* J Cell Biochem, 1993. **51**(4): p. 426-35.
138. Weaver, J.C., *Electroporation theory. Concepts and mechanisms.* Methods Mol Biol, 1995. **47**: p. 1-26.
139. Zorec, B., et al., *Skin electroporation for transdermal drug delivery: the influence of the order of different square wave electric pulses.* Int J Pharm, 2013. **457**(1): p. 214-23.
140. Vanbever, R., M.A. Leroy, and V. Preat, *Transdermal permeation of neutral molecules by skin electroporation.* J Control Release, 1998. **54**(3): p. 243-50.
141. Vanbever, R. and V. Préat, *Factors affecting transdermal delivery of metoprolol by electroporation.* Bioelectrochemistry and Bioenergetics, 1995. **38**(1): p. 223-228.
142. Sung, K.C., et al., *Transdermal delivery of nalbuphine and its prodrugs by electroporation.* Eur J Pharm Sci, 2003. **18**(1): p. 63-70.
143. Lin, F., et al., *A novel prototype device for electroporation-enhanced DNA vaccine delivery simultaneously to both skin and muscle.* Vaccine, 2011. **29**(39): p. 6771-80.
144. Zhang, L., et al., *Enhanced delivery of naked DNA to the skin by non-invasive in vivo electroporation.* Biochim Biophys Acta, 2002. **1572**(1): p. 1-9.
145. Chou, T.-h.W., S. Biswas, and S. Lu, *Gene Delivery Using Physical Methods*, in *Gene Delivery to Mammalian Cells: Volume 1: Nonviral Gene Transfer Techniques*, W.C. Heiser, Editor. 2004, Humana Press: Totowa, NJ. p. 147-165.
146. Chang, D.C. and T.S. Reese, *Changes in membrane structure induced by electroporation as revealed by rapid-freezing electron microscopy.* Biophysical Journal, 1990. **58**(1): p. 1-12.
147. Mehier-Humbert, S. and R.H. Guy, *Physical methods for gene transfer: improving the kinetics of gene delivery into cells.* Adv Drug Deliv Rev, 2005. **57**(5): p. 733-53.
148. Jinturkar, K.A., M.N. Rathi, and A. Misra, *3 - Gene Delivery Using Physical Methods*, in *Challenges in Delivery of Therapeutic Genomics and Proteomics*. 2011, Elsevier: London. p. 83-126.
149. Gothelf, A., L.M. Mir, and J. Gehl, *Electrochemotherapy: results of cancer treatment using enhanced delivery of bleomycin by electroporation.* Cancer Treat Rev, 2003. **29**(5): p. 371-87.
150. Bigey, P., M.F. Bureau, and D. Scherman, *In vivo plasmid DNA electrotransfer.*

Current Opinion in Biotechnology, 2002. **13**(5): p. 443-447.
151. Chiarella, P., et al., *Electroporation of skeletal muscle induces danger signal release and antigen-presenting cell recruitment independently of DNA vaccine administration.* Expert Opin Biol Ther, 2008. **8**(11): p. 1645-57.
152. Todorova, B., et al., *Electroporation as a vaccine delivery system and a natural adjuvant to intradermal administration of plasmid DNA in macaques.* Sci Rep, 2017. **7**(1): p. 4122.
153. Mehier-Humbert, S. and R.H. Guy, *Physical methods for gene transfer: Improving the kinetics of gene delivery into cells.* Advanced Drug Delivery Reviews, 2005. **57**(5): p. 733-753.
154. Vanbever, R. and V.V. Preat, *In vivo efficacy and safety of skin electroporation.* Adv Drug Deliv Rev, 1999. **35**(1): p. 77-88.
155. Jadoul, A., J. Bouwstra, and V.V. Preat, *Effects of iontophoresis and electroporation on the stratum corneum. Review of the biophysical studies.* Adv Drug Deliv Rev, 1999. **35**(1): p. 89-105.
156. Prausnitz, M.R., *The effects of electric current applied to skin: A review for transdermal drug delivery.* Advanced Drug Delivery Reviews, 1996. **18**(3): p. 395-425.
157. Choi, S.-O., et al., *An electrically active microneedle array for electroporation.* Biomedical microdevices, 2010. **12**(2): p. 263-273.
158. Wei, Z., et al., *A flexible microneedle array as low-voltage electroporation electrodes for in vivo DNA and siRNA delivery.* Lab on a Chip, 2014. **14**(20): p. 4093-4102.
159. Li, L., F. Saade, and N. Petrovsky, *The future of human DNA vaccines.* J Biotechnol, 2012. **162**(2-3): p. 171-82.
160. Khan, K.H., *DNA vaccines: roles against diseases.* Germs, 2013. **3**(1): p. 26-35.
161. Liu, M.A., *DNA vaccines: a review.* J Intern Med, 2003. **253**(4): p. 402-10.
162. Xiang, S.D., et al., *Delivery of DNA vaccines: an overview on the use of biodegradable polymeric and magnetic nanoparticles.* Wiley Interdisciplinary Reviews: Nanomedicine and Nanobiotechnology, 2010. **2**(3): p. 205-218.
163. Ibraheem, D., A. Elaissari, and H. Fessi, *Gene therapy and DNA delivery systems.* International Journal of Pharmaceutics, 2014. **459**(1): p. 70-83.
164. Elouahabi, A. and J.M. Ruysschaert, *Formation and intracellular trafficking of lipoplexes and polyplexes.* Mol Ther, 2005. **11**(3): p. 336-47.
165. Boussif, O., et al., *A versatile vector for gene and oligonucleotide transfer into cells in culture and in vivo: polyethylenimine.* Proc Natl Acad Sci U S A, 1995. **92**(16): p. 7297-301.
166. Pires, P., et al., *Interaction of cationic liposomes and their DNA complexes with monocytic leukemia cells.* Biochim Biophys Acta, 1999. **1418**(1): p. 71-84.
167. Simoes, S., et al., *Mechanisms of gene transfer mediated by lipoplexes associated with targeting ligands or pH-sensitive peptides.* Gene Ther, 1999. **6**(11): p. 1798-807.
168. Brunner, S., et al., *Cell cycle dependence of gene transfer by lipoplex, polyplex and recombinant adenovirus.* Gene Ther, 2000. **7**(5): p. 401-7.
169. Tros de Ilarduya, C., Y. Sun, and N. Duzgunes, *Gene delivery by lipoplexes and polyplexes.* Eur J Pharm Sci, 2010. **40**(3): p. 159-70.
170. Cho, C.-S., *Design and Development of Degradable Polyethylenimines for*

Delivery of DNA and Small Interfering RNA: An Updated Review. ISRN Materials Science, 2012. **2012**: p. 24.

171. Boussif, O., et al., *A versatile vector for gene and oligonucleotide transfer into cells in culture and in vivo: polyethylenimine.* Proceedings of the National Academy of Sciences of the United States of America, 1995. **92**(16): p. 7297-301.
172. Intra, J. and A.K. Salem, *Characterization of the transgene expression generated by branched and linear polyethylenimine-plasmid DNA nanoparticles in vitro and after intraperitoneal injection in vivo.* J Control Release, 2008. **130**(2): p. 129-38.
173. Dunlap, D.D., et al., *Nanoscopic structure of DNA condensed for gene delivery.* Nucleic Acids Research, 1997. **25**(15): p. 3095-3101.
174. Godbey, W.T., K.K. Wu, and A.G. Mikos, *Poly(ethylenimine) and its role in gene delivery.* Journal of Controlled Release, 1999. **60**(2): p. 149-160.
175. Neu, M., D. Fischer, and T. Kissel, *Recent advances in rational gene transfer vector design based on poly(ethylene imine) and its derivatives.* Journal of Gene Medicine, 2005. **7**(8): p. 992-1009.
176. Neu, M., D. Fischer, and T. Kissel, *Recent advances in rational gene transfer vector design based on poly(ethylene imine) and its derivatives.* J Gene Med, 2005. **7**(8): p. 992-1009.
177. Choosakoonkriang, S., et al., *Biophysical characterization of PEI/DNA complexes.* J Pharm Sci, 2003. **92**(8): p. 1710-22.
178. Zinselmeyer, B.H., et al., *The lower-generation polypropylenimine dendrimers are effective gene-transfer agents.* Pharm Res, 2002. **19**(7): p. 960-7.
179. Fischer, D., et al., *In vitro cytotoxicity testing of polycations: influence of polymer structure on cell viability and hemolysis.* Biomaterials, 2003. **24**(7): p. 1121-31.
180. Eichman, J.D., et al., *The use of PAMAM dendrimers in the efficient transfer of genetic material into cells.* Pharm Sci Technolo Today, 2000. **3**(7): p. 232-245.
181. Zhu, L. and R.I. Mahato, *Lipid and polymeric carrier-mediated nucleic acid delivery.* Expert Opinion on Drug Delivery, 2010. **7**(10): p. 1209-1226.
182. Haensler, J. and F.C. Szoka, Jr., *Polyamidoamine cascade polymers mediate efficient transfection of cells in culture.* Bioconjug Chem, 1993. **4**(5): p. 372-9.
183. Kukowska-Latallo, J.F., et al., *Efficient transfer of genetic material into mammalian cells using Starburst polyamidoamine dendrimers.* Proceedings of the National Academy of Sciences of the United States of America, 1996. **93**(10): p. 4897-4902.
184. Sonawane, N.D., F.C. Szoka, Jr., and A.S. Verkman, *Chloride accumulation and swelling in endosomes enhances DNA transfer by polyamine-DNA polyplexes.* J Biol Chem, 2003. **278**(45): p. 44826-31.
185. Lee, J.H., et al., *Polyplexes assembled with internally quaternized PAMAM-OH dendrimer and plasmid DNA have a neutral surface and gene delivery potency.* Bioconjug Chem, 2003. **14**(6): p. 1214-21.
186. Waite, C.L., et al., *Acetylation of PAMAM dendrimers for cellular delivery of siRNA.* BMC Biotechnol, 2009. **9**: p. 38.
187. Tang, M.X., C.T. Redemann, and F.C. Szoka, Jr., *In vitro gene delivery by degraded polyamidoamine dendrimers.* Bioconjug Chem, 1996. **7**(6): p. 703-14.

188. Thapa, B. and R. Narain, *1 - Mechanism, current challenges and new approaches for non viral gene delivery*, in *Polymers and Nanomaterials for Gene Therapy*. 2016, Woodhead Publishing. p. 1-27.
189. Aramaki, Y., et al., *Recognition of charged liposomes by rat peritoneal and splenic macrophages: effects of fibronectin on the uptake of charged liposomes.* European Journal of Pharmaceutical Sciences, 1995. **3**(2): p. 63-70.
190. Mutsaers, S.E. and J.M. Papadimitriou, *Surface charge of macrophages and their interaction with charged particles.* J Leukoc Biol, 1988. **44**(1): p. 17-26.
191. Foged, C., et al., *Interaction of dendritic cells with antigen-containing liposomes: effect of bilayer composition.* Vaccine, 2004. **22**(15-16): p. 1903-13.
192. Gregoriadis, G., et al., *A role for liposomes in genetic vaccination.* Vaccine, 2002. **20**: p. B1-B9.
193. Hawley-Nelson, P., *Lipofectamine reagent : a new higher efficiency polycationic liposome transfection reagent.* Focus, 1993. **15**: p. 73-79.
194. Zhou, F. and L. Huang, *Liposome-mediated cytoplasmic delivery of proteins: an effective means of accessing the MHC class I-restricted antigen presentation pathway.* Immunomethods, 1994. **4**(3): p. 229-35.
195. Davies, D.J., R.J. Ward, and J.R. Heylings, *Multi-species assessment of electrical resistance as a skin integrity marker for in vitro percutaneous absorption studies.* Toxicol In Vitro, 2004. **18**(3): p. 351-8.
196. Niyomtham, N., et al., *Synthesis and in vitro transfection efficiency of spermine-based cationic lipids with different central core structures and lipophilic tails.* Bioorganic & Medicinal Chemistry Letters, 2015. **25**(3): p. 496-503.
197. Opanasopit, P., et al., *Cationic niosomes an effective gene carrier composed of novel spermine-derivative cationic lipids: effect of central core structures.* Pharm Dev Technol, 2017. **22**(3): p. 350-359.
198. Franz, T.J., *Kinetics of cutaneous drug penetration.* Int J Dermatol, 1983. **22**(9): p. 499-505.
199. Wang, P.M., et al., *Precise microinjection into skin using hollow microneedles.* J Invest Dermatol, 2006. **126**(5): p. 1080-7.
200. Prausnitz, M.R., *Microneedles for transdermal drug delivery.* Advanced Drug Delivery Reviews, 2004. **56**(5): p. 581-587.
201. Abbas, A.K., A.H.H. Lichtman, and S. Pillai, *Cellular and Molecular Immunology E-Book*. 2011: Elsevier Health Sciences.
202. Kindt, T.J., et al., *Kuby Immunology*. 2007: W. H. Freeman.
203. Kupper, T.S. and R.C. Fuhlbrigge, *Immune surveillance in the skin: mechanisms and clinical consequences.* Nat Rev Immunol, 2004. **4**(3): p. 211-22.
204. Flynn, P.M., et al., *Influence of needle gauge in Mantoux skin testing.* Chest, 1994. **106**(5): p. 1463-5.
205. Sheikhi Mehrabadi, F., W. Fischer, and R. Haag, *Dendritic and lipid-based carriers for gene/siRNA delivery (a review).* Current Opinion in Solid State and Materials Science, 2012. **16**(6): p. 310-322.
206. Dincer, S., M. Turk, and E. Piskin, *Intelligent polymers as nonviral vectors.* Gene Ther, 2005. **12 Suppl 1**: p. S139-45.
207. Cooper, M.J., *CHAPTER 2 - Noninfectious Gene Transfer and Expression Systems for Cancer Gene Therapy A2 - LATTIME, EDMUND C*, in *Gene Therapy of Cancer (Second Edition)*, S.L. Gerson, Editor. 2002, Academic

Press: San Diego. p. 31-52.
208. Peng, J., et al., *An antisense oligonucleotide carrier based on amino silica nanoparticles for antisense inhibition of cancer cells.* Nanomedicine, 2006. **2**(2): p. 113-20.
209. Hengge, U.R., B. Dexling, and A. Mirmohammadsadegh, *Safety and Pharmacokinetics of Naked Plasmid DNA in the Skin: Studies on Dissemination and Ectopic Expression11Presented in part at the 28th Annual Meeting of the European Society for Dermatological Research, Montpellier, France, September 22–25, 1999.* Journal of Investigative Dermatology, 2001. **116**(6): p. 979-982.
210. Banga, A.K., *Microporation applications for enhancing drug delivery.* Expert Opin Drug Deliv, 2009. **6**(4): p. 343-54.
211. Yang, J., H. Liu, and X. Zhang, *Design, preparation and application of nucleic acid delivery carriers.* Biotechnol Adv, 2014. **32**(4): p. 804-17.
212. Amiji, M.M., *Polymeric Gene Delivery: Principles and Applications*. 2004: CRC Press.
213. Hahn, P. and E. Scanlan, *Gene delivery into mammalian cells: an overview on existing approaches employed in vitro and in vivo.* Top Curr Chem, 2010. **296**: p. 1-13.
214. Marchini, C., et al., *Structural Stability and Increase in Size Rationalize the Efficiency of Lipoplexes in Serum.* Langmuir, 2009. **25**(5): p. 3013-3021.
215. Sandrine, A., et al., *Serum as a modulator of lipoplex-mediated gene transfection: dependence of amphiphile, cell type and complex stability.* The Journal of Gene Medicine, 2000. **2**(6): p. 465-476.
216. Pojo, M., et al., *In vitro evaluation of the cytotoxicity and cellular uptake of CMCht/PAMAM dendrimer nanoparticles by glioblastoma cell models.* Journal of Nanoparticle Research, 2013. **15**(5): p. 1621.
217. Roberts, J.C., M.K. Bhalgat, and R.T. Zera, *Preliminary biological evaluation of polyamidoamine (PAMAM) Starburst dendrimers.* J Biomed Mater Res, 1996. **30**(1): p. 53-65.
218. Liblau, R.S., S.M. Singer, and H.O. McDevitt, *Th1 and Th2 CD4+ T cells in the pathogenesis of organ-specific autoimmune diseases.* Immunol Today, 1995. **16**(1): p. 34-8.
219. Curfs, J.H., J.F. Meis, and J.A. Hoogkamp-Korstanje, *A primer on cytokines: sources, receptors, effects, and inducers.* Clinical Microbiology Reviews, 1997. **10**(4): p. 742-780.
220. Constant, S.L. and K. Bottomly, *Induction of Th1 and Th2 CD4+ T cell responses: the alternative approaches.* Annu Rev Immunol, 1997. **15**: p. 297-322.

มหาวิทยาลัยศิลปากร

VITA

NAME	Boonnada Pamornpathomkul
DATE OF BIRTH	08 July 1990
PLACE OF BIRTH	Bangkok
INSTITUTIONS ATTENDED	2013-Present: Doctor of Philosophy, Ph.D. in Pharmaceutical Technology, Faculty of Pharmacy, Silpakorn University, Thailand. 2017: Visiting student, School of Pharmacy, Queen's University, Belfast, United Kingdom. 2009-2013: Bachelor of pharmacy (2nd class honors), Pharmaceutical Science, Faculty of Pharmacy, Silpakorn University, Thailand.
HOME ADDRESS	89 Soi.Puttaraksa 2, Puttaraksa Rd, Tumbon Sanamchan, Amphoe Muang, Nakhon Pathom 73000
PUBLICATION	1. Boonnada Pamornpathomkul, Tanasait Ngawhirunpat, Ismaiel A. Tekko, Lalitkumar Vora, Helen O. McCarthy, Ryan F. Donnelly. Dissolving polymeric microneedle arrays for local targeted acyclovir delivery. European Journal of Pharmaceutical Sciences. 2018;121:200-9. 2. Boonnada Pamornpathomkul, Nattisa Niyomtham, Boon-Ek Yingyongnarongkul, Chutinun Prasitpuriprecha, Theerasak Rojanarata, Tanasait Ngawhirunpat, and Praneet Opanasopit. Cationic Niosomes for Enhanced Skin Immunization of Plasmid DNA-Encoding Ovalbumin via Hollow Microneedles. AAPS PharmSciTech. 2018;19(1):481-8. 3. Boonnada Pamornpathomkul, Adisak Wongkajornsilp, Wanida Laiwattanapaisal, Theerasak Rojanarata, Praneet Opanasopit, Tanasait Ngawhirunpat. A combined approach of hollow microneedles and nanocarriers for skin immunization with plasmid DNA encoding ovalbumin. International journal of nanomedicine. 2017;12:885-98. 4. Boonnada Pamornpathomkul Theerasak Rojanarata, Praneet Opanasopit, Tanasait Ngawhirunpat. Enhancement of Skin Permeation and Skin Immunization of Ovalbumin Antigen via Microneedles. AAPS PharmSciTech. 2017;18(7):2418-26. 5. Boonnada Pamornpathomkul, Sureewan Duangjit, Suvida Laohapatarapant, Theerasak Rojanarata, Praneet Opanasopit, Tanasait Ngawhirunpat. Transdermal delivery of fluorescein isothiocyanate-dextrans using the combination of microneedles and low-frequency sonophoresis. Asian Journal of Pharmaceutical Sciences.

2015;10(5):415-24.
6. Sureewan Duangjit, Boonnada Pamornpathomkul, Praneet Opanasopit, Theerasak Rojanarata, Yasuko Obata, Kozo Takayama, Tanasait Ngawhirunpat. Role of the charge, carbon chain length, and content of surfactant on the skin penetration of meloxicam-loaded liposomes. International Journal of Nanomedicine. 2014;9:2005-17.
7. Thirapit Subongkot, Boonnada Pamornpathomkul, Theerasak Rojanarata, Praneet Opanasopit, Tanasait Ngawhirunpat. Investigation of the mechanism of enhanced skin penetration by ultradeformable liposomes. International Journal of Nanomedicine. 2014;9:3539-50.
8. Ponwanit Charoenputtakun, Boonnada Pamornpathomkul, Theerasak Rojanarata, Praneet Opanasopit, Tanasait Ngawhirunpat. Terpene composited lipid nanoparticles for enhanced dermal delivery of all-trans-retinoic acids. Biological & Pharmaceutical Bulletin. 2014;37(7):1139-48.

AWARD RECEIVED

• A certificate of achievement for excellence in contributing to the enhancement of the Faculty of Pharmacy, Silpakorn University's reputation, 5 April 2018, Faculty of Pharmacy, Silpakorn University, Thailand.
• An excellent oral presentation
Development of Dissolving Microneedle Arrays for Acyclovir Delivery, The 10th Annual Northeast Pharmacy Research Conference of 2018, 17-18 March 2018, Faculty of Pharmaceutical Sciences, Khon Kaen University, Thailand.
• The Royal Golden Jubilee Ph.D. Programme Scholarship, RGJ (co-funding with the National Vaccine Institute)